View metadata, citation and similar papers at core.ac.uk

brought to you by CORE

provided by UT Digital Repository

Copyright

by

Di Xiao

2007

The Dissertation Committee for Di Xiao
certifies that this is the approved version of the following dissertation:

Berry Phase Modification to Electron Density of States and Its Applications

Committee:

Qian Niu, Supervisor

Allan H. MacDonald

Michael P. Marder

Maxim Tsoi

Sanjay K. Barnejee

Berry Phase Modification to Electron Density of States and Its Applications

by

Di Xiao, B.S.

Dissertation

Presented to the Faculty of the Graduate School of

The University of Texas at Austin

in Partial Fulfillment

of the Requirements

for the Degree of

Doctor of Philosophy

The University of Texas at Austin

May 2007

Dedicated to my wife Yuan.

Acknowledgments

Over the years, I have enjoyed reading the acknowledgment part of books, dissertations, or anything that comes with one. The reason is simple. Obviously, the content of a scientific publication is always up to rigorous examinations, but the acknowledgment can be justified only by the author himself, and no one else. It is inspiring that despite all the ups and downs in the course of preparation, in the end everybody comes away with someone who they are grateful to. Now upon the completion of my dissertation, I truly feel that I am blessed to ride this great journey with many great people. Here are my humble salutations to all of them.

First and foremost, I would like to offer my sincere thanks to Dr. Qian Niu for his kind support and relentless guidance for all these years. Finding him is always as easy as a knock on the next door and discussing physics with him is one of the most enjoyable things to do, not to mention all the good jokes he has made. I especially appreciate his faith in me. He was more than just a supervisor.

I also want to thank the members of Dr. Niu's group, including former students Drs. Biao Wu, Roberto Diener, Chuangwei Zhang, and Dimitrie Culcer (a.k.a., Changqi Wen), and former postdocs Drs. Jie Liu, Yugui Yao, and Ping Zhang. In particular, I owe a great deal to Dr. Junren Shi, with whom I published my very first paper (of course there is always *the* supervisor). I extend my thanks to the current students of Dr. Niu, Chi-Piao Chuu, Mingxi Jiang, and Shengyuan Yang, the postdoc Dr. Wang Yao, and the visiting professor Dr. Dennis Clougherty.

Many thanks are also due to Drs. Allan MacDonald, Maxim Tsoi, James Erskine, and all members of Dr. MacDonald's group for many helpful discussions. I am also grateful to Dr. Michael Marder for a careful reading of the manuscript and many valuable suggestions.

This list would not be complete without the mention of Dr. Zhenyu Zhang. I am grateful to him for his kind and generous support and showing me the door to scientific research at an early stage.

I own much to my parents and sister Mandy for always believing in me and encouraging me to achieve my goals. I hope that I have made them proud by finishing this dissertation.

Finally, I would like to acknowledge the support of my loving wife. I am grateful to find such a brilliant, funny, and caring person as the love in my life. Her example of determination and emotional support during difficult times have been invaluable. Yuan, this would not be possible without you.

Di Xiao

The University of Texas at Austin
May 2007

Berry Phase Modification to Electron Density of States and Its Applications

Publication No. _____

Di Xiao, Ph.D.

The University of Texas at Austin, 2007

Supervisor: Qian Niu

We study the Berry phase correction to the electron density of states and present a number of its applications. It is now well recognized that the Berry phase of the electronic wave function plays an important role in the dynamics of Bloch electrons. For instance, the electron will acquire an anomalous velocity term transverse to the applied electric field, giving rise to an intrinsic contribution to the anomalous Hall effect. On the other hand, we find that the Berry phase also has a fundamental effect on the electron phase space, and leads to a modification of the phase-space density of states. This surprising result has a number of applications, which we shall discuss in detail. We first derive an explicit expression of the orbital magnetization (zero and finite temperature), where it is shown that contributions to the orbital

magnetization can be classified into a local rotation of the electron and global center-of-mass motion. Based on this formula, we develop a theory of the Berry-phase effect in anomalous transport in ferromagnets driven by statistical forces such as the gradient of temperature or chemical potential. We also study the Berry phase effect on magnetotransport, showing that a linear (in field) magnetoresistance is possible in ferromagnets. Finally, we propose that in graphene with broken inversion symmetry, a valley Hall effect exists and the finite valley polarization can be detected by measuring the magnetization.

Contents

Chapter 1

Introduction

1.1 Geometric Phase

One of the most fundamental differences between quantum mechanics and its classical counterpart is the phase factor associated with each quantum state, which is absent in classical mechanics. In fact, it is probably not an exaggeration to say that it is this very phase factor that makes quantum mechanics such an intriguing subject and gives rise to so many fascinating phenomena.

Among these phenomena, we shall discuss the Aharonov-Bohm (AB) effect [1] in detail since it gives a very nice example illustrating the geometric phase in quantum mechanics. Let us consider the experiment shown in Fig. 1.1. In the absence of the magnetic field, this is the classic double-slit experiments with electrons from the source going through the double slits, then forming an interference pattern on the screen. Now, we turn on the magnetic field $\boldsymbol{B}$ confined in a very thin solenoid. From a classical point of view, since the two paths C_1 and C_2 are far away from the solenoid, the magnetic field cannot have an effect on the electrons. Therefore the interference patter should remain the same. However, in quantum mechanics, it is the vector potential $\boldsymbol{A}$ rather than the field $\boldsymbol{B}$ enters into the Schrodinger equation, i.e.,

$$\frac{1}{2m}(-i\hbar\boldsymbol{\nabla} + e\boldsymbol{A})^2\psi = \varepsilon\psi \ , \tag{1.1}$$

where m is the electron mass and ε is the energy. We choose the convention that the electron charge is $-e$. The physical quantities should be invariant with respect

to the following gauge transformation

$$\boldsymbol{A} \rightarrow \boldsymbol{A} + \boldsymbol{\nabla}\chi \ , \tag{1.2}$$

where χ is an arbitrary function. Accordingly, the wave function can at most change by a phase factor under this transformation,

$$\psi \rightarrow e^{i\phi}\psi \ . \tag{1.3}$$

It is straightforward to verify that $\boldsymbol{\nabla}\phi = -(e/\hbar)\boldsymbol{\nabla}\chi$. Therefore the electron moving along the path C_i will acquire a phase

$$\phi_i = -i\frac{e}{\hbar}\int_{C_i} d\boldsymbol{l}\cdot\boldsymbol{A}(\boldsymbol{r}) \ , \tag{1.4}$$

and electrons from different paths will have a phase difference

$$\Delta\phi = \frac{e}{\hbar}\oint_C d\boldsymbol{l}\cdot\boldsymbol{A}(\boldsymbol{r}) = \frac{e}{\hbar}\int_S d\boldsymbol{S}\cdot\boldsymbol{B} \ , \tag{1.5}$$

where S is the surface enclosed by the loop $C = C_1 + C_2$. We have used the Stokes theorem to convert the line integral into a surface integral. As a result, one should be able to observe a phase shift of the interference patter on the screen. It is noteworthy that although ϕ_i depends on the gauge choice of the vector potential $\boldsymbol{A}$, the phase $\Delta\phi$ an electron acquired along a *closed* loop is gauge invariant.

In fact, the AB effect is a particular example of the more general geometric phase in quantum mechanics. It was first discovered by Pancharatnam in 1956 [2], and rediscovered by Berry in 1984 [3]. Since Berry is responsible for making this concept known to the physics and mathematics community, the geometric phase is also called the Berry phase. In order to show the existence of the Berry phase, we shall follow Berry's original paper [3]. Let us consider a system described by the Hamiltonian $H(\boldsymbol{R})$ that is a function of a set of parameters $\boldsymbol{R} = \{R_1, R_2, \cdots, R_n\}$. To explore an analogy with the AB effect, we shall consider the case of three parameters. The adiabatic evolution of the system can be described by the path of the $\boldsymbol{R}$ point in the parameter space as time changes. At time t_1 we assume the system is in one of its eigenstates $|\psi_0(\boldsymbol{R}(t_1))\rangle$. The adiabatic condition requires that the system stays in the eigenstate $|\psi_0(\boldsymbol{R}(t))\rangle$ during the evolution. We can therefore

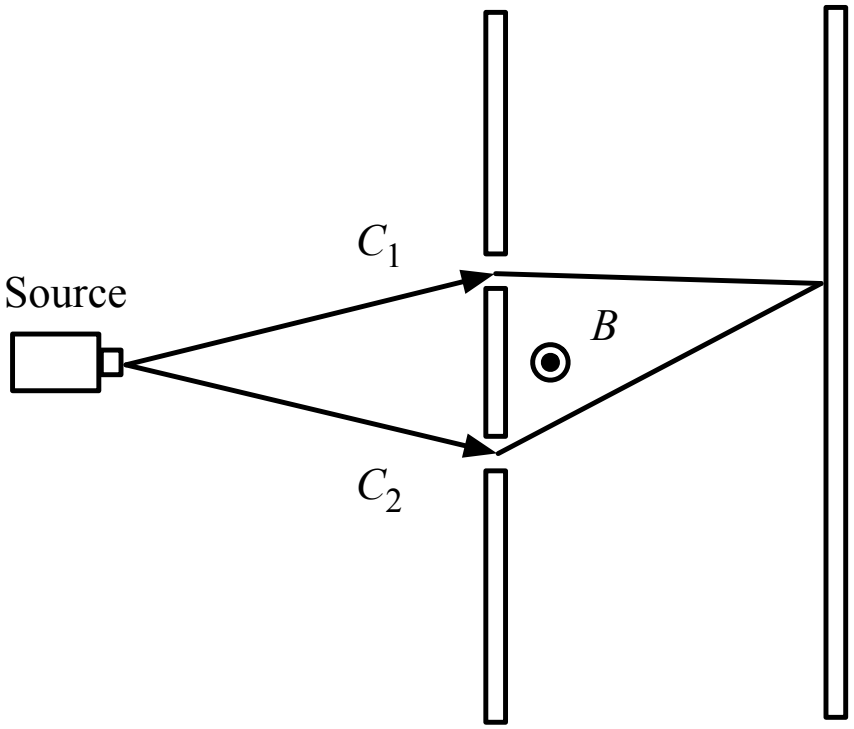

Figure 1.1: Schematic showing of the Aharonov-Bohm Effect in a double-slit experiment.

write the state at time t as

$$|\psi_0(t)\rangle = \exp\Big[-\frac{i}{\hbar}\int_{t_1}^{t} dt\, \varepsilon_0(\boldsymbol{R}(t))\Big] \exp(i\phi_B)|\psi_0(\boldsymbol{R}(t))\rangle, \tag{1.6}$$

where $\varepsilon_0(\boldsymbol{R})$ is the energy of the eigenstates $|\psi_0(\boldsymbol{R})\rangle$. The first exponential is the usual dynamical phase, and the second one, $\exp(i\phi_B)$, is the so called Berry phase. To find ϕ_B, we insert the above expression into the the Schrödinger equation

$$i\frac{\partial}{\partial t}|\psi_0(t)\rangle = H(\boldsymbol{R}(t))|\psi_0(t)\rangle \ , \tag{1.7}$$

and we have

$$\phi_B = \int_{C_{\boldsymbol{R}}} d\boldsymbol{R} \cdot \langle\psi_0(\boldsymbol{R})|i\boldsymbol{\nabla}_{\boldsymbol{R}}|\psi_0(\boldsymbol{R})\rangle \ , \tag{1.8}$$

where $C_{\boldsymbol{R}}$ is the path in the parameter space. If we compare the above equation with Eq. (1.4), we can see that the Berry phase and the AB phase have the same mathematical structure, with the quantity

$$\boldsymbol{A}(\boldsymbol{R}) = \langle\psi_0(\boldsymbol{R})|i\boldsymbol{\nabla}_{\boldsymbol{R}}|\psi_0(\boldsymbol{R})\rangle \tag{1.9}$$

playing the same role as the vector potential, but in parameter space. If we make a gauge transformation

$$|\psi_0(\boldsymbol{R})\rangle \to e^{i\chi(\boldsymbol{R})}|\psi_0(\boldsymbol{R})\rangle \ , \tag{1.10}$$

then $\boldsymbol{A}(\boldsymbol{R})$ transforms as

$$\boldsymbol{A}(\boldsymbol{R}) \to \boldsymbol{A}(\boldsymbol{R}) - \boldsymbol{\nabla}_{\boldsymbol{R}}\chi(\boldsymbol{R}) \ . \tag{1.11}$$

We can also define a quantity, the Berry curvature, as

$$\boldsymbol{\Omega}(\boldsymbol{R}) = \boldsymbol{\nabla} \times \boldsymbol{A}(\boldsymbol{R}) \ . \tag{1.12}$$

While the vector potential $\boldsymbol{A}(\boldsymbol{R})$ depends on the gauge choice of $|\psi_0(\boldsymbol{R})\rangle$, the Berry curvature $\boldsymbol{\Omega}(\boldsymbol{R})$ is gauge invariant. Just like the magnetic field $\boldsymbol{B}$ will have an effect on the electron motion through the Lorentz force $-e\dot{\boldsymbol{r}} \times \boldsymbol{B}$, the Berry curvature will also have an effect on the dynamics of the parameter $\boldsymbol{R}$. As we shall see later, this is exactly the case for the Berry phase effect on Bloch electron dynamics.

1.2 Semiclassical Model

The semiclassical theory of Bloch electron dynamics plays a very important role in our understanding of electronic spectral and transport properties of solids. For example, so far the most common, and perhaps also the most accurate, probes of the Fermi surface rely on a class of magneto-oscillatory effects, such as the de Haas-van Alphen oscillation. These effects can be easily understood in terms of quantization of the semiclassical electron orbits in the presence of a magnetic field. Another example is the semiclassical transport theory of conduction in metals and semiconductors. Armed with the Boltzmann equation, even within the simplest relaxation time approximation, the semiclassical theory provides a successful account of various transport phenomena, and lays the foundation of modern electronics.

In the semiclassical approach, each electron is described by a wave packet constructed from Bloch functions under the following condition. The spread Δk of the wave packet in the momentum space should be small compared with the dimensions of the Brillouin zone so that it is meaningful to speak of the momentum $\boldsymbol{k}$ of the electron. This requirement implies that in the real space the spread Δr of the wave packet is on the scale of hundreds of unit cells. Therefore, in order for the semiclassical description to be valid, external perturbations must vary slowly over the dimensions of Δr. The wave packet can be written as

$$|W(\boldsymbol{r}_c, \boldsymbol{k}_c)\rangle = \int d\boldsymbol{k}\, a(\boldsymbol{k}) e^{i\boldsymbol{k}\cdot(\boldsymbol{r}-\boldsymbol{r}_c)} |u_n(\boldsymbol{k})\rangle \ , \tag{1.13}$$

where $\boldsymbol{r}_c$ and $\boldsymbol{k}_c$ are the wave packet centers in the real and momentum space, respectively, $a(\boldsymbol{k})$ is the expansion coefficient whose exact form is not important as long as the above requirement on the wave packet spread is satisfied, and $|u_n(\boldsymbol{k})\rangle$ is the periodic part of the Bloch function, $|\psi_n(\boldsymbol{k})\rangle = e^{i\boldsymbol{k}\cdot\boldsymbol{r}}|u_n(\boldsymbol{k})\rangle$. The spirit of the semiclassical model is that the fast varying periodic lattice potential is taken into account by the use of the Bloch functions $|u_n(\boldsymbol{k})\rangle$ while the slowly varying external perturbations are treated semiclassically.

In the presence of weak electric ($\boldsymbol{E}$) and magnetic ($\boldsymbol{B}$) fields, the equation of motion of the wave packet center is usually given in the following form [4] (we have

neglected the subscript c on the electron position and momentum):

$$\dot{\boldsymbol{r}} = \frac{1}{\hbar}\frac{\partial \varepsilon_n(\boldsymbol{k})}{\partial \boldsymbol{k}} \,, \tag{1.14a}$$

$$\hbar\dot{\boldsymbol{k}} = -e\boldsymbol{E} - e\dot{\boldsymbol{r}} \times \boldsymbol{B} \,, \tag{1.14b}$$

where $\varepsilon_n(\boldsymbol{k})$ is the unperturbed band energy of the electron. According to this set of equations, the electron dynamics is *solely* determined by the band energy $\varepsilon_n(\boldsymbol{k})$. In fact, the quantity $\varepsilon_n(\boldsymbol{k})$ is so important that techniques developed to calculate the band structure have become an independent field in solid state physics.

Surprisingly, despite its wide usage and great success, this semiclassical model has never been rigorous justified. To best put the situation, I shall simply quote from Ashcroft and Mermin [4],

> Perhaps a suitable attitude to take is this: If there were no underlying microscopic quantum theory of electrons in solids, one could still imagine a semiclassical mechanics (...) that was brilliantly confirmed by its account of observe electronic behavior, ..., and only very much later given a more fundamental derivation as a limiting form of quantum mechanics.

It turns out that this more fundamental derivation comes near seventy years later after Bloch's seminal paper [5] on the quantum mechanics of electrons in crystal lattices.

1.3 Berry Phase Modified Equations of Motion

The wave packet (1.13) is expanded in the basis of the cell function $|u_n(\boldsymbol{k})\rangle$, which is the eigenstate of the following effective Hamiltonian

$$H(\boldsymbol{k}) = \frac{\hbar}{2m}(-i\boldsymbol{\nabla} + \boldsymbol{k})^2 + V(\boldsymbol{r}) \,, \tag{1.15}$$

where $V(\boldsymbol{r})$ is the periodic lattice potential. Then according to the theory presented in Sec. 1.1, if the electron adiabatically moves from $\boldsymbol{k}_1$ to $\boldsymbol{k}_2$, which can be done by simply applying an electric field, it will acquire a Berry phase. As a result, there will also be a Berry curvature in the parameter space, which is just the momentum

space in our case, given by

$$\boldsymbol{\Omega}_n(\boldsymbol{k}) = \boldsymbol{\nabla}_{\boldsymbol{k}} \times \langle u_n(\boldsymbol{k}) | i\boldsymbol{\nabla}_{\boldsymbol{k}} | u_n(\boldsymbol{k}) \rangle \ . \tag{1.16}$$

This Berry curvature acts like a magnetic field in the momentum space and will drive the electron motion.

A rigorous derivation of the semiclassical dynamics of Bloch electrons was found recently by Chang and Niu [6], and Sundaram and Niu [7]. The equations of motion, in the presence of weak electric and magnetic fields, are given by

$$\dot{\boldsymbol{r}} = \frac{1}{\hbar}\frac{\partial \tilde{\varepsilon}_n(\boldsymbol{k})}{\partial \boldsymbol{k}} - \dot{\boldsymbol{k}} \times \boldsymbol{\Omega}(\boldsymbol{k}) \ , \tag{1.17a}$$

$$\hbar\dot{\boldsymbol{k}} = -e\boldsymbol{E} - e\dot{\boldsymbol{r}} \times \boldsymbol{B} \ . \tag{1.17b}$$

Compared to the conventional equations of motion (1.14), there are two major differences:

1. The electron acquires an extra velocity $-\dot{\boldsymbol{k}} \times \boldsymbol{\Omega}_n(\boldsymbol{k})$ that is proportional to the Berry curvature.

2. In addition, the electron energy has a correction due to the orbital magnetic moment of the wave packet, $\tilde{\varepsilon}_n(\boldsymbol{k}) = \varepsilon_n(\boldsymbol{k}) - \boldsymbol{m}_n(\boldsymbol{k}) \cdot \boldsymbol{B}$, where

$$\boldsymbol{m}_n(\boldsymbol{k}) = -i\frac{e}{\hbar}\langle \boldsymbol{\nabla}_{\boldsymbol{k}} u_n(\boldsymbol{k})| \times [H(\boldsymbol{k}) - \varepsilon_n(\boldsymbol{k})] |\boldsymbol{\nabla}_{\boldsymbol{k}} u_n(\boldsymbol{k})\rangle \ . \tag{1.18}$$

   The magnetic moment $\boldsymbol{m}_n(\boldsymbol{k})$ originates from the self-rotation of the wave packet.

Symmetry considerations show [7] that for single band, if the crystal has both the time-reversal and inversion symmetry, then both $\boldsymbol{\Omega}_n(\boldsymbol{k})$ and $\boldsymbol{m}_n(\boldsymbol{k})$ vanish. However, if either symmetry is broken, then the Berry phase term will appear and have a profound effect on transport as well equilibrium properties.

One of the applications of the Berry phase approach is the anomalous Hall effect (AHE). In ferromagnet, a spontaneous Hall current can be induced by an electric field in the absence of a magnetic field. The origin of the AHE has been a controversial subject. Now it is agreed that the contributions to the AHE can be classified into two categories, the Berry-phase induced intrinsic contribution and the

scattering-dependent extrinsic contribution, including skew scattering [8] and side jump [9]. We shall focus on the intrinsic contribution here. In the presence of an electric field, the electron velocity is given by

$$\dot{\boldsymbol{r}} = \frac{1}{\hbar}\frac{\partial \varepsilon_n(\boldsymbol{k})}{\partial \boldsymbol{k}} + \frac{e}{\hbar}\boldsymbol{E} \times \boldsymbol{\Omega}_n(\boldsymbol{k}) \; . \tag{1.19}$$

By summing over all occupied electron state, we obtain a Hall current that is independent of scattering

$$\boldsymbol{j}_{\rm AH} = -\frac{e^2}{\hbar}\boldsymbol{E} \times \sum_n \int \frac{d\boldsymbol{k}}{(2\pi)^3} f_n(\boldsymbol{k}) \boldsymbol{\Omega}_n(\boldsymbol{k}) \; , \tag{1.20}$$

where $f_n(\boldsymbol{k})$ is the Fermi-Dirac distribution function. Numerical calculations in ferromagnetic semiconductors [10], oxides [11], and transition metals [12] have shown that this intrinsic contribution is the dominant contribution to the AHE in these materials.

1.4 Outline of this Work

In this work we study the Berry phase correction to the electron density of states and present a number of its applications. In Chap. 2 we show that the Berry phase also has a fundamental effect on the electron phase space, and leads to a modification of the phase-space density of states. This surprising result has a number of applications, which we shall discuss in detail. We first derive in Chap. 3 an explicit expression of the orbital magnetization (zero and finite temperature), where it is shown that contributions to the orbital magnetization can be classified into a local rotation of the electron and global center-of-mass motion. Based on this formula, we develop a theory of the Berry-phase effect in anomalous transport in ferromagnets driven by statistical forces such as the gradient of temperature or chemical potential, which is presented in Chap. 4. In Chap. 5 we study the Berry phase effect on magnetotransport, showing that a linear (in field) magnetoresistance is possible in ferromagnets. Finally, in Chap. 6 we propose that in graphene with broken inversion symmetry, a valley Hall effect exists and the finite valley polarization can be detected by measuring the magnetization.

Chapter 2

Berry Phase Correction to Electron Density of States in Solids

2.1 Introduction

Semiclassical dynamics of Bloch electrons in external fields has provided a powerful theoretical framework to account for various properties of metals, semiconductors and insulators [4]. In recent years, it has become increasingly clear that essential modification of the semiclassical dynamics is necessary for a proper understanding of a number of phenomena. It was known earlier that global geometric phase effects [3, 13] on Bloch states are very important for insulators in our understanding of the quantum Hall effect [14], quantized adiabatic pumps [15], and electric polarization [16, 17]. It was shown [6, 7] later that geometric phase also modifies the local dynamics of Bloch electrons and thus affects the transport properties of metals and semiconductors. Recently these ideas have been successfully applied to the anomalous Hall effect in ferromagnetic semiconductors and metals [10, 11, 12, 18], as well as spin transport [19, 20].

In this chapter, we reveal a general property of the Berry phase modified semiclassical dynamics which has been overlooked so far: the violation of Liou-

This chapter is adapted from D. Xiao, J. Shi, and Q. Niu, Phys. Rev. Lett. **95**, 137204 (2005).
Copyright © 2005 American Physical Society.

ville's theorem for the conservation of phase space volume. Liouville's theorem was originally established for standard classical Hamiltonian dynamics, and its importance cannot be over emphasized as it serves as a foundation for classical statistical physics. The Berry phase makes, in general, the equations of motion noncanonical [21, 22, 6, 7, 23], leading to a violation of Liouville's theorem. Nevertheless, we are able to remedy the situation by modifying the density of states in phase space.

This modified phase-space density of states enters naturally in the semiclassical expression for the expectation value of physical quantities, and has profound effects on equilibrium as well as transport properties. We demonstrate this with several examples. First, we consider a Fermi sea of electrons in a weak magnetic field, and show that the Fermi sea volume can be changed linearly by the field. Second, we show how the Berry phase formula for the intrinsic anomalous Hall conductivity may be derived from equilibrium thermodynamics using the Středa formula [24]. Third, we provide a general derivation of an orbital-magnetization formula which is convenient for first-principles calculations.

In addition, we present an effective quantum mechanics for Bloch electrons in solids by quantizing the semiclassical dynamics with the geometric phase. The density of states enters in a nontrivial manner into the commutators of the phase space coordinates, and relates directly to the minimal uncertainty volume in the phase space.

2.2 Breakdown of the Liouville's Theorem

To begin with, we write down the semiclassical equations of motion for a Bloch electron in weak electric and magnetic fields [7]

$$\dot{\boldsymbol{r}} = \frac{1}{\hbar}\frac{\partial \varepsilon_n(\boldsymbol{k})}{\partial \boldsymbol{k}} - \dot{\boldsymbol{k}} \times \boldsymbol{\Omega}_n(\boldsymbol{k}) \,, \tag{2.1a}$$

$$\hbar\dot{\boldsymbol{k}} = -e\boldsymbol{E}(\boldsymbol{r}) - e\dot{\boldsymbol{r}} \times \boldsymbol{B}(\boldsymbol{r}) \,, \tag{2.1b}$$

where $\boldsymbol{\Omega}_n(\boldsymbol{k})$ is the Berry curvature of electronic Bloch states defined by $\boldsymbol{\Omega}_n(\boldsymbol{k}) = \mathrm{i}\langle \boldsymbol{\nabla}_{\boldsymbol{k}} u_n(\boldsymbol{k})| \times |\boldsymbol{\nabla}_{\boldsymbol{k}} u_n(\boldsymbol{k})\rangle$ with $|u_n(\boldsymbol{k})\rangle$ being the periodic part of Bloch waves in the nth band, $\varepsilon_n(\boldsymbol{k})$ is the band energy with a correction due to the orbital magnetic moment [see Eq. (2.10) and above]. For crystals with broken time-reversal symmetry

(such as ferromagnetic materials) or spatial inversion symmetry (such as GaAs), the Berry curvature $\boldsymbol{\Omega}_n(\boldsymbol{k})$ is nonzero.

To show the violation of Liouville's theorem, we consider the time evolution of a volume element $\Delta V = \Delta\boldsymbol{r}\Delta\boldsymbol{k}$ in the phase space. The equation of motion for ΔV is given by $(1/\Delta V)\mathrm{d}\Delta V/\mathrm{d}t = \boldsymbol{\nabla}_{\boldsymbol{r}} \cdot \dot{\boldsymbol{r}} + \boldsymbol{\nabla}_{\boldsymbol{k}} \cdot \dot{\boldsymbol{k}}$ [25]. A straightforward but somewhat tedious calculation (see Appendix A) shows that the right hand side is equal to $-\mathrm{d}\ln(1 + e\boldsymbol{B} \cdot \boldsymbol{\Omega}/\hbar)/\mathrm{d}t$, which is a total time derivative. Therefore we can solve for the time evolution of the volume element and obtain

$$\Delta V = \Delta V_0/(1 + e\boldsymbol{B} \cdot \boldsymbol{\Omega}_n/\hbar) \; . \tag{2.2}$$

The fact that the Berry curvature is generally $\boldsymbol{k}$ dependent (and the magnetic field can also depend on $\boldsymbol{r}$) implies that the phase space volume element changes during time evolution of the state variables $(\boldsymbol{r}, \boldsymbol{k})$.

Nevertheless, we have a remedy to this breakdown of Liouville's theorem. Equation (2.2) shows that the volume element is a local function of the state variables (through the magnetic field and the Berry curvature) and has nothing to do with the history of time evolution. We can thus introduce a modified density of states

$$D_n(\boldsymbol{r}, \boldsymbol{k}) = (2\pi)^{-d}(1 + e\boldsymbol{B} \cdot \boldsymbol{\Omega}_n/\hbar) \; , \tag{2.3}$$

such that the number of states in the volume element, $D_n(\boldsymbol{r}, \boldsymbol{k})\Delta V$, remains constant in time, where d is the spatial dimensionality of the system. The prefactor $(2\pi)^{-d}$ is obtained by demanding that the density of states $D_n(\boldsymbol{r}, \boldsymbol{k})$ reduces to the conventional form when the Berry curvature vanishes. As will be shown later, this density of states corresponds to the minimal quantum uncertainty volume of the state variables. Therefore, it does serve as the semiclassical measure for the number of quantum states per unit volume in the phase space. Based on this understanding, we write the classical phase-space probability density as

$$\rho_n(\boldsymbol{r}, \boldsymbol{k}, t) = D_n(\boldsymbol{r}, \boldsymbol{k}) f_n(\boldsymbol{r}, \boldsymbol{k}, t) \; , \tag{2.4}$$

with $f_n(\boldsymbol{r}, \boldsymbol{k}, t)$ being the occupation number of the state labeled by $(\boldsymbol{r}, \boldsymbol{k})$. Probability conservation demands that $\rho_n(\boldsymbol{r}, \boldsymbol{k}, t)$ satisfies the continuity equation in phase space. On the other hand, our density of states satisfies $\mathrm{d}D_n/\mathrm{d}t = -(\boldsymbol{\nabla}_{\boldsymbol{r}} \cdot \dot{\boldsymbol{r}} + \boldsymbol{\nabla}_{\boldsymbol{k}} \cdot$

$\dot{\boldsymbol{k}})D_n$. It then follows that the occupation number introduced above has the desired property of being invariant along the trajectory, i.e., $\mathrm{d}f_n/\mathrm{d}t = 0$ [1].

We can thus write the real space density of a physical observable $\hat{O}$ in the form [26]

$$\bar{O}(\boldsymbol{R}) = \sum_n \int \mathrm{d}\boldsymbol{k} D_n(\boldsymbol{r},\boldsymbol{k}) f_n(\boldsymbol{r},\boldsymbol{k},t) \langle \hat{O}\delta(\hat{\boldsymbol{r}} - \boldsymbol{R})\rangle_{\boldsymbol{r}\boldsymbol{k}n} \tag{2.5}$$

where $\langle\cdots\rangle_{\boldsymbol{r}\boldsymbol{k}n}$ denotes the expectation value in the wave-packet state centered at ($\boldsymbol{r}$, $\boldsymbol{k}$) with the band index n. In the spatially homogeneous case, it reduces to:

$$\bar{O} = \sum_n \int \mathrm{d}\boldsymbol{k} D_n(\boldsymbol{k}) f_n(\boldsymbol{k}) O_n(\boldsymbol{k}) \ , \tag{2.6}$$

where $O_n(\boldsymbol{k})$ is the expectation value of $\hat{O}$ in a Bloch state. For simpler notation, we will drop the band index n and assume that the integral over $\boldsymbol{k}$ includes the sum over n.

We now discuss the magnitude of the correction term $e\boldsymbol{B}\cdot\boldsymbol{\Omega}/\hbar$ to the density of states in Eq. (2.3). The Berry curvature for several materials has been calculated before using first-principles method [11, 12]. Over large regions of the Brillouin zone, its magnitude is on the order of a^2 with a being the lattice constant. Thus, $e\boldsymbol{B}\cdot\boldsymbol{\Omega}/\hbar \sim eBa^2/\hbar$ is the ratio of the magnetic flux through a unit cell to the magnetic flux quantum, and can be 10^{-2} to 10^{-3} for a magnetic field of 1 tesla. In the vicinity of some isolated points, the Berry curvature can be several orders of magnitude higher, leading to bigger effects for measurement. In the following, we will present a number of applications of our formula Eq. (2.6).

2.3 Examples

In our first example, we consider the quantity of electron density and show that the Fermi sea volume can be changed linearly by a magnetic field when the Berry curvature is non-zero. Assuming zero temperature and using Eq. (2.3), we have the

[1] In the presence of collision, the function satisfies the usual Boltzmann equation:

$$\frac{df_n}{dt} \equiv \Big(\frac{\partial}{\partial t} + \dot{\boldsymbol{r}}\cdot\nabla_{\boldsymbol{r}} + \dot{\boldsymbol{k}}\cdot\nabla_{\boldsymbol{k}}\Big) f_n(\boldsymbol{k},\boldsymbol{r},t) = \Big(\frac{\partial f_n}{\partial t}\Big)_{\mathrm{coll}}$$

The right hand side denotes the collision contribution.

electron density as

$$n_e = \int^{\mu} \frac{\mathrm{d}\boldsymbol{k}}{(2\pi)^d} \left(1 + \frac{e\boldsymbol{B}\cdot\boldsymbol{\Omega}}{\hbar}\right) , \tag{2.7}$$

where the upper limit means that the integral is over states with energies below the chemical potential μ. Noting that the electron density is fixed by the background charge density, we conclude that the Fermi volume must change with the magnetic field. To first order, this change is given by

$$\delta V_F = -\int^{\mu_0} \mathrm{d}\boldsymbol{k}\, \frac{e\boldsymbol{B}\cdot\boldsymbol{\Omega}}{\hbar} . \tag{2.8}$$

We note that while Landau levels make the Fermi sea volume oscillate with the field, the effect described above gives an overall shift on average. Such a shift has important implications for Fermi-surface related behaviors such as transport properties. For instance, in metals, it can induce a magnetoresistance linearly depending on the magnetic field. On the other hand, in band insulators the $\boldsymbol{k}$ space is limited to the Brillouin zone. Electrons must populate a higher band if $(e/\hbar)\int_{\mathrm{BZ}} \mathrm{d}\boldsymbol{k}\,\boldsymbol{B}\cdot\boldsymbol{\Omega}$ is negative. When this quantity is positive, holes must appear at the top of the valence bands. Discontinuous behavior of physical properties in a magnetic field is therefore expected for band insulators with non-zero integral of the Berry curvatures (Chern numbers).

In our second example, we show a connection between our phase space density of states to the intrinsic anomalous Hall effect, which is due to spin-orbit coupling in the band structure of a ferromagnetic crystal. In the context of the quantum Hall effect, Středa derived a formula relating the Hall conductivity to the field derivative of the electron density at a fixed chemical potential [24], $\sigma_{xy} = -e(\partial n_e/\partial B_z)_\mu$. There is a simple justification of this relation by a thermodynamic argument by considering the following adiabatic process in two dimensions. A time dependent magnetic flux generates an electric field with an emf around the boundary of some region; and the Hall current leads to a net flow of electrons across the boundary and thus a change of electron density inside. This argument can be straightforwardly applied to the case of anomalous Hall effect and to three dimensions. By taking the derivative of the electron density (2.7) with respect to $\boldsymbol{B} = B\hat{\boldsymbol{z}}$ at fixed chemical potential, we find that

$$\sigma_{xy} = -\frac{e^2}{\hbar}\int^{\mu} \frac{\mathrm{d}\boldsymbol{k}}{(2\pi)^d}\Omega_z . \tag{2.9}$$

This is an intrinsic effect because it is independent of scattering, and thus differs from conventional skew scattering and side jump mechanisms [10, 11, 12, 18].

As a third example of application, we now derive a semiclassical formula for orbital magnetization. In the semiclassical picture, a Bloch electron is modeled by a wave packet in a Bloch band, which is found to rotate about its center of mass in general, yielding an intrinsic magnetic moment given by $\boldsymbol{m}(\boldsymbol{k}) = -\mathrm{i}(e/2\hbar)\langle\boldsymbol{\nabla}_{\boldsymbol{k}}u| \times [\hat{H}_0(\boldsymbol{k}) - \varepsilon_0(\boldsymbol{k})]|\boldsymbol{\nabla}_{\boldsymbol{k}}u\rangle$, where $\hat{H}_0$ is the Hamiltonian [2]. In the presence of a weak magnetic field $\boldsymbol{B}$, the electron band structure energy $\varepsilon_0(\boldsymbol{k})$ (which may already include Zeeman energy from spin magnetization) acquires a correction term from this intrinsic orbital moment [6, 7], $\varepsilon(\boldsymbol{k}) = \varepsilon_0(\boldsymbol{k}) - \boldsymbol{m}(\boldsymbol{k}) \cdot \boldsymbol{B}$. For an equilibrium ensemble of electrons, the total orbital magnetization can be found from the total energy, which is given by Eq. (2.6) as,

$$E = \int^{\mu} \frac{\mathrm{d}\boldsymbol{k}}{(2\pi)^d}\Big(1 + \frac{e\boldsymbol{B}\cdot\boldsymbol{\Omega}}{\hbar}\Big)\Big(\varepsilon_0(\boldsymbol{k}) - \boldsymbol{m}(\boldsymbol{k})\cdot\boldsymbol{B}\Big)\,. \tag{2.10}$$

Taking the differential of E with respect to $\boldsymbol{B}$, we obtain the magnetization at zero magnetic field to be

$$\begin{aligned}\boldsymbol{M} &= \int^{\mu_0} \frac{\mathrm{d}\boldsymbol{k}}{(2\pi)^d}\Big(\boldsymbol{m}(\boldsymbol{k}) + \frac{e\boldsymbol{\Omega}}{\hbar}\big[\mu_0 - \varepsilon_0(\boldsymbol{k})\big]\Big) \\ &= \frac{e}{2\hbar}\int^{\mu_0} \frac{\mathrm{d}\boldsymbol{k}}{(2\pi)^d}\mathrm{i}\Big\langle\frac{\partial u}{\partial \boldsymbol{k}}\Big| \times [2\mu_0 - \varepsilon_0(\boldsymbol{k}) - \hat{H}_0]\Big|\frac{\partial u}{\partial \boldsymbol{k}}\Big\rangle\,.\end{aligned} \tag{2.11}$$

In the upper line of the above expression, the first term is the contribution from the intrinsic orbital moment of each Bloch electron, and the second term comes from the explicit field dependence of the density of states and the resulting change in the Fermi volume in Eq. (2.8). We expect this effect to be important in ferromagnetic materials with strong spin-orbit coupling.

Gat and Avron obtained an equivalent result for the special case of Hofstadter model [27]. Our derivation provides a more general formula that is applicable to other systems. Following the discussions on band insulators in our first example, there will be a discontinuity of the orbital magnetization if the integral of the Berry curvature over the Brillouin zone, or the anomalous Hall conductivity, is non-zero

[2] There is a typo in Ref. [7]. The expression for orbital magnetic moment in Eq. (3.6) misses a factor of $-1/2$. This term is equivalent to the Rammal-Wilkinson term as discussed in Ref. [23].

and quantized. Depending on the direction of the field, the chemical potential μ_0 in the above formula should be taken at the top of the valence bands or the bottom of the conduction bands. The size of the discontinuity is given by the quantized anomalous Hall conductivity times E_g/e, where E_g is the energy gap. For insulators with zero Chern numbers, the orbital magnetization can be directly evaluated from Wannier functions, with result consistent with our general formula [28]. Our general formula can also be derived from a full quantum mechanical linear response analysis [29].

2.4 General Form and Effective Quantum Mechanics

The central result of this paper, equation (2.3), can be extended to the more general case when Berry curvature includes the components of $\overleftrightarrow{\Omega}^{\boldsymbol{kr}}$ as well as $\overleftrightarrow{\Omega}^{\boldsymbol{kk}}$ and $\overleftrightarrow{\Omega}^{\boldsymbol{rr}}$ [7]. In this case, we introduce the Berry curvature in phase space,

$$\overleftrightarrow{\boldsymbol{\Omega}} = \begin{pmatrix} \overleftrightarrow{\Omega}^{\boldsymbol{rr}} & \overleftrightarrow{\Omega}^{\boldsymbol{rk}} \\ \overleftrightarrow{\Omega}^{\boldsymbol{kr}} & \overleftrightarrow{\Omega}^{\boldsymbol{kk}} \end{pmatrix} , \tag{2.12}$$

where each block is a 3×3 matrix; $\overleftrightarrow{\Omega}^{\boldsymbol{rk}} = -(\overleftrightarrow{\Omega}^{\boldsymbol{kr}})^T$. The phase space density of states then reads,

$$D = (2\pi)^{-d} \sqrt{\det(\overleftrightarrow{\boldsymbol{\Omega}} - \overleftrightarrow{\mathbf{J}})} \, . \tag{2.13}$$

with $\overleftrightarrow{\mathbf{J}} = \left(\begin{smallmatrix} 0 & \overleftrightarrow{\mathrm{I}} \\ -\overleftrightarrow{\mathrm{I}} & 0 \end{smallmatrix} \right)$. In the special case of electromagnetic perturbations with $\overleftrightarrow{\Omega}^{\boldsymbol{kk}}_{ab} = \epsilon_{abc}\Omega_c$, $\overleftrightarrow{\Omega}^{\boldsymbol{rr}}_{ab} = -(e/\hbar)\epsilon_{abc}B_c$ and $\overleftrightarrow{\Omega}^{\boldsymbol{kr}} = 0$, it reduces to (2.3). On the other hand, when either $\overleftrightarrow{\Omega}^{\boldsymbol{kk}}$ or $\overleftrightarrow{\Omega}^{\boldsymbol{rr}}$ vanishes, it has a simpler form

$$D = (2\pi)^{-d} \det(\overleftrightarrow{\mathrm{I}} - \overleftrightarrow{\Omega}^{\boldsymbol{rk}}) \, . \tag{2.14}$$

This result has found application in the study of spin-force induced charge-Hall effect [30].

Finally, we show how the density of states emerges naturally in the effective quantum mechanics of Bloch electrons. Although our system is not canonical, it can nevertheless be quantized following a standard procedure developed for non-holonomic systems with second class constraints [31, 32]. First, one redefines the Poisson bracket $\{f, g\}^* = (\partial f/\partial \xi^a) M_{ab} (\partial g/\partial \xi^b)$, where ξ^a are the components of

phase space coordinates $\boldsymbol{\xi} \equiv (\boldsymbol{r},\ \boldsymbol{k})$ and $\overleftrightarrow{\mathbf{M}} = (\overleftrightarrow{\boldsymbol{\Omega}} - \overleftrightarrow{\mathbf{J}})^{-1}$. Our equations of motion (2.1) can then be written as $\dot{\xi}^a = \{\xi^a, \varepsilon\}^*$, where the energy $\varepsilon(\boldsymbol{\xi})$ plays the role as the Hamiltonian function. Then, one promotes the Poisson brackets into quantum commutators:

$$[\hat{\xi}^a, \hat{\xi}^b] = \mathrm{i}M_{ab} \ , \tag{2.15}$$

where $\hat{\xi}^a$ is the quantum operator corresponding to the phase space coordinates. It then follows that a phase space point acquires a minimal uncertainty volume given by [33]

$$\min\Big(\prod_a \Delta\xi^a\Big) = 2^{-d}\Big[\det(\overleftrightarrow{\boldsymbol{\Omega}} - \overleftrightarrow{\mathbf{J}})\Big]^{-1/2} \ . \tag{2.16}$$

This can be understood as the phase space volume occupied by a single quantum state, therefore Eq. (2.13), which is proportional to the reciprocal of this volume, can naturally be regarded as the semiclassical expression for the number of quantum states per unit volume in the phase space.

Equation (2.15) presents the effective quantum mechanics of Bloch electrons. As a demonstration for the validity of the quantization scheme as well as the quantum effect of the phase space density of states, we consider a simple toy model of two dimensional electron system with a constant Berry curvature, subjected to a uniform magnetic field. The commutators read,

$$\begin{aligned} &[\hat{x}, \hat{y}] = \mathrm{i}\frac{\Omega}{1 + (e/\hbar)B\Omega} \ , \quad [\hat{k}_x, \hat{k}_y] = -\mathrm{i}\frac{(e/\hbar)B}{1 + (e/\hbar)B\Omega} \ , \\ &[\hat{x}, \hat{k}_x] = [\hat{y}, \hat{k}_y] = \mathrm{i}\frac{1}{1 + (e/\hbar)B\Omega} \ . \end{aligned} \tag{2.17}$$

In the absence of the Berry curvature, we reduce the problem to a known case with the familiar nontrivial commutator $[\hat{k}_x, \hat{k}_y] = -\mathrm{i}(e/\hbar)B$. In the absence of the B field, we have the nontrivial commutator $[\hat{x}, \hat{y}] = \mathrm{i}\Omega$ discussed extensively in the literature on non-commutative geometry. It is interesting to see that in the presence of both fields, we do not just have a combination of these nontrivial commutators. Instead, we have a nontrivial density of states which enters into all of the commutators.

Assuming $\varepsilon(\boldsymbol{k}) = \hbar^2\boldsymbol{k}^2/2m$, the system can be solved algebraically to yield the energy spectrum and degeneracy. We found that the spectrum consists of a set of Landau levels with the renormalized cyclotron frequency $\omega_c = \omega_c^0/[1 + (e/\hbar)B\Omega]$,

where $\omega_c^0 = eB/m$ is the usual cyclotron frequency [34]. At the same time, it is more important to note that each Landau level still has the same degeneracy eB/h as in the absence of the Berry curvature. It is known that this degeneracy is directly related to the quantized Hall conductance e^2/h for a filled Landau level [3]. Had the density of states not entered in the commutators, the Landau level degeneracy would be modified, violating the topological requirement that the Hall conductance for a filled Landau level is quantized.

Before closing, we note that the phase space density of states also enters naturally in the alternative quantization scheme with Feynman path integral. The S matrix is calculated by [31]

$$\langle \text{out}|S|\text{in}\rangle = \int \prod_t [D(\boldsymbol{\xi}) \mathrm{d}\boldsymbol{\xi}] \exp\Big[\frac{\mathrm{i}}{\hbar}\int L \mathrm{d}t\Big] \,. \tag{2.18}$$

where L is the Lagrangian for our system [7],

$$L = \frac{1}{2}\dot{\xi}^a J_{ab} \xi^b - \varepsilon(\boldsymbol{\xi}) + \dot{\xi}^a \mathcal{A}_a(\boldsymbol{\xi}) \tag{2.19}$$

with $\mathcal{A}_a(\boldsymbol{\xi}) \equiv \mathrm{i}\langle u(\boldsymbol{\xi})|\nabla_\alpha u(\boldsymbol{\xi})\rangle$ being the phase space gauge potentials associated with the Berry curvature field $\overleftrightarrow{\boldsymbol{\Omega}}$.

2.5 Summary

In summary, we have found a Berry phase correction to the phase space density of states for Bloch electrons. This correction emerges naturally in both semiclassical and quantum mechanics of Bloch electrons, and has profound effects on the equilibrium and transport properties. Because of the fundamental change introduced by this correction, it could have important implications on other aspects of condensed matter physics, such as the Fermi liquid theory. For instance, in the presence of a magnetic field, interaction between electrons can change the Fermi sea volume by modifying the Berry curvature and thus the phase space density of states.

[3] The Hall conductance is given by $\sigma = ne/B$, where n is the electron density. The quantized value is obtained if we substitute the degeneracy density for n.

Chapter 3

Orbital magnetization of Bloch electrons

3.1 Introduction

In solids, magnetism is either due to the orbital currents of the electrons, or to their spins. While the latter has enjoyed a continuous and growing research attention over decades, orbital magnetism remains a somewhat poorly understood subject. Recently, this problem has attracted much attention [27, 35, 28].

In this chapter, we first generalize the zero-temperature formula for orbital magnetization to finite temperatures. By studying a finite system, it is shown that the magnetization consists of a orbital moment contribution and a free current contribution. A thermodynamic derivation of the Hall effect and Nernst effect is given based on the Streda formula. In the end, possible extension to the quantum Hall insulators is discussed.

Our theory of orbital magnetization is built on recent development [6, 7, 35] of the semiclassical dynamics of Bloch electrons that has been successfully applied to the anomalous Hall effect (AHE) [10, 11, 12] and spin transport [19, 26] in magnetic materials and nanostructures. In the semiclassical approach, each electron in a given band is described by a wave packet $|W(\boldsymbol{r},\boldsymbol{k})\rangle$ centered at $(\boldsymbol{r},\boldsymbol{k})$ in the phase space. It has been found [6, 7] that in addition to the spin magnetic moment, the wave packet also carries an *intrinsic* orbital magnetic moment $\boldsymbol{m}(\boldsymbol{k})$ that is proportional to the expectation value of the angular momentum operator, i.e.,

$\boldsymbol{m}(\boldsymbol{k}) = -(e/2m_e)\langle W|(\hat{\boldsymbol{r}} - \boldsymbol{r}) \times \hat{\boldsymbol{p}}|W\rangle$, where $-e$ and m_e is the electron charge and mass, respectively. Interestingly, this magnetic moment $\boldsymbol{m}(\boldsymbol{k})$ is insensitive to the precise shape and size of the wave packet or any external perturbation. Another relevant and intriguing aspect of the Bloch electron dynamics is the non-commutativity of the position and momentum operators due to the Berry phase effect, which leads to a field-dependent density of states in the phase space [35]. Accordingly, the usual conversion of a quantum-state summation to a $\boldsymbol{k}$-space integral in the semiclassical limit becomes

$$\sum_{\boldsymbol{k}} \to \int [d\boldsymbol{k}](1 + \frac{e}{\hbar}\boldsymbol{B} \cdot \boldsymbol{\Omega}) \ , \tag{3.1}$$

where $[d\boldsymbol{k}]$ is a shorthand for $d\boldsymbol{k}/(2\pi)^d$, $\boldsymbol{B}(\boldsymbol{r})$ is the magnetic field, and $\boldsymbol{\Omega}(\boldsymbol{k})$ is the Berry curvature of the Bloch states. The explicit expressions for $\boldsymbol{\Omega}(\boldsymbol{k})$ and $\boldsymbol{m}(\boldsymbol{k})$ will be given later.

3.2 General Formula

Armed with the semiclassical theory for Bloch electron dynamics, we now derive the orbital magnetization at finite temperatures. For a system with a fixed chemical potential, the magnetization is most easily obtained by $\boldsymbol{M} = -(\partial G/\partial \boldsymbol{B})_{\mu,T}$, where $G(\mu, T, \boldsymbol{B})$ is the grand canonical potential. Neglecting the Zeeman spin energy, we have [1]

$$\begin{aligned} G &= -\frac{1}{\beta}\sum_{\boldsymbol{k}} \log(1 + e^{-\beta(\varepsilon_M - \mu)}) \\ &= -\frac{1}{\beta}\int [d\boldsymbol{k}](1 + \frac{e}{\hbar}\boldsymbol{B} \cdot \boldsymbol{\Omega}) \log(1 + e^{-\beta(\varepsilon_M - \mu)}) \ , \end{aligned} \tag{3.2}$$

where the electron energy $\varepsilon_M = \varepsilon(\boldsymbol{k}) - \boldsymbol{m}(\boldsymbol{k}) \cdot \boldsymbol{B}$ includes a correction due to the orbital magnetic moment $\boldsymbol{m}(\boldsymbol{k})$. The conversion rule (3.1) with the Berry-phase modified density of states is used to obtain the second line. It then follows that at zero magnetic field,

$$\boldsymbol{M} = \int [d\boldsymbol{k}] f \boldsymbol{m} + \frac{1}{\beta}\int [d\boldsymbol{k}] \frac{e}{\hbar}\boldsymbol{\Omega} \log(1 + e^{-\beta(\varepsilon - \mu)}) \ , \tag{3.3}$$

[1] Here we assume the magnetic field is sufficiently weak so that the crystal momentum $\boldsymbol{k}$ is still a good quantum number.

where $f(\boldsymbol{k})$ is the Fermi-Dirac distribution function. Since our derivation is carried out for a system without boundaries, the orbital magnetization appears to be a bulk property.

The first term in Eq. (3.3) is the expected contribution from the orbital magnetic moment $\boldsymbol{m}(\boldsymbol{k})$ of each wave packet. In fact, the contribution of the spin magnetic moment can easily be incorprated by including the Zeeman energy term $-g(e/m_e)\boldsymbol{S}\cdot\boldsymbol{B}$ in the grand canonical potential (3.2), where g is the Landé factor and $\boldsymbol{S}$ is the spin. Then each wave packet will contribute a total magnetic moment of $\tilde{\boldsymbol{m}}(\boldsymbol{k}) = \boldsymbol{m}(\boldsymbol{k}) + g(e/m)\boldsymbol{S}$ to the magnetization. Since the orbital moment responds to the magnetic field in the exact way as the spin moment does, the former is indistinguishable from the latter in a measurement of the magnetization [2]. This also implies a $\boldsymbol{k}$-dependent g factor.

3.3 Boudary Current Contribution

Now we turn to the second term in Eq. (3.3) with an odd-looking logarithm function as the statistical weighing factor. It comes from the explicit field-dependence of the density of states, and can be regarded as the boundary current contribution due to the AHE. To see this, we consider a finite system of electrons in a two-dimensional lattice with a confining potential $V(\boldsymbol{r})$. We further assume that the potential $V(\boldsymbol{r})$ varies slowly at atomic length scale so that the wave packet description of the electron is still valid. In the bulk where $V(\boldsymbol{r})$ vanishes identically, the electron energy is just the bulk band-energy; near the boundary, it will be tilted up due to the increase of $V(\boldsymbol{r})$. Thus to a good approximation, we can write the electron energy as

$$\tilde{\varepsilon}(\boldsymbol{r},\boldsymbol{k}) = \varepsilon(\boldsymbol{k}) + V(\boldsymbol{r})\ . \tag{3.4}$$

The energy spectrum in real space is sketched in Fig. 3.1. For a wave packet near the boundary, it will feel a force $\boldsymbol{\nabla}V(\boldsymbol{r})$ due to the presence of the confining potential. Consequently, the electron acquires an anomalous velocity $(1/\hbar)\boldsymbol{\nabla}V\times\boldsymbol{\Omega}$ [6, 7] whose

[2] Here our starting point is the Pauli equation, where the spin is regarded as an intrinsic property of the electron. In fact, if one constructs a wave packet using the positive energy eigenstates of the Dirac equation, it will possess an orbital magnetic moment whose magnitude is exactly the Bohr magneton. Therefore in the Dirac description, the electron spin actually comes from the *spinning* of the wave packet, which restores the literal meaning of "spin". Details are presented in C.-P. Chuu, M.-C. Chang, and Q. Niu (to be published).

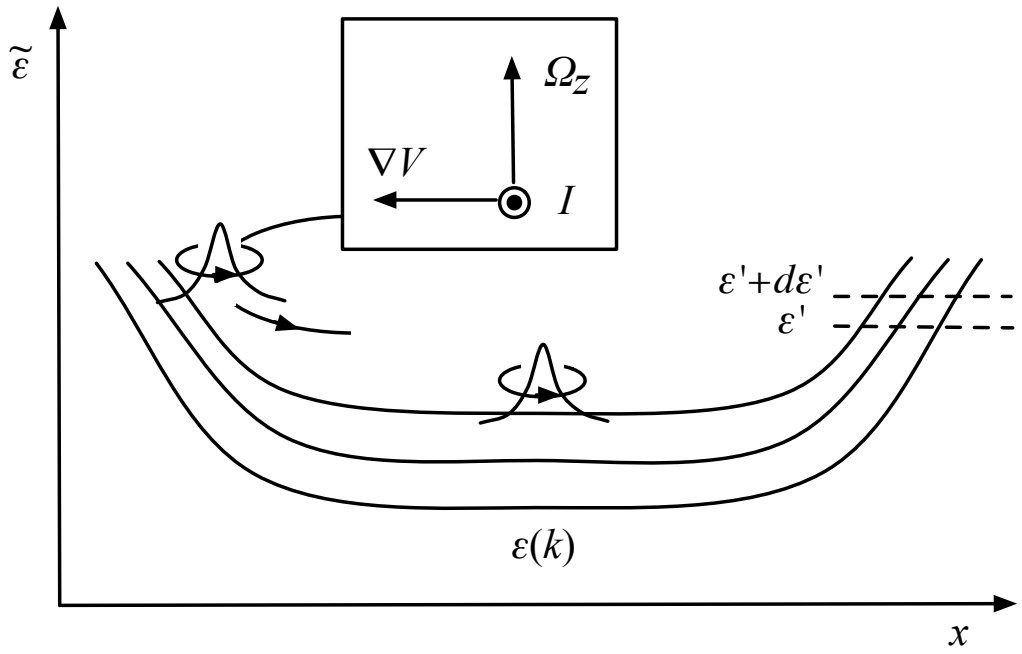

Figure 3.1: Electron energy $\tilde{\varepsilon}$ in a slowly varying confining potential $V(\boldsymbol{r})$. In addition to the self-rotation, wave packets near the boundary will also move along the boundary due to the potential V. Level spacings between different bulk $\boldsymbol{k}$-states are exaggerated; they are continuous in the semiclassical limit. The insert shows directions of the Berry curvature, the effective force, and the current carried by a wave packet on the left boundary. Electron charge is $-e$ ($e < 0$).

direction is parallel with the boundary. Because electrons on opposite boundaries have opposite velocities, they form a macroscopic circuit. The corresponding current (of the dimension "current density × width" in 2D) is

$$\begin{aligned} I = & \int d\varepsilon' \, f(\varepsilon') \int [d\boldsymbol{k}] \Theta(\varepsilon' - \varepsilon(\boldsymbol{k})) \\ & \times \int dx \, \frac{dV}{dx} \frac{e}{\hbar} \Omega_z(\boldsymbol{k}) \delta(\tilde{\varepsilon}(\boldsymbol{r}, \boldsymbol{k}) - \varepsilon') \; . \end{aligned} \tag{3.5}$$

The first integral $\int d\varepsilon' \, f(\varepsilon')$ is the usual statistical average with the distribution function; the second integral $\int [d\boldsymbol{k}] \Theta(\varepsilon' - \varepsilon(\boldsymbol{k}))$ means that only states below energy ε' contribute to the current I at energy ε'; and the third integral $\int dx \, \delta(\tilde{\varepsilon}(\boldsymbol{r}, \boldsymbol{k}) - \varepsilon')$ places the requirement that the electron energy at the point x has to fall into the interval $[\varepsilon', \varepsilon' + d\varepsilon']$ (Fig. 3.1). The integral over dx is confined to the space where $V(\boldsymbol{r})$ varies appreciately. Now recall that if there is a current I flows in a closed circuit with a sufficiently small area A, then the magnetic moment is given by $I \cdot A$. Therefore the magnetization (magnetic moment per unit area) has the magnitude of the current I. Since this boundary current corresponds to the macroscopic orbital motion of the wave packet center that is free to drift around, we call this contribution the "free current" contribution. Integrating Eq. (3.5) we obtain

$$M_c = \frac{1}{e} \int d\varepsilon \, f(\varepsilon) \sigma_z^{\mathrm{AH}}(\varepsilon) \; , \tag{3.6}$$

where $\sigma_z^{AH}(\varepsilon)$ is

$$\sigma_z^{\mathrm{AH}}(\varepsilon) = \frac{e^2}{\hbar} \int [d\boldsymbol{k}] \Theta(\varepsilon - \varepsilon(\boldsymbol{k})) \Omega_z(\boldsymbol{k}) \; . \tag{3.7}$$

This is the zero-temperature formula (with Fermi energy ε') for the intrinsic anomalous Hall conductivity that has been extensively studied recently [10, 11, 12]. In fact, integrating the second integral of Eq. (3.3) by parts, we can eliminate the logarithm function and obtain the same expression of M_c due to the boundary current. The total magnetization thus is

$$M_z = \int [d\boldsymbol{k}] f(\boldsymbol{k}) m_z(\boldsymbol{k}) + \frac{1}{e} \int d\varepsilon \, f(\varepsilon) \sigma_z^{\mathrm{AH}}(\varepsilon) \; . \tag{3.8}$$

3.4 Thermodynamic Derivation of the Hall and Nernst Coefficient

This situation vividly resembles the equivalence between the bulk picture [14] and the edge picture [36] in the quantum Hall effect (QHE). The fact that M_c can be understood either as a bulk contribution or a boundary contribution shows that it is truly a topological property of the system. However, one should not confuse our boundary current with the edge current discussed by Halperin in the QHE (therefore in the paragraph the words "boundary" and "edge" mean different quantities). Their difference is best viewed by considering an insulator with nonzero Berry curvature but with a zero Chern number, as discussed by Thonhauser *et al.* [28]. The edge current is due to the edge states existing in the energy gap above the Fermi energy. The quantum Hall conductance of such a system is zero [14], meaning there is no net edge current (we do not rule out the possibility of non-chiral edge states). On the other hand, it does not prevent the existence of a boundary current below the Fermi energy discussed above. Numerical analysis of the motion of Wannier functions near the boundary also verifies this observation [28]. Actually, if the time-reversal symmetry is present, $\varepsilon(\boldsymbol{k}) = \varepsilon(-\boldsymbol{k})$, $\boldsymbol{\Omega}(\boldsymbol{k}) = -\boldsymbol{\Omega}(-\boldsymbol{k})$, and $\boldsymbol{m}(\boldsymbol{k}) = -\boldsymbol{m}(-\boldsymbol{k})$; both the moment and current contributions vanish. In fact, time-reversal symmetry prohibits the existence of a nonzero magnetization. If the time-reversal symmetry is broken, M_c in general is nonzero, leading to the appearance of a boundary current.

In the quantum Hall effect, the relation between the Hall current and the magnetization is given in the elegant Středa formula [24], i.e., $\sigma_{xy} = -e(\partial n/\partial B)_{\mu,T} = -e(\partial M/\partial \mu)_{B,T}$ (the last step is by the Maxwell relation). However, if we apply this equation directly to the AHE, it does not lead to the well-studied anomalous Hall conductivity. A direct calculation shows that the total magnetization M in the Středa formula should be replaced by only the free current contribution $M_{\rm c}$, i.e.,

$$\sigma_{xy} = -e\Big(\frac{\partial M_c}{\partial \mu}\Big)_{T,B} = -\int d\varepsilon\, \frac{\partial f}{\partial \mu}\sigma_z^{\rm AH}(\varepsilon)\ . \tag{3.9}$$

This is consistent with our understanding that $M_{\rm m}$ comes from the localized motion around the electron center thus does not appear in a transport measurement. Based on this understanding, we postulate that the off-diagonal Peltier coefficient should

be given by [37]

$$\alpha_{xy} = T\Big(\frac{\partial M_c}{\partial T}\Big)_{T,B} = \int d\varepsilon \, \frac{\partial f}{\partial \mu}(\varepsilon - \mu)\sigma_z^{\mathrm{AH}}(\varepsilon) \; , \tag{3.10}$$

where $j_x^Q = \alpha_{xy} E_y$ with j_x^Q the heat current. This coefficient α_{xy} can be measured in the Nernst experiment [38].

The above result (3.10) can be justified by a simple thermodynamic argument. In two dimension, a changing magnetic field induces an electric field around some area; the change of the entropy density S inside this area then corresponds to the heat current flow. We immediately have $\alpha_{xy} = T(\partial S/\partial t)/(\partial B/\partial t)$. Neglecting the electron interaction and assuming the system is at the clean limit, we can take the adiabatic limit and obtain $\alpha_{xy} = T(\partial S/\partial B)_{\mu,T}$. Note that the electron spin is neglected because the Zeeman energy will change the chemical potential. However, based on our understanding of the magnetization, the intrinsic orbital moment also couples to the magnetic field directly, therefore has to be neglected as well. Write the grand canonical potential as

$$dG = -SdT - nd\mu - M_c dB_o - M_m dB_z \; , \tag{3.11}$$

where B_o is the part that enters into the Hamiltonian through mechanical moment $\boldsymbol{p} + (e/\hbar)\boldsymbol{A}$ and only affect the orbital motion of the electron, and B_z couples to the magnetic moment directly through some Zeeman-like energy term; M_m is the electron moment contribution. The thermodynamic process described above actually corresponds to changing B_o while fixing B_z. Therefore $\alpha_{xy} = T(\partial M_c/\partial T)_{T,B_o}$.

Now we write down the explicit expression for the Berry curvature $\boldsymbol{\Omega}(\boldsymbol{k})$ and the magnetic moment $\boldsymbol{m}(\boldsymbol{k})$. Both of them are properties of the band structure of the crystal. They are evaluated directly using the single-electron Bloch states:

$$\boldsymbol{\Omega}(\boldsymbol{k}) = i\langle \boldsymbol{\nabla}_{\boldsymbol{k}} u| \times |\boldsymbol{\nabla}_{\boldsymbol{k}} u\rangle \; , \tag{3.12}$$

$$\boldsymbol{m}(\boldsymbol{k}) = -i(e/2\hbar)\langle \boldsymbol{\nabla}_{\boldsymbol{k}} u| \times [\hat{H}(\boldsymbol{k}) - \varepsilon(\boldsymbol{k})]|\boldsymbol{\nabla}_{\boldsymbol{k}} u\rangle \; , \tag{3.13}$$

where $|u(\boldsymbol{k})\rangle$ is the periodic part of the Bloch function, and $\hat{H}(\boldsymbol{k})$ and $\varepsilon(\boldsymbol{k})$ are the unperturbed Hamiltonian and band energy, respectively. They are nonzero in the presence of broken time-reversal or spatial-inversion symmetry. These $\boldsymbol{k}$-

space expressions (3.12) and (3.13) can be readily implemented in first-principles calculations.

So far we have discussed the orbital magnetization in the context of the anomalous Hall effect. Our result can also be applied to electrons in a periodic lattice with a quantizing magnetic field where the wave packet is constructed by magnetic Bloch functions [6]. Similar results have been obtained in a recent paper by Středa [39].

Chapter 4

Berry Phase Effect in Anomalous Thermoelectric Transport

4.1 Introduction

The phenomena of transport fall into two categories: those due to a mechanical force, such as the electric field on charges, and those driven by a statistical force, such as the gradient of temperature or chemical potential. The mechanical force exists on the microscopic level and can be described by a perturbation to the Hamiltonian for the carriers, while the statistical force manifests on the macroscopic level and makes sense only through the statistical distribution of the carriers. It has been established [6, 7] that the Berry phase of Bloch states has a profound effect on transport driven by a mechanical force. This is through the mechanism that the group velocity of a Bloch electron acquires an anomalous term proportional to the mechanical force, i.e.,

$$\dot{\boldsymbol{r}} = \frac{1}{\hbar}\frac{\partial \varepsilon_n(\boldsymbol{k})}{\partial \boldsymbol{k}} + \frac{e}{\hbar}\boldsymbol{E} \times \boldsymbol{\Omega}_n(\boldsymbol{k}) \,, \tag{4.1}$$

where $\varepsilon_n(\boldsymbol{k})$ is the band energy, $-e\boldsymbol{E}$ is the mechanical force due to the external electric field, and $\boldsymbol{\Omega}_n(\boldsymbol{k})$ is the Berry curvature, the Berry phase per unit area in

This chapter is adapted from D. Xiao, Y. Yao, F. Zhong, and Q. Niu, Phys. Rev. Lett. **97**, 026603 (2006). Copyright © American Physical Society.

$\boldsymbol{k}$-space. Evaluation of the Hall current from the anomalous term reproduces the Karplus-Luttinger formula [40] for the anomalous Hall conductivity. Calculations based on the Berry phase effect have found much success in explaining anomalous Hall effects (AHE) in ferromagnets of semiconductors [10], oxides [11] and transition metals [12]. Recent experiments [41, 42] give further convincing evidence in support of this theory.

A natural question is whether and how the Berry phase also manifests itself in transport driven by a statistical force. On the one hand, the anomalous velocity vanishes in the absence of a mechanical force, eliminating the obvious cause for a Berry phase effect in this case. On the other hand, this conclusion would introduce a number of basic contradictions to the standard transport theory. First, a chemical potential gradient would be distinct from the electrical force, violating the basis for the Einstein relation for transport. Second, a temperature gradient would not induce an intrinsic charge Hall current, violating the Mott relation [see Eq. (4.10) below] between the AHE and the anomalous Nernst effect (ANE), where a transverse current is produced by a temperature gradient in ferromagnets. Third, as will be made clear below, it would be impossible to establish the Onsager relation between cross transport coefficients connecting thermoelectric Hall currents and forces. In addition, a recent experiment on the ANE in the spinel ferromagnet $CuCr_2Se_{4-x}Br_x$ [38] found weak dependence on scattering, suggesting that there should indeed be a Berry-phase induced intrinsic mechanism.

In this chapter, we solve the puzzle by showing how the Berry phase effect manifests itself in thermoelectric transport driven by a statistical force. It turns out that the local current of carriers acquires an extra term from the carrier magnetic moment in the presence of a non-uniform distribution which arises from the gradient of temperature or chemical potential. However, the complete theory also relies on a proper deduction of magnetization current [43], and requires a deeper understanding of the orbital magnetization. It was found that there is a Berry-phase correction to the magnetization [35, 28], and here we generalize it to the case of finite temperatures which is needed for thermoelectric transport. This Berry phase correction eventually enters into the transport current produced by the statistical force, playing the counterpart as the anomalous velocity term due to a mechanical force.

We have thus found perfect harmony between statistical and mechanical

forces even in the presence of Berry phase effect. The basic transport relations of Einstein, Mott, and Onsager continue to hold, which gives strong support for the validity of our theory. Finally, we also provide a reality check on the Berry phase effect in the ANE by calculating the intrinsic anomalous Nernst conductivity α_{xy} [1] for $CuCr_2Se_{4-x}Br_x$ using first-principles method. The obtained doping dependence curve agrees well with available experimental data [38]. Our calculation also predicts a peak-valley structure between the data points, at a place where the anomalous Hall conductivity has a sudden sign and magnitude change.

4.2 Local and transport currents.

In the conventional Boltzmann transport theory, one considers a statistical distribution $g(\boldsymbol{r}, \boldsymbol{k})$ of carriers in the phase space of position and crystal momentum. The distribution function satisfies the Boltzmann equation with a collision integral whose form depends on the details of the collision process. The current density is given by $\boldsymbol{J} = -e \int [d\boldsymbol{k}]\, g(\boldsymbol{r}, \boldsymbol{k}) \dot{\boldsymbol{r}}$, where $\int [d\boldsymbol{k}]$ is a shorthand for $\int d\boldsymbol{k}/(2\pi)^3$, and a summation over band index has been omitted for simple notation. In the absence of a mechanical force, the electron velocity is simply $\dot{\boldsymbol{r}} = \partial\varepsilon(\boldsymbol{k})/\hbar\partial\boldsymbol{k}$. It is then apparent that the anomalous velocity term due to the Berry phase drops out of the expression for the current.

However, the above picture is naïve in that the carrier is treated as a structureless point particle. The quantum representation of the carrier is in fact a wave packet, which has a finite spread in the phase space. The wave packet generally rotates about its center position, as illustrated in Fig. 4.1, giving rise to an orbital magnetic moment $\boldsymbol{m}(\boldsymbol{k}) = -(e/2)\langle W|(\hat{\boldsymbol{r}} - \boldsymbol{r}_c) \times \hat{\boldsymbol{v}}|W\rangle$, where $|W\rangle$ is the wave packet and $\hat{\boldsymbol{v}}$ is the velocity operator [6, 7]. A careful coarse graining analysis [26] (see also Appendix B) shows that the correct expression for the *local* current has an extra term:

$$\boldsymbol{J} = -e \int [d\boldsymbol{k}]\, g(\boldsymbol{r}, \boldsymbol{k}) \dot{\boldsymbol{r}} + \boldsymbol{\nabla} \times \int [d\boldsymbol{k}]\, f(\boldsymbol{r}, \boldsymbol{k}) \boldsymbol{m}(\boldsymbol{k}) \,, \tag{4.2}$$

where the magnetic moment enters explicitly. In the extra term we have replaced

[1] In the presence of both an electric field and a temperature gradient, the transverse current is given by $j_x = \sigma_{xy} E_y + \alpha_{xy}(-\nabla_y T)$. It is thus natural to call α_{xy} the Nernst conductivity as σ_{xy} is conventionally called the Hall conductivity. Note however in Ref. [38] α_{xy} was called the Peltier term.

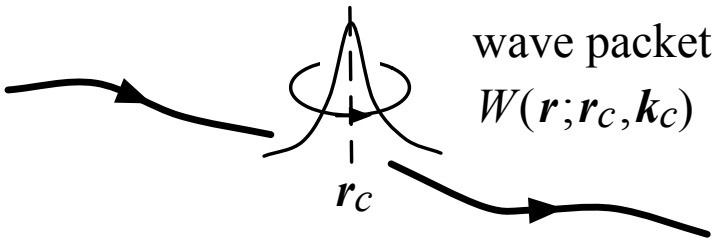

Figure 4.1: The wave packet description of a charge carrier whose center is $(\boldsymbol{r}_c, \boldsymbol{k}_c)$. A wave packet generally possesses two kinds of motion: the center of mass motion and the self-rotation around its center. Both of them contribute to the local current density as given in Eq. (4.2).

$g(\boldsymbol{r}, \boldsymbol{k})$ with the local equilibrium Fermi-Dirac distribution $f(\boldsymbol{r}, \boldsymbol{k})$ for a linear-order calculation. When the temperature or chemical potential varies in space, the extra term will be proportional to the gradient of these thermodynamic quantities and is therefore non-negligible.

For transport studies, it is important to discount the contribution from the magnetization current, a point which has attracted much discussion in the past. It was argued that the magnetization current cannot be measured by conventional transport experiments (For the most recent comprehensive work, see Ref. [43]). Therefore, one introduces the concept of *transport* current, defined by

$$\boldsymbol{j} = \boldsymbol{J} - \boldsymbol{\nabla} \times \boldsymbol{M}(\boldsymbol{r}) \,, \tag{4.3}$$

where $\boldsymbol{M}(\boldsymbol{r})$ is the magnetization density. This is entirely analogous to the classic distinction between microscopic current and free current [44].

It is also important to realize that the magnetization density is not simply a statistical sum of the carrier magnetic moments. It has been shown recently that there is a Berry phase correction to the magnetization [35, 28]. The contribution from the carrier magnetic moments to the local current will be subtracted out in the transport current, but the Berry phase correction to the magnetization will give rise to an extra term in the transport current. Earlier work concentrate on the zero temperature magnetization, and we provide an extension to the finite temperature case below. Using Eq. (4.6) for the magnetization, we find that the transport current

is given by

$$\boldsymbol{j} = -e\int [d\boldsymbol{k}] g(\boldsymbol{r},\boldsymbol{k})\dot{\boldsymbol{r}} - \boldsymbol{\nabla}\times\frac{1}{\beta}\int [d\boldsymbol{k}]\frac{e}{\hbar}\boldsymbol{\Omega}(\boldsymbol{k})\log(1+e^{-\beta(\varepsilon-\mu)})\,, \tag{4.4}$$

where $\beta = 1/k_B T$, and the Berry curvature is defined by $\boldsymbol{\Omega}(\boldsymbol{k}) = \boldsymbol{\nabla}_{\boldsymbol{k}}\times\langle u|i\boldsymbol{\nabla}_{\boldsymbol{k}}|u\rangle$ with $|u\rangle$ being the periodic amplitude of the Bloch wave.

The above expression gives a complete account of the transport current in ferromagnets, and for crystals with nonzero Berry curvatures in general. The first term is the usual expression for the charge current, which vanishes at local equilibrium (assuming the absence of a mechanical force), i.e., $g(\boldsymbol{r},\boldsymbol{k}) = f(\boldsymbol{r},\boldsymbol{k})$. Nonequilibrium correction to first order in the gradient of temperature or chemical potential yields a result strongly depending on the relaxation process, and a transverse current can result from skew scattering due to spin-orbit coupling [45]. The second term is new, which results from the Berry phase correction to the magnetization. It is also first order in the statistical force, but is independent of the relaxation time, and is therefore an intrinsic property of the system.

4.3 Orbital magnetization at finite temperatures

The orbital magnetization of Bloch electrons has been an outstanding problem in solid state physics. Recently, different approaches [35, 28] have been used to derive a formula at zero temperature, where Berry phase is found to play an important role. In order to study thermoelectric transport, we need to generalize it to finite temperatures. Our derivation is made easy by using the field-dependent density of states introduced in Ref. [35], where it was shown that in the weak-field limit, a quantum-state summation $\sum_{\boldsymbol{k}}\mathcal{O}(\boldsymbol{k})$ of some physical quantity $\mathcal{O}(\boldsymbol{k})$ should be converted to a $\boldsymbol{k}$-space integral according to $\int[d\boldsymbol{k}](1+e\boldsymbol{B}\cdot\boldsymbol{\Omega}/\hbar)\mathcal{O}(\boldsymbol{k})$.

The equilibrium magnetization density can be obtained from the grand canonical potential, which, within first order in the magnetic field, may be written as

$$\begin{aligned} F &= -\frac{1}{\beta}\sum_{\boldsymbol{k}}\log(1+e^{-\beta(\varepsilon_M-\mu)}) \\ &= -\frac{1}{\beta}\int[d\boldsymbol{k}](1+\frac{e}{\hbar}\boldsymbol{B}\cdot\boldsymbol{\Omega})\log(1+e^{-\beta(\varepsilon_M-\mu)})\,, \end{aligned} \tag{4.5}$$

where the electron energy $\varepsilon_M = \varepsilon(\boldsymbol{k}) - \boldsymbol{m}(\boldsymbol{k}) \cdot \boldsymbol{B}$ includes a correction due to the orbital magnetic moment $\boldsymbol{m}(\boldsymbol{k})$. The magnetization is then the field derivative at fixed temperature and chemical potential, $\boldsymbol{M} = -(\partial F/\partial \boldsymbol{B})_{\mu,T}$, with the result

$$\boldsymbol{M}(\boldsymbol{r}) = \int [d\boldsymbol{k}]\, f(\boldsymbol{r},\boldsymbol{k})\boldsymbol{m}(\boldsymbol{k}) + \frac{1}{\beta}\int [d\boldsymbol{k}]\, \frac{e}{\hbar}\boldsymbol{\Omega}(\boldsymbol{k}) \log(1 + e^{-\beta(\varepsilon-\mu)}) \; . \tag{4.6}$$

For generality, we have included a position dependence to cover the situation of local equilibrium with a position dependent temperature and chemical potential.

We have thus derived a general expression for the equilibrium orbital magnetization density, valid at zero magnetic field but at arbitrary temperatures. The first term is just a statistical sum of the orbital magnetic moments of the carriers originating from self-rotation of the carrier wavepackets. It has been derived in Ref. [6, 7] with the expression $\boldsymbol{m}(\boldsymbol{k}) = -i(e/2\hbar)\langle \boldsymbol{\nabla}_{\boldsymbol{k}} u| \times [\hat{H}(\boldsymbol{k}) - \varepsilon(\boldsymbol{k})]|\boldsymbol{\nabla}_{\boldsymbol{k}} u\rangle$, where $\hat{H}(\boldsymbol{k})$ is the crystal Hamiltonian acting on $|u\rangle$. It has the same symmetry properties as the Berry curvature. The second term of Eq. (4.6) is the Berry phase correction to the orbital magnetization. It is of topological nature, arising from a bulk consideration on the one hand as in the above derivation, and being connected to a boundary current circulation on the other. Interestingly, it is this second term that eventually enters the transport current.

4.4 Anomalous thermoelectric transport.

With the aid of Eq. (4.4) it is straightforward to calculate various thermoelectric response to statistical forces. For example, a chemical potential gradient will produce, through the second term, a Hall current given by $-\boldsymbol{\nabla}\mu \times (e/\hbar)\int [d\boldsymbol{k}] f(\boldsymbol{k})\boldsymbol{\Omega}(\boldsymbol{k})$. This is the same as the Berry-phase induced anomalous Hall current in response to an electric field if one substitutes $\boldsymbol{\nabla}\mu/e$ for the field. It is gratifying to see that the Einstein relation continues to hold in the presence of the Berry phase effect.

In the presence of a temperature gradient, an intrinsic Hall current also results from the second term of Eq. (4.4),

$$\boldsymbol{j}_{\rm in} = -\frac{\boldsymbol{\nabla} T}{T} \times \frac{e}{\hbar}\int [d\boldsymbol{k}]\boldsymbol{\Omega}[(\varepsilon - \mu)f + k_B T \log(1 + e^{-\beta(\varepsilon-\mu)})] \; . \tag{4.7}$$

One can then extract an anomalous Nernst conductivity α_{xy} defined by $j_x =$

$\alpha_{xy}(-\nabla_y T)$. On a different route, we can also obtain the same result by invoking a fictitious gravitational field [46], establishing the Einstein relation between this mechanical force and the temperature gradient.

Interestingly, by integration by parts, α_{xy} can be written into the following more suggestive form

$$\alpha_{xy} = -\frac{1}{e}\int d\varepsilon\, \frac{\partial f}{\partial \mu}\sigma_{xy}(\varepsilon)\frac{\varepsilon-\mu}{T}\ , \tag{4.8}$$

where $\sigma_{xy}(\varepsilon)$ is the intrinsic anomalous Hall conductivity at zero temperature with Fermi energy ε, given by

$$\sigma_{xy}(\varepsilon) = -\frac{e^2}{\hbar}\int [d\boldsymbol{k}]\,\Theta(\varepsilon-\varepsilon_{\boldsymbol{k}})\Omega_z(\boldsymbol{k})\ . \tag{4.9}$$

At low temperatures, the above relation reduces to

$$\alpha_{xy} = \frac{\pi^2}{3}\frac{k_B^2 T}{e}\sigma'_{xy}(\varepsilon_F)\ . \tag{4.10}$$

Such relations between the electrical and thermoelectric conductivities are known as Mott relations. They were proved for non-magnetic materials without or with a magnetic field [47, 48]. Our result extends the validity of this relation to ferromagnets and other systems with a Berry curvature, and justifies the usage of Eq. (4.10) in Ref. [38].

The reciprocal of the ANE is the generation of a transverse heat current by an electric field. The Onsager relation dictates that the Berry phase should also affect the latter. To show this explicitly, we consider the energy current carried by a wave packet $\langle W|(\hat{H}\hat{\dot{\boldsymbol{r}}}+\hat{\dot{\boldsymbol{r}}}\hat{H})/2|W\rangle = \varepsilon\dot{\boldsymbol{r}} - \boldsymbol{E}\times\boldsymbol{m}(\boldsymbol{k})$, where the second term is from the field correction to the local Hamiltonian. Assuming a uniform temperature and chemical potential [2], we obtain the *local* energy current to first order in the electric field:

$$\boldsymbol{J}^E = \int [d\boldsymbol{k}]\, g(\boldsymbol{k})\varepsilon\dot{\boldsymbol{r}} - \boldsymbol{E}\times\int [d\boldsymbol{k}]\, f(\boldsymbol{k})\boldsymbol{m}(\boldsymbol{k})\ , \tag{4.11}$$

where the electron velocity $\dot{\boldsymbol{r}}$ is given by Eq. (4.1). However, the energy current

[2] It corresponds to the so-called "rapid case" in Ref. [46] where the perturbation is periodic in time with a frequency that is large compared to the hydrodynamic relaxation rates set by the system size but small compared to the microscopic relaxation time.

also has a magnetization part from an "energy" magnetization [43]. In the present case, it is given by $-\boldsymbol{E}\times\boldsymbol{M}$, which is nothing but the material-dependent part of the Poynting vector $\boldsymbol{E}\times\boldsymbol{H}$ describing the energy flow (with $\boldsymbol{H}=\boldsymbol{B}/\mu_0-\boldsymbol{M}$) [44]. Since this energy flow exists in an equilibrium state, it does not correspond to a transport current thus must be subtracted from $\boldsymbol{J}^E$ to yield the *transport* energy current $\boldsymbol{j}^E=\boldsymbol{J}^E+\boldsymbol{E}\times\boldsymbol{M}$. Based on our expression (4.6) for the magnetization density, we finally find the Berry phase correction to the heat current (defined by $\boldsymbol{j}^Q\equiv\boldsymbol{j}^E-\mu\boldsymbol{j}$):

$$\boldsymbol{j}^Q_{\rm in}=\boldsymbol{E}\times\frac{e}{\hbar}\int[d\boldsymbol{k}]\boldsymbol{\Omega}[(\varepsilon-\mu)f+k_BT\log(1+e^{-\beta(\varepsilon-\mu)})]\,, \tag{4.12}$$

while the usual expression for the heat current is $\int[d\boldsymbol{k}]\,g(\boldsymbol{k})(\varepsilon-\mu)\boldsymbol{v}$, where $\boldsymbol{v}$ is the usual group velocity determined by the band energy. In this case, the Berry phase correction comes from both the anomalous velocity and the orbital magnetization. Comparison with Eq. (4.7) shows that the Onsager relation is indeed satisfied, providing a strong evidence for the validity of our theory.

4.5 Comparison with experiment.

The intrinsic anomalous Nernst conductivity α_{xy} only depends on the band structure and Berry curvature, so it can be evaluated for crystals based on first principles methods. Here we report our result for $CuCr_2Se_{4-x}Br_x$ and compare with the experiment [38]. The band structure and Berry curvature are calculated following the procedures in Ref. [12], using the generalized gradient approximation for the exchange-correlation potential. Such calculations are very extensive, and, to reduce the work load, we assume that doping affects the Fermi energy but not the band structure, which is justified for the present compounds [49].

The calculated α_{xy} is plotted in Fig. 4.2 as a function of doping x together with the experimental data from Ref. [38]. The comparison is *quantitatively* good, except for the data point at $x=0.25$. This is however a rather special point, because it was reported [38] that, for unknown reasons, α_{xy} is not really proportional to T for $x=0.25$. At low temperatures, a proportional relation is expected from the Mott relation, which is followed strictly by all the data points at other doping densities.

We also note that while our theory predicts a pronounced peak-valley struc-

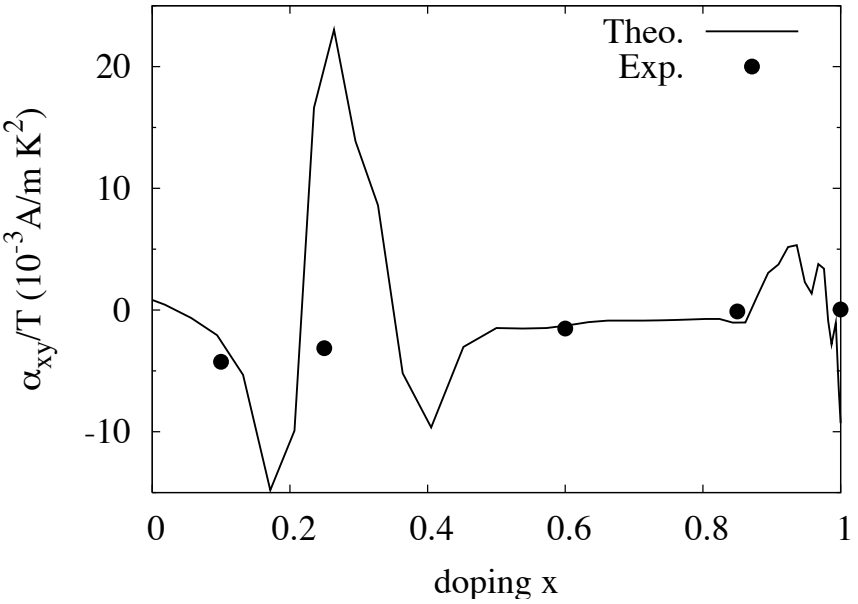

Figure 4.2: The intrinsic anomalous Nernst conductivity α_{xy} (divide by the temperature T) of $CuCr_2Se_{4-x}Br_x$ as a function of the Br content x. The calculated curve is compared with experimental results • extracted from Ref. [38].

ture around $x = 0.3$, the available experimental data at present is too sparse to confirm or disprove it. The oscillatory behavior results from the complicated band structure of this material, and occurs when the Fermi energy (which depends on doping) goes through a region of spin-orbit induced energy gap. Detailed explanation based on the numerical calculations will be presented elsewhere [49]. An indirect experimental evidence for this peak is that it occurs at a place where the anomalous Hall conductivity has a sudden change of sign and magnitude around $x = 0.3$ according to Ref. [41]. Such a correlation is expected from the Mott relation (4.10) and the fact that the Fermi energy changes approximately linearly with the doping density [49]. Nevertheless, more direct experimental results are clearly needed for a careful comparison with our theory.

Chapter 5

Reciprocal Spin-Hall Effect: Charge Transport Under the Influence of a Nonuniform Perturbation

5.1 Introduction

Recently, great research interests have been devoted to the spin-Hall effect in doped semiconductors [19, 20], where the spin-orbit interaction can give rise to an intrinsic spin current perpendicular to the applied electric field. Despite strong experimental evidence [50, 51], a clear understanding of this effect is far from complete. For instance, there is no definite relation between bulk spin current and boundary spin accumulation, making it difficult to extract the spin-Hall conductivity from experimental data. Moreover, using the conventional definition of spin current, one is led to the dubious conclusion that even in simple band insulators (i.e., bands with zero Chern numbers) the spin-Hall conductivity can be nonzero [52, 53, 54].

To overcome the above difficulties, we recently proposed a proper definition of spin current [55], which, unlike the conventional one, allows us to establish the Onsager reciprocal relation of the charge and spin currents and their corresponding forces. This result puts recent electrical measurements [56, 57, 58] of the spin-Hall

effect on a firm ground, i.e, one can first detect the charge Hall current induced by a spin force, then deduce the corresponding spin-Hall conductivity from the Onsager relation. In practice, the spin force can be realized by the gradient of a Zeeman field or a spin-dependent chemical potential. On the other hand, while the properly defined spin current vanishes in insulators with localized orbitals as desired [55], what happens in band insulators still remains an open question. It is thus timely and interesting to investigate the reciprocal spin-Hall effect in detail.

Apart from its practical value, study of the reciprocal spin-Hall effect is also posing a new challenge to the present theory of charge transport. It has been found that the electron motion can be driven by a momentum-space Berry curvature, giving rise to a transverse anomalous velocity in the presence of an electric field [7]. In insulators, this velocity term leads to the celebrated TKNN formula for the quantum Hall effect [14], while in metals and semiconductors, it gives an intrinsic contribution to the anomalous Hall current [10, 11, 12]. However, these theories are concerned about charge transport under a uniform perturbation (the electric field can be written as the time derivative of a uniform vector potential). In the general scenario where the system is perturbed by a nonuniform field, there are other Berry curvatures defined in the mixed position-momentum space that also affects the electron motion [7]. Their effect on the transport properties of solids is yet to be explored.

In this chapter we develop a semiclassical theory for charge transport under the influence of a nonuniform perturbation. We consider only the intrinsic mechanism, where the Hall current is driven by the Berry phase in the Bloch bands, and depends only on the equilibrium part of the carrier distribution function. We show that for systems perturbed by a nonuniform field, it is necessary to include the Berry curvature in the mixed position-momentum space. It turns out that this Berry curvature affects the charge transport through two different ways. In addition to appearing in the equations of motion, it also modifies the phase-space density of states [35], which leads to a nontrivial change in the local chemical potential as explained below. Finally, the complete theory also needs a proper deduction of the magnetization current, whose connection to the Berry-phase effect is revealed recently [59].

After deriving the general formalism, we then apply our theory to the reciprocal spin-Hall effect. We first demonstrate the formulation by verifying the Onsager

relation for the Rashba model. After that, we focus on insulators. In a single-band insulator our result reduces to the familiar expression for the quantum Hall effect, i.e., the current is given by a product of the Chern number and the chemical potential difference between opposite boundaries in appropriate units. We thus reach the conclusion that the reciprocal spin-Hall conductivity σ_{yx}^{cs} vanishes if the Chern number is zero. Furthermore, σ_{yx}^{cs} is quantized only when the spin s_z is a good quantum number. In a two-band insulator with time-reversal symmetry, we show that the value of σ_{yx}^{cs} depends on the boundary condition. For smooth boundaries σ_{yx}^{cs} vanishes identically, while for sharp boundaries σ_{yx}^{cs} is determined by the expectation value of s_z in the edge states. We also discuss the relation between our theory and a recently proposed Streda-like formula for the spin-Hall conductivity [60].

5.2 General Formalism

We start by considering a two-dimensional electron gas under the influence of a nonuniform external field $h(\boldsymbol{r})$ coupled to some operator Q. Generalizations to three dimensions shall be straightforward. The Hamiltonian takes the general form

$$H = H_0(\boldsymbol{k}) + h(\boldsymbol{r})Q \;, \tag{5.1}$$

where $H_0(\boldsymbol{k})$ is the unperturbed Hamiltonian. To access transport properties, we adopt the formalism of semiclassical wave-packet dynamics [7], which is a powerful tool for studying the influence of slowly varying perturbations on the dynamics of Bloch electrons. Consider a wave packet $|W(\boldsymbol{r}_c, \boldsymbol{k}_c)\rangle$ sharply centered at $(\boldsymbol{r}_c, \boldsymbol{k}_c)$. Due to its narrow distribution in real space, it is sufficient to construct the wave packet using the eigenstates $|u(h(\boldsymbol{r}_c), \boldsymbol{k})\rangle$ of H_c, where $H_c = H_0(\boldsymbol{k}) + h(\boldsymbol{r}_c)Q$ is the local Hamiltonian felt by this wave packet. As it moves in the phase space, the wave packet $|W(\boldsymbol{r}_c, \boldsymbol{k}_c)\rangle$ will acquire a Berry phase that depends on both $\boldsymbol{r}_c$ and $\boldsymbol{k}_c$. According to Ref. [7], the Berry phase also modifies the local dynamics of Bloch electrons. Assume the force term $\boldsymbol{F} = \boldsymbol{\nabla} h(\boldsymbol{r})$ is along the x-axis. To first order in F we have $\hbar \dot{k}_x = -F \partial_h \varepsilon$ and $\hbar \dot{k}_y = 0$ with $\varepsilon(\boldsymbol{k}, \boldsymbol{r})$ being the electron energy obtained from H_c. The orbital motion of the wave-packet center is given by (the subscript c

is dropped)

$$\hbar\dot{x} = (1 - F\Omega_{k_x h})\partial_{k_x}\varepsilon + F\partial_{k_x}\delta\varepsilon \ , \tag{5.2a}$$

$$\hbar\dot{y} = \partial_{k_y}\varepsilon + F\partial_{k_y}\delta\varepsilon - F\Omega_{k_x k_y}\partial_h\varepsilon - F\Omega_{k_y h}\partial_{k_x}\varepsilon \ , \tag{5.2b}$$

where $\Omega_{\alpha\beta}$ is the Berry curvature defined by $\Omega_{\alpha\beta} = -2\,\mathrm{Im}\langle\partial_\alpha u|\partial_\beta u\rangle$, and $F\delta\varepsilon$ is the gradient correction to the electron energy with $\delta\varepsilon = -\,\mathrm{Im}\langle\partial_h u|(\varepsilon - H_c)|\partial_{k_x} u\rangle$. Since we are interested in a linear order calculation in F, we have used the identity $\partial_x = F\partial_h$ to write $\Omega_{kx} = F\Omega_{kh}$. Here the Berry curvature $\Omega_{\alpha\beta}$ has the meaning of the Berry phase per unit area in the α-β plane. One can see that in addition to the familiar $\boldsymbol{k}$-space Berry curvature $\Omega_{k_x k_y}$ [10, 11, 12], $\Omega_{k_x h}$ and $\Omega_{k_y h}$ also enter into the equations of motion (5.2).

Next we discuss the Berry-phase effect on thermodynamic quantities. In a recent work [35] it is shown that the electron density of states in the phase space can be modified by a Berry phase term. In the case of a nonzero $\Omega_{k_x x}$, the modified density of states reads [1]

$$D(\boldsymbol{r}, \boldsymbol{k}) = (1 + F\Omega_{k_x h})/(2\pi)^2 \ . \tag{5.3}$$

Accordingly, the electron density is given by

$$n(\boldsymbol{r}) = \int [d\boldsymbol{k}](1 + F\Omega_{k_x h}) f(\mu - \varepsilon) \ , \tag{5.4}$$

where $[d\boldsymbol{k}]$ is a shorthand for $d\boldsymbol{k}/(2\pi)^d$, and $f(\mu - \varepsilon)$ is the Fermi-Dirac distribution function that depends on local variables such as the chemical potential $\mu(\boldsymbol{r})$ and temperature $T(\boldsymbol{r})$. For simplicty we assume the isothermal condition always holds and set the temperature to zero. The local chemical potential is thus determined

[1] Although the complete formulation of the Berry-phase modification to the electron density of states is given in Ref. [35], here we provide an heuristic argument for self completeness. Consider a one-dimensional system with a nonzero Ω_{kx}. It is well-known that the area $\mathcal{A}$ of a closed orbit $\mathcal{C}$ in the phase space is quantized according to $\mathcal{A} = \oint_{\mathcal{C}} k dx = 2\pi(n + \frac{1}{2}) - \gamma_B$, where γ_B is the Berry phase accumulated along the loop $\mathcal{C}$. The Berry phase γ_B can be expressed as an area integral $\gamma_B = \int_{\mathcal{A}} d\mathcal{A}\,\Omega_{kx}$. Thus the phase-space area between two neighboring orbits is $\delta\mathcal{A} = 2\pi/(1 + \bar{\Omega}_{kx})$, where $\bar{\Omega}_{kx}$ is the average of Ω_{kx} over the annular area $\delta\mathcal{A}$. Recall that $\delta\mathcal{A}$ has the meaning of the phase-space volume occupied by a single quantum state, which is inversely proportional to the density of states $D(\boldsymbol{r}, \boldsymbol{k})$ in the phase space. Because Ω_{kx} explicitly depends on k and x, we find that $D(\boldsymbol{r}, \boldsymbol{k})$ is no longer uniform and on average we have $\bar{D}(\boldsymbol{r}, \boldsymbol{k}) = (1 + \bar{\Omega}_{kx})/2\pi$.

by the highest occupied energy level $\varepsilon(k_F, \boldsymbol{r})$.

In magnetic materials, a nonuniform $h(\boldsymbol{r})$ will in general induce a nonuniform magnetization $\boldsymbol{M}(\boldsymbol{r})$. As a result, a magnetization current appears in the bulk and contributes to the local current density. The orbital magnetization is given by [35, 28]

$$\boldsymbol{M}(\boldsymbol{r}) = \int [d\boldsymbol{k}][\boldsymbol{m}(\boldsymbol{k}) + \frac{e}{\hbar}(\mu - \varepsilon)\boldsymbol{\Omega}_{\boldsymbol{k}}]\Theta(\mu - \varepsilon) \ , \tag{5.5}$$

where $\boldsymbol{m}(\boldsymbol{k})$ is the intrinsic orbital moment of the wave packet, and $(\boldsymbol{\Omega}_{\boldsymbol{k}})_\alpha = \frac{1}{2}\epsilon_{\alpha\beta\gamma}\Omega_{k_\beta k_\gamma}$. Since we only need calculate the magnetization current linear in $\boldsymbol{\nabla} h$, we can evaluate Eq. (5.5) for a uniform field h and then use $\boldsymbol{\nabla} \times \boldsymbol{M} = \boldsymbol{\nabla} h \times \partial \boldsymbol{M}/\partial h$. The effect of the magnetization current has been discussed in the context of anomalous Nernst effect in ferromagnets [59]. To calculate the transport current $\boldsymbol{j}$, the magnetization current should be subtracted from the local current, i.e., $\boldsymbol{j} = \boldsymbol{j}^{\text{local}} - \boldsymbol{\nabla} \times \boldsymbol{M}(\boldsymbol{r})$. During this procedure, the magnetic moment contribution is canceled out, and only the second term in Eq. (5.5), the Berry-phase correction to orbital magnetization, survives (details is present in Ref. [59]).

Finally, the transport current is given by (up to first-order of the perturbation)

$$\boldsymbol{j} = -e \int d\boldsymbol{k}\, D(\boldsymbol{r}, \boldsymbol{k}) g(\boldsymbol{r}, \boldsymbol{k}) \dot{\boldsymbol{r}} - \boldsymbol{\nabla} \times \frac{e}{\hbar} \int [d\boldsymbol{k}](\mu - \varepsilon)\boldsymbol{\Omega}_{\boldsymbol{k}}\Theta(\mu - \varepsilon) \ , \tag{5.6}$$

where $g(\boldsymbol{r}, \boldsymbol{k})$ is the distribution function. Compared to the usual Boltzmann theory, this equation has two interesting aspects due to the Berry-phase effect. The first term is from the Boltzmann theory. However, a position- and momentum-dependent density of states $D(\boldsymbol{r}, \boldsymbol{k})$ is introduced to account for the nontrivial geometry of the phase space [35]. The second term results from the subtraction of the magnetization current. Equation (5.6) is the central result of our paper.

It is noteworthy that in the special case when $[H_0, Q] = 0$, the local basis $|u(\boldsymbol{k})\rangle$ will not depend on h hence $\Omega_{k_x h}$ and $\Omega_{k_y h}$ vanishes. The perturbation $h(\boldsymbol{r}_c)Q$ simply shifts the electron energy. An example for that is the electrical perturbation with $h(\boldsymbol{r})$ being the electric potential $\phi(\boldsymbol{r})$ and Q the electron charge $-e$. On the contrary, in the reciprocal spin-Hall effect, $h(\boldsymbol{r})$ has the meaning of a Zeeman field and Q becomes the spin s_z. Since H_0 usually includes the spin-orbit interaction, $[H_0, \sigma_z] \neq 0$, the Berry curvature $\Omega_{k_x h}$ and $\Omega_{k_y h}$ will appear and play a role.

5.3 Reciprocal Spin-Hall Effect

Now we apply our theory to the reciprocal spin-Hall effect. Inserting Eqs. (5.2) and (5.3) into Eq. (5.6) yields

$$\begin{aligned} j_y = -\frac{e}{\hbar}F\int [d\boldsymbol{k}](&\Omega_{k_xh}\partial_{k_y}\varepsilon - \Omega_{k_yh}\partial_{k_x}\varepsilon + \partial_h\Omega_{k_xk_y}\varepsilon \\ &- \partial_h\Omega_{k_xk_y}\mu - \Omega_{k_xk_y}\partial_h\mu + \partial_{k_y}\delta\varepsilon)\Theta(\mu-\varepsilon) \\ &- \frac{e}{\hbar}F\Big(\int [d\boldsymbol{k}]\Omega_{k_xh}\Big)\langle\partial_{k_y}\varepsilon\rangle_{\varepsilon_F} \ , \end{aligned} \tag{5.7}$$

where $\langle\partial_{k_y}\varepsilon\rangle_{\varepsilon_F}$ is the average of $\partial_{k_y}\varepsilon$ on the Fermi surface, which vanishes in systems with rotational symmetry around z-axis. For a linear-order calculation, the integral can be evaluated at the limit $h \to 0$ since j_y is explicitly proportional to ∇h. It is straightforward to show that for the Rashba model $H_R(\boldsymbol{k}) = k^2/2m + \alpha(\boldsymbol{k}\times\boldsymbol{\sigma})\cdot\hat{z}$, the reciprocal spin-Hall conductivity is $\sigma^{cs}_{yx} = -e/8\pi$ in the clean limit. A comparison with Ref. [55] shows that the Onsager relation is satisfied, i.e., $\sigma^{cs}_{yx} = -\sigma^{sc}_{xy}$, where σ^{sc}_{xy} is the spin-Hall conductivity. A linear-response study on the conserved spin current in semiconductors can be found in Ref. [61].

In the following we turn our attention to the reciprocal spin-Hall effect in insulators. In this situation, Eq. (5.7) can be greatly simplified, and physical meaning of those Berry curvature terms become clear. By doing so we can also safely ignore the impurity scattering in the bulk because there is no available phase space for scattering events to occur. Before any in-depth discussion, we verify that the longitudinal current $j_x = \int_{\rm BZ} d\boldsymbol{k}\, D(\boldsymbol{r},\boldsymbol{k})\dot{x}$ vanishes. This is only true if we use the modified density of states $D(\boldsymbol{r},\boldsymbol{k})$ given in Eq. (5.3).

We first consider a single-band insulator. The last term in Eq. (5.7), the Fermi surface contribution, vanishes. $\int_{\rm BZ}[d\boldsymbol{k}]\partial_{k_y}\varepsilon$ also vanishes. We assume that varying h does not close the bulk energy gap. (Since h can be infinitesimal, this condition is always satisfied.) By integration by parts the first three terms can be written as

$$(\partial_{k_y}\Omega_{hk_x} + \partial_{k_x}\Omega_{k_yh} + \partial_h\Omega_{k_xk_y})\varepsilon = 0 \ . \tag{5.8}$$

The sum in the parentheses actually gives the monopole density in the parameter space spanned by (h, k_x, k_y), which vanishes by our assumption. The remaining

terms give a current of

$$j_y = \frac{e}{\hbar} F \partial_h (\mu \int_{BZ} [d\boldsymbol{k}] \Omega_{k_x,k_y}) = \frac{e}{h} C F \partial_h \mu \ , \tag{5.9}$$

where in the second step we used the fact that the Chern number C is unchanged as long as the bulk energy gap remains open [62]. One should not confuse the Plank constant h in the denominator with the Zeeman field derivative ∂_h. We can see that the reciprocal spin-Hall conductivity σ_{yx}^{cs} will be quantized in units of $e/4\pi$ only if s_z is a good quantum number so that $\partial_h \mu = \pm\hbar/2$. Integrating j_y in the x-direction yields

$$I_y = -\frac{e}{h} C(\mu_L - \mu_R) \ , \tag{5.10}$$

where μ_L and μ_R are chemical potentials at opposite boundaries. This is the exact formula for the Hall current as in the quantum Hall effect. Had we not included the magnetization current, such an agreement cannot be obtained. It also gives the desired property that for a single-band insulator with a zero Chern number, the (reciprocal) spin-Hall conductivity vanishes. It is straightforward to verify that for multi-band insulators with zero Chern number for each band, σ_{xy}^{cs} vanishes too.

Next we consider a two-band insulator with time-reversal symmetry so that the total Chern number is zero. To be specific, the model we have in mind is the Kane-Mele model on the honeycomb lattice [63, 64]. In the absence of the Rashba spin-orbit interaction, s_z is a good quantum number; the model reduces to two independent copies of the Haldane model [65] with opposite signs of $s_z = \mp\hbar/2$ and Chern numbers $C_{\uparrow,\downarrow} = \pm 1$. If the impurity scattering is spin-independent, there is no channel for the two spin components to exchange particles. Thus for each of them a chemical potential can be defined. The total reciprocal spin-Hall conductivity is simply given by the sum of each copy,

$$\sigma_{yx}^{cs} = -\frac{e}{2\pi} \ . \tag{5.11}$$

This is consistent with the Onsager relation.

If we turn on the Rashba spin-orbit interaction, s_z is no longer a good quantum number, therefore the picture of two independent species of electrons becomes questionable. The possibility of impurity scattering in the bulk is ruled out; we only need focus on the boundary states. We first consider the smooth boundary

condition with a slowly varying confining potential $V(\boldsymbol{r})$ so that the semiclassical picture still holds. Hence, each bulk state with energy $\varepsilon(\boldsymbol{k})$ corresponds to a state in the vicinity of the boundaries with energy $\varepsilon(\boldsymbol{k}) + V(\boldsymbol{r})$. The interchange between electrons from the two different bands can happen through scattering on the boundary. Thus a steady state measurement of the reciprocal spin-Hall effect will give us a vanishing σ_{yx}^{cs}. On the other hand, under the sharp boundary condition we can follow Kane and Mele's argument [64], i.e., there is a pair of edge modes and intra-pair scattering is forbidden due to time-reversal symmetry. Hence we can still define two different chemical potentials for electrons from different edge modes. In this case, the reciprocal spin-Hall conductivity is

$$\sigma_{yx}^{cs} = \frac{e}{h} \sum_{\alpha} C_{\alpha} \partial_h \mu_{\alpha} = \frac{e}{h} \sum_{\alpha} C_{\alpha} \langle s_z \rangle_{\alpha}^{\text{edge}} \,, \tag{5.12}$$

where α is the band index. We see that the smooth and sharp boundary conditions lead to entirely different results. This is in sharp contrast to the quantum Hall effect, which is insensitive to the boundary condition because it is topologically protected. We suspect that the quantum spin-Hall effect is not entirely determined by the topological property of the system.

Finally we comment on a recently proposed Streda-like formula for the spin-Hall conductivity σ_{xy}^{sc} [60], where it is shown that $\sigma_{xy}^{sc} \propto \partial M_{\text{orbit}}/\partial h$. However, it is clear from our derivation for the reciprocal spin-Hall current that $\partial M_{\text{orbit}}/\partial h$ only corresponds to the magnetization current; there is no obvious reason that other contributions such as the first term in Eq. (5.6) will vanish. Then by Onsager relation, the Streda formula for σ_{xy}^{sc} is only part of the story; there are other contributions missing.

Chapter 6

Berry Phase Effect on Magnetotransport

6.1 Introduction

The problem of magnetoresistance in metals and semiconductors has a long history, and a large amount of work has been devoted to this subject. According to conventional theory [66], in a weak magnetic field the magnetoresistance of a crystal behaves as

$$\frac{\Delta\rho}{\rho_0} \sim (\omega_c\tau)^2 \,, \quad (\omega_c\tau \ll 1) \tag{6.1}$$

where $\omega_c = eB/m^*$ is the cyclotron frequency and τ is the relaxation time. The effect of the magnetic field is to always increase the resistance. On the other hand, in the strong field limit, the details of the collision processes are suppressed and the details of the Fermi surface enhanced. Thus the magnetoresistance is largely determined by the Fermi surface topology. It has three quite different behaviors:

$$\frac{\Delta\rho}{\rho_0} \sim \begin{cases} \text{saturation}, & \text{non-equal densities of electrons and holes,} \\ (\omega_c\tau)^2, & \text{equal densities of electrons and holes,} \\ \omega_c\tau, & \text{open Fermi surface.} \end{cases} \qquad (\omega_c\tau \gg 1) \tag{6.2}$$

Recently Weitering's group measured the magnetotransport properties of Mn_5Ge_3. We show that the experiment was done at the low field limit. Consider

the conductivity of a crystal $\sigma = ne^2\tau/m^*$, and the quantity $\omega_c\tau = eB\tau/m^*$. Here we treat the electron effective mass and the cyclotron mass as the same. Combining these two expressions together gives

$$\omega_c\tau = \frac{B\sigma}{ne} = \frac{B}{\rho ne} \ . \tag{6.3}$$

From the data we find $\min \rho_{xx} = 15 \times 10^{-8}\ \Omega \cdot \mathrm{m}$ and $\min n = 5 \times 10^{28}\ \mathrm{m}^{-3}$. Thus $\omega_c\tau \sim 10^{-3}B$; even for the highest field 20 T in the experiment, $\omega_c\tau \sim 0.02$. Contradicting to the conventional result (6.1), their data clearly shows a linear magnetoresistance with a temperature-dependent slope that ranges from positive to negative.

The conventional result is obtained in the framework of semiclassical transport theory, which is built upon two basic ingredients: the equations of motion describing the dynamics of each particle and the Boltzmann equation governing the evolution of the distribution function. It has been shown [7] that one of the ingredients, the equations of motion, has to be modified if the spatial-inversion or/and time-reversal symmetry of the crystal is broken. Typical systems that need such modifications include crystals with spin-orbit coupling; and Mn_5Ge_3 is one of them. In view of this observation, we propose a novel mechanism for a possible linear magnetoresistance in metals and semiconductors with broken symmetries.

The plan of this chapter is as following. We will first briefly review the semiclassical dynamics of Bloch electrons. Then we derive the general solution of the Boltzmann equation at low field limit. For demonstration we apply our formula to two-dimensional systems with Rashba spin-orbit coupling. We will also discuss the high field limit.

6.2 Semiclassical Dynamics

In this section we briefly review the theory for semiclassical dynamics of Bloch electrons and its consequence on electron density of states in phase space. Within the semiclassical approach, each electron in a given band is described by a wave packet narrowly localized around $(\boldsymbol{r}, \boldsymbol{k})$ in phase space. It is shown [7] that the

dynamics of the wave packet center satisfies the following equations of motion

$$\dot{\boldsymbol{r}} = \frac{1}{\hbar}\frac{\partial \varepsilon_M}{\partial \boldsymbol{k}} - \dot{\boldsymbol{k}} \times \boldsymbol{\Omega}(\boldsymbol{k}) \,, \tag{6.4a}$$

$$\hbar\dot{\boldsymbol{k}} = -e\boldsymbol{E}(\boldsymbol{r}) - e\dot{\boldsymbol{r}} \times \boldsymbol{B}(\boldsymbol{r}) \,. \tag{6.4b}$$

There are two major modifications to the conventional equations of motion widely presented in standard textbooks (for example, see Ref. [4]):

1. The band structure energy needs a correction term that accounts for the orbital magnetization of the wave packet, i.e., $\varepsilon_M(\boldsymbol{k}) \equiv \varepsilon_0(\boldsymbol{k}) - \boldsymbol{m}(\boldsymbol{k}) \cdot \boldsymbol{B}$. We shall discuss the magnetic moment $\boldsymbol{m}(\boldsymbol{k})$ in detail later.

2. An extra term proportional to the Berry curvature $\boldsymbol{\Omega}(\boldsymbol{k})$ of the Bloch state appears in the velocity expression. The Berry curvature is defined by $\boldsymbol{\Omega}(\boldsymbol{k}) \equiv \mathrm{i}\langle \boldsymbol{\nabla}_{\boldsymbol{k}} u(\boldsymbol{k})| \times |\boldsymbol{\nabla}_{\boldsymbol{k}} u(\boldsymbol{k})\rangle$, where $|u(\boldsymbol{k})\rangle$ is the periodic part of the Bloch waves.

The magnetic moment $\boldsymbol{m}(\boldsymbol{k})$ and the Berry curvature $\boldsymbol{\Omega}(\boldsymbol{k})$ vanish for crystals with both spatial-inversion and time-reversal symmetry. But if the crystal lacks either of these symmetries, a complete description of electron dynamics requires the use of the modified equations of motion (6.4).

The explicit appearance of the Berry curvature term has profound effect on the electron dynamics. In a recent work [35] we showed that in the presence of both the magnetic field and the Berry curvature, the density of states in phase space is no longer uniform. To account for this change, the expression for the density of a physical observable $\hat{Q}$ must use the properly defined density of states, i.e.,

$$\langle Q \rangle = \int [\mathrm{d}\boldsymbol{k}] D(\boldsymbol{k}) f(\boldsymbol{r}, \boldsymbol{k}) Q(\boldsymbol{k}) \,, \tag{6.5}$$

where $[\mathrm{d}\boldsymbol{k}]$ is a shorthand of $\mathrm{d}\boldsymbol{k}/(2\pi)^d$ and $D(\boldsymbol{k})$ is the modified density of states

$$D(\boldsymbol{k}) \equiv 1 + \frac{e}{\hbar}\boldsymbol{B} \cdot \boldsymbol{\Omega} \,. \tag{6.6}$$

The introduction of a field-dependent density of states implies that the distribution function can be altered by a magnetic field. To see this, let us consider

the electron density of a closed system in equilibrium

$$n = \int [\mathrm{d}\boldsymbol{k}] D(\boldsymbol{k}) f(\varepsilon_M, \mu) \ . \tag{6.7}$$

Upon the application of a magnetic field, it is changed by

$$\delta n = \int [\mathrm{d}\boldsymbol{k}] \Big[\frac{e}{\hbar} f \boldsymbol{B} \cdot \boldsymbol{\Omega} + \frac{\partial f}{\partial \varepsilon} (\delta\varepsilon - \delta\mu) \Big] \ . \tag{6.8}$$

Since the electron density is fixed, we obtain

$$\int [\mathrm{d}\boldsymbol{k}] \frac{\partial f}{\partial \varepsilon} (\delta\mu - \delta\varepsilon) = \int [\mathrm{d}\boldsymbol{k}] \frac{e}{\hbar} f \boldsymbol{B} \cdot \boldsymbol{\Omega} \ . \tag{6.9}$$

This result shows that the distribution function will adjust itself to an external magnetic field. It still has the form of an equilibrium distribution but both the electron energy ε and the chemical potential μ has changed. This modified distribution function then serves as the initial condition for the Boltzmann equation.

It is useful to write $\dot{\boldsymbol{r}}$ and $\dot{\boldsymbol{k}}$ as functions of $\boldsymbol{r}$ and $\boldsymbol{k}$. A few steps of algebra on equations (6.4) yields

$$D(\boldsymbol{k}) \dot{\boldsymbol{r}} = \boldsymbol{v} + \boldsymbol{E} \times \boldsymbol{\Omega} + (\boldsymbol{v} \cdot \boldsymbol{\Omega}) \boldsymbol{B} \ , \tag{6.10a}$$

$$D(\boldsymbol{k}) \dot{\boldsymbol{k}} = -\boldsymbol{E} - \boldsymbol{v} \times \boldsymbol{B} - (\boldsymbol{E} \cdot \boldsymbol{B}) \boldsymbol{\Omega} \ , \tag{6.10b}$$

where $\boldsymbol{v} \equiv \partial \varepsilon_M / \hbar \partial \boldsymbol{k}$ is the "normal" velocity of the electron. When writing down the above equations, we use the units system where the electric and magnetic field absorb a factor of $e/\hbar$.

6.3 Uniform Magnetic Field

Semiclassical motion of a Bloch electron in a uniform magnetic field is important to understand various magneto-effect in solids. In this case, the equations of motion reduce to

$$D(\boldsymbol{k}) \dot{\boldsymbol{r}} = \boldsymbol{v} + (\boldsymbol{v} \cdot \boldsymbol{\Omega}) \boldsymbol{B} \ , \tag{6.11a}$$

$$D(\boldsymbol{k}) \dot{\boldsymbol{k}} = -\boldsymbol{v} \times \boldsymbol{B} \ . \tag{6.11b}$$

At first look it is very odd that there is an anomalous velocity term proportional to $\boldsymbol{B}$, which means there will be a current along the field direction. We show that after averaging over the distribution function, this current is actually zero. The current corresponding to the anomalous velocity is

$$\begin{aligned}\boldsymbol{j}_B &= -e\boldsymbol{B}\int[\mathrm{d}\boldsymbol{k}]f\boldsymbol{v}\cdot\boldsymbol{\Omega}\\ &= -\frac{e}{\hbar}\boldsymbol{B}\int[\mathrm{d}\boldsymbol{k}]\boldsymbol{\nabla}_{\boldsymbol{k}}F\cdot\boldsymbol{\Omega}\\ &= -\frac{e}{\hbar}\boldsymbol{B}\Big(\int[\mathrm{d}\boldsymbol{k}]\boldsymbol{\nabla}_{\boldsymbol{k}}(F\boldsymbol{\Omega})-\int[\mathrm{d}\boldsymbol{k}]F\boldsymbol{\nabla}_{\boldsymbol{k}}\cdot\boldsymbol{\Omega}\Big)\,,\end{aligned}\tag{6.12}$$

where $F(\varepsilon)=-\int_{\varepsilon}^{\infty}f(\varepsilon')\mathrm{d}\varepsilon'$ and $f(\varepsilon)=\partial F/\partial\varepsilon$. The first term vanishes [1] and if there is no magnetic monopole in $\boldsymbol{k}$-space, the second term also vanishes. In above calculation we did not consider the change of the Fermi surface. Since it always comes in the form $(\partial f/\partial/\mu)\delta\mu=-(\partial f/\partial/\varepsilon)\delta\mu$ we can use the same technique to prove that the corresponding current also vanishes.

We assume the field is along the z-axis. From the second equation of (6.11) we can see that motion in $\boldsymbol{k}$-space is confined in the xy-plane and is completely determined once the energy ε and the z component of the wave vector k_z is given. Let us calculate the period of the cyclotron motion. The time for the wave vector to move from $\boldsymbol{k}_1$ to $\boldsymbol{k}_2$ is

$$t_2-t_1=\int_{t_1}^{t_2}\mathrm{d}t=\int_{\boldsymbol{k}_1}^{\boldsymbol{k}_2}\frac{\mathrm{d}k}{|\dot{\boldsymbol{k}}|}\,.\tag{6.13}$$

From the equations of motion (6.11) we have

$$|\dot{\boldsymbol{k}}|=\frac{B|\boldsymbol{v}_\perp|}{D(\boldsymbol{k})}=\frac{B|(\partial\varepsilon/\partial\boldsymbol{k})_\perp|}{\hbar D(\boldsymbol{k})|}\,.\tag{6.14}$$

On the other hand, the quantity $(\partial\varepsilon/\partial\boldsymbol{k})_\perp$ has a very nice geometric intepretation. Let $\Delta\boldsymbol{k}$ denotes the vector in the plane connecting points on neighboring orbits of energy ε and $\varepsilon+\Delta\varepsilon$, respectively (Fig. 6.1). Then

[1] For any periodic function $F(\boldsymbol{k})$ with the periodicity of a reciprocal Bravais lattice, the following identity holds for integrals taken over a Brillouin zone, $\in_{\mathrm{BZ}}\mathrm{d}\boldsymbol{k}\,\boldsymbol{\nabla}_{\boldsymbol{k}}F(\boldsymbol{k})=0$. To see this, consider $I(\boldsymbol{k}')=\int\mathrm{d}\boldsymbol{k}\,F(\boldsymbol{k}+\boldsymbol{k}')$. Because $F(\boldsymbol{k})$ is periodic in $\boldsymbol{k}$, $I(\boldsymbol{k}')$ should not depend on $\boldsymbol{k}'$. Therefore, $\boldsymbol{\nabla}_{\boldsymbol{k}'}I(\boldsymbol{k}')=\int\mathrm{d}\boldsymbol{k},\boldsymbol{\nabla}_{\boldsymbol{k}'}F(\boldsymbol{k}+\boldsymbol{k}')=\int\mathrm{d}\boldsymbol{k}\boldsymbol{\nabla}_{\boldsymbol{k}}F(\boldsymbol{k}+\boldsymbol{k}')=0$. Setting $\boldsymbol{k}'=0$ gives the desired

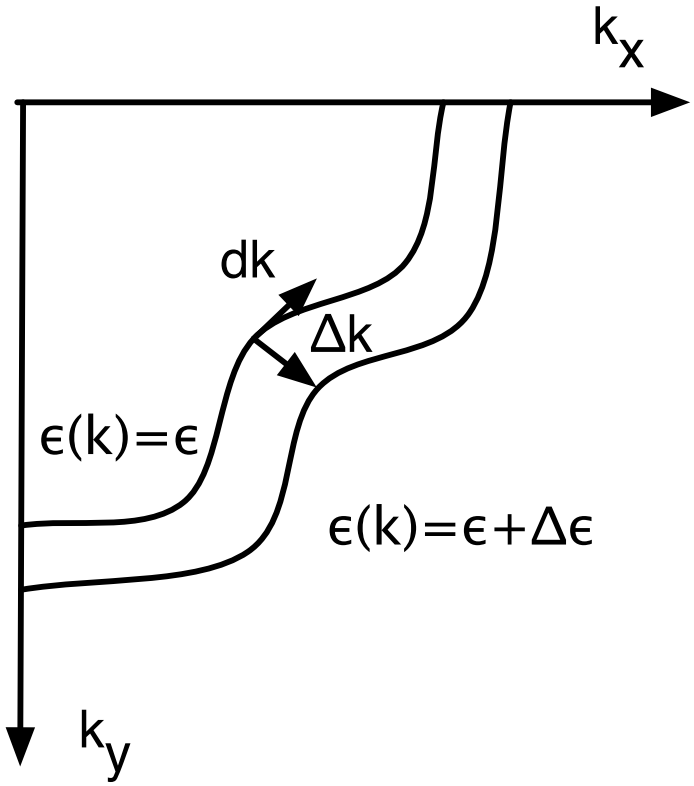

Figure 6.1: The geometry of orbit dynamics. The magnetic field is along the z-axis. The orbit is limited in the xy plane in $\boldsymbol{k}$-space.

$$\Delta\varepsilon = (\partial\varepsilon/\partial\boldsymbol{k})\cdot\Delta\boldsymbol{k} = |(\partial\varepsilon/\partial/\boldsymbol{k})_\perp|\Delta\boldsymbol{k}\ . \tag{6.15}$$

Thus

$$t_2 - t_1 = \frac{\hbar}{B}\int_{\boldsymbol{k}_1}^{\boldsymbol{k}_2}\frac{D(\boldsymbol{k})\Delta\boldsymbol{k}\,\mathrm{d}k}{\Delta\varepsilon}\ . \tag{6.16}$$

Introducing the 2D electron density for given ε and k_z

$$n_2(\varepsilon, k_z) = \iint_{k_z,\varepsilon(\boldsymbol{k})<\varepsilon}\frac{D(\boldsymbol{k})\,\mathrm{d}k_x\mathrm{d}k_y}{(2\pi)^2}\ , \tag{6.17}$$

the period of a cyclotron motion can be written as

$$T = (2\pi)^2\frac{\hbar}{B}\frac{\partial n_2(\varepsilon, k_z)}{\partial\varepsilon}\ . \tag{6.18}$$

6.4 High Field Limit

In this section we study the high field limit. We consider the configuration where the electric and magnetic fields are perpendicular to each other, i.e., $\boldsymbol{E} = E\hat{\boldsymbol{x}}$, $\boldsymbol{B} = B\hat{\boldsymbol{z}}$ and $\boldsymbol{E}\cdot\boldsymbol{B} = 0$. In the absence of electric field, the motion of $\boldsymbol{k}$ satisfies

$$D(\boldsymbol{k})\dot{\boldsymbol{k}} = -\boldsymbol{v}\times\boldsymbol{B}\ . \tag{6.19}$$

Multiplying $\times\boldsymbol{B}$ on both sides gives

$$D(\boldsymbol{k})\dot{\boldsymbol{k}}\times\boldsymbol{B} = B^2\boldsymbol{v}_\perp\ . \tag{6.20}$$

Since we have assumed $\boldsymbol{E}\perp\boldsymbol{B}$, then $\boldsymbol{E}\cdot\boldsymbol{v} = \boldsymbol{E}\cdot\boldsymbol{v}_\perp = D(\boldsymbol{k})\boldsymbol{E}\cdot(\dot{\boldsymbol{k}}\times\boldsymbol{B})/B^2$. Inserting this expression into the Boltzmann equation and integrating by parts yields

$$\begin{aligned} g &= f + \frac{\hbar}{B^2}\frac{\partial f}{\partial\varepsilon}(\boldsymbol{B}\times\boldsymbol{E})\cdot\int_{-\infty}^{t}\mathrm{d}t'\,\mathrm{e}^{-(t-t')/\tau}\dot{\boldsymbol{k}} \\ &= f + \frac{\hbar}{B^2}\frac{\partial f}{\partial\varepsilon}(\boldsymbol{B}\times\boldsymbol{E})\cdot(\boldsymbol{k} - \langle\boldsymbol{k}\rangle)\ , \end{aligned} \tag{6.21}$$

expression. It is also true if $\boldsymbol{F}(\boldsymbol{k})$ is a vector function.

where $\langle \boldsymbol{k} \rangle$ is the average over relaxation time,

$$\langle \boldsymbol{k} \rangle = \frac{1}{\tau} \int_{-\infty}^{t} \mathrm{d}t' \, \mathrm{e}^{-(t-t')/\tau} \boldsymbol{k}(t') \; . \tag{6.22}$$

In the hight field limit, $\omega_c \tau \gg 1$, the electron can finish several turns between two successive collisions. We can therefore set $\langle \boldsymbol{k} \rangle = 0$, assuming all orbits are closed. Using (2.6), we write the total current as

$$\begin{aligned} \boldsymbol{j} &= -e \int [\mathrm{d}\boldsymbol{k}] D(\boldsymbol{k}) g(\boldsymbol{k}) \dot{\boldsymbol{r}} \\ &= -e \int [\mathrm{d}\boldsymbol{k}] \Big(f + \frac{\hbar}{B^2} \frac{\partial f}{\partial \varepsilon} (\boldsymbol{B} \times \boldsymbol{E}) \cdot \boldsymbol{k} \Big) \Big(\boldsymbol{v} + \boldsymbol{E} \times \boldsymbol{\Omega} + (\boldsymbol{v} \cdot \boldsymbol{\Omega}) \boldsymbol{B} \Big) \; . \end{aligned} \tag{6.23}$$

We then expand the product to linear order of $\boldsymbol{E}$:

$$\boldsymbol{j} = -e \int [\mathrm{d}\boldsymbol{k}] \Big(f \boldsymbol{E} \times \boldsymbol{\Omega} + \frac{\hbar}{B^2} \frac{\partial f}{\partial \varepsilon} [(\boldsymbol{B} \times \boldsymbol{E}) \cdot \boldsymbol{k}] [\boldsymbol{v} + (\boldsymbol{v} \cdot \boldsymbol{\Omega}) \boldsymbol{B}] \Big) \; . \tag{6.24}$$

The first term is the anomalous Hall current [10],

$$\boldsymbol{j}_{AH} = -e \int [\mathrm{d}\boldsymbol{k}] f \boldsymbol{E} \times \boldsymbol{\Omega} = -e \boldsymbol{E} \times \boldsymbol{\sigma}_{AH} \; , \quad \text{with} \quad \boldsymbol{\sigma}_{AH} \equiv \int [\mathrm{d}\boldsymbol{k}] f \boldsymbol{\Omega} \; . \tag{6.25}$$

The second term is the normal Hall current

$$\begin{aligned} \boldsymbol{j}_H &= -\frac{e}{B^2} \int [\mathrm{d}\boldsymbol{k}] \frac{\partial f}{\partial \boldsymbol{k}} [\boldsymbol{k} \cdot (\boldsymbol{B} \times \boldsymbol{E})] \\ &= -\frac{e}{B^2} \int [\mathrm{d}\boldsymbol{k}] \Big(\frac{\partial}{\partial \boldsymbol{k}} [f \boldsymbol{k} \cdot (\boldsymbol{B} \times \boldsymbol{E})] - f \frac{\partial}{\partial \boldsymbol{k}} [\boldsymbol{k} \cdot (\boldsymbol{B} \times \boldsymbol{E})] \Big) \\ &= -e \frac{\boldsymbol{E} \times \boldsymbol{B}}{B^2} \tilde{n}, \quad \text{with} \quad \tilde{n} = \int [\mathrm{d}\boldsymbol{k}] f \; . \end{aligned} \tag{6.26}$$

Note that $\boldsymbol{k}$ is not a periodic function so in general the first integral in the second line does not vanish. However, for closed orbits, we can always choose the Brillouin zone so that no orbits pass through the boundaries and either all states at the zone boundary are occupied (hole-like) or all are unoccupied (electron-like), as shown in Fig. 6.2. In this calculation we consider the electron-like band. For hole-like bands, one only needs to replace the f with $f - 1$ then the same argument follows. The

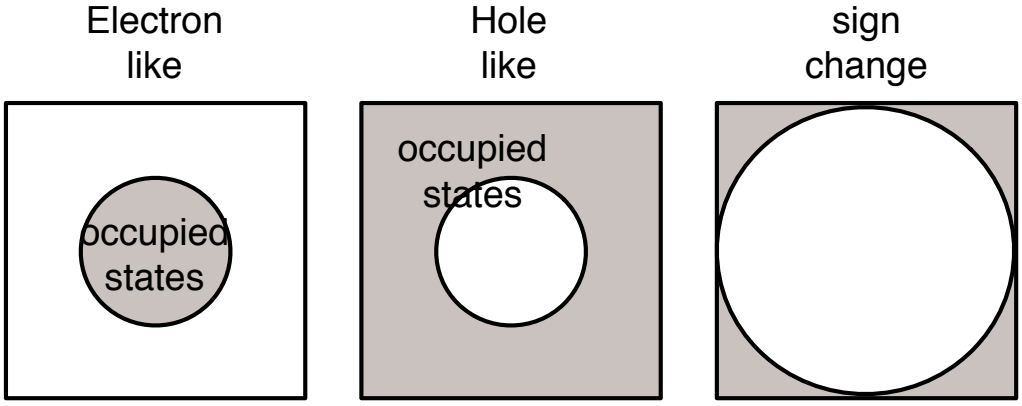

Figure 6.2: Electron-like, hole-like and the critical orbits for the Hall effect. When the orbit grows to exceeds the zone boundary, it is possible to observe a sign change of the charge carrier.

third term is a current along the $\boldsymbol{B}$ field [2]

$$\begin{aligned}\boldsymbol{j}_B &= -e\frac{\boldsymbol{B}}{B^2}\int[\mathrm{d}\boldsymbol{k}](\frac{\partial f}{\partial \boldsymbol{k}}\cdot\boldsymbol{\Omega})[\boldsymbol{k}\cdot(\boldsymbol{B}\times\boldsymbol{E})] \\ &= -e\frac{\boldsymbol{B}}{B^2}\int[\mathrm{d}\boldsymbol{k}]\Big(\frac{\partial}{\partial \boldsymbol{k}}(f\boldsymbol{\Omega}[\boldsymbol{k}\cdot(\boldsymbol{B}\times\boldsymbol{E})]) - f\boldsymbol{\Omega}\cdot\frac{\partial}{\partial \boldsymbol{k}}[\boldsymbol{k}\cdot(\boldsymbol{B}\times\boldsymbol{E})]\Big) \\ &= -e\frac{\boldsymbol{B}[(\boldsymbol{E}\times\boldsymbol{B})\cdot\boldsymbol{\sigma}_{AH}]}{B^2} = e\frac{\boldsymbol{B}[(\boldsymbol{E}\times\boldsymbol{\sigma}_{AH})\cdot\boldsymbol{B}]}{B^2}\,.\end{aligned} \tag{6.27}$$

Introducing the unit vector $\boldsymbol{b} = \boldsymbol{B}/B$, the total current is

$$\begin{aligned}\boldsymbol{j} &= \boldsymbol{j}_{AH} + \boldsymbol{j}_H + \boldsymbol{j}_B \\ &= -e\Big(\boldsymbol{E}\times\boldsymbol{\sigma}_{AH} + \boldsymbol{E}\times\boldsymbol{b}\frac{\tilde{n}}{B} - [(\boldsymbol{E}\times\boldsymbol{\sigma}_{AH})\cdot\boldsymbol{b}\Big) \\ &= -e\Big((\boldsymbol{E}\times\boldsymbol{\sigma}_{AH})_\perp + \boldsymbol{E}\times\boldsymbol{b}\frac{\tilde{n}}{B}\Big)\,.\end{aligned} \tag{6.28}$$

Recalling that $\boldsymbol{E}\cdot\boldsymbol{B} = 0$, so $(\boldsymbol{E}\times\boldsymbol{\sigma})_\perp = \boldsymbol{E}\times\sigma_z\boldsymbol{b} = (\boldsymbol{E}\times\boldsymbol{B})(\boldsymbol{B}\cdot\boldsymbol{\Omega})/B^2$. Thus

$$\boldsymbol{j} = -e\frac{\boldsymbol{E}\times\boldsymbol{B}}{B^2}\int[\mathrm{d}\boldsymbol{k}]f(\boldsymbol{k})(1+\boldsymbol{B}\cdot\boldsymbol{\Omega}) = -e\frac{\boldsymbol{E}\times\boldsymbol{B}}{B^2}\int[\mathrm{d}\boldsymbol{k}]f(\boldsymbol{k})D(\boldsymbol{k})\,. \tag{6.29}$$

[2] We assume there is no magnetic monopole in the $\boldsymbol{k}$-space, i.e., $\boldsymbol{\nabla}_{\boldsymbol{k}}\cdot\boldsymbol{\Omega} = 0$.

According to (2.6) the integral is the exact electron density. Therefore in the high field limit we reach the following conclusion: the total current in crossed electric and magnetic fields is the Hall current as calculated from free electron model

$$\boldsymbol{j} = -e\frac{\boldsymbol{E}\times\boldsymbol{B}}{B^2}n\ , \tag{6.30}$$

and has no dependence on the relaxation time τ. This result ensures that even in the presence of anomalous Hall effect, the hight field Hall current gives the "real" electron density.

In above calculation we ignored the change of Fermi surface. This should not affect our final conclusion because by definition the electron density should be the integral of the modified distribution function, which already includes the Fermi surface change.

Let us now consider the hole-like band. The expression for $\boldsymbol{j}_{AH}$ remains the same. In the normal Hall current the charge carrier density should be calculated using $1-f$. The same goes to $\boldsymbol{j}_B$. We have

$$\boldsymbol{j}_H^{\text{hole}} = \boldsymbol{j}_H + e\frac{\boldsymbol{E}\times\boldsymbol{B}}{B^2}\int[\mathrm{d}\boldsymbol{k}]\ , \tag{6.31}$$

$$\boldsymbol{j}_B^{\text{hole}} = \boldsymbol{j}_B - e\frac{\boldsymbol{B}}{B^2}(\boldsymbol{B}\times\boldsymbol{E})\cdot\int[\mathrm{d}\boldsymbol{k}]\boldsymbol{\Omega}\ . \tag{6.32}$$

Then we have for hole-like bands, the total current is given by

$$\boldsymbol{j}^{\text{hole}} = e\frac{\boldsymbol{E}\times\boldsymbol{B}}{B^2}\int[\mathrm{d}\boldsymbol{k}]D(\boldsymbol{k})[1-f(\boldsymbol{k})] - e\boldsymbol{E}\times\int[\mathrm{d}\boldsymbol{k}]\boldsymbol{\Omega}\ . \tag{6.33}$$

So for the hole-like band, there is an additonal term in the current expression proportional to the Chern number (the second integral) of the band.

6.5 The Low Field Limit

We now exam the Boltzmann equation after the necessary modification to the equations of motion. The Boltzmann equation governs the evolution of the distribution function, which describes the number of electrons in state $(\boldsymbol{r},\boldsymbol{k})$. In the collisionless case, since the total number of electrons along a trajectory in phase space is

conserved, we can write down the continuity equation for f,

$$\frac{df}{dt} = \frac{\partial f}{\partial t} + \dot{\boldsymbol{r}} \cdot \frac{\partial f}{\partial \boldsymbol{r}} + \dot{\boldsymbol{k}} \cdot \frac{\partial f}{\partial \boldsymbol{k}} = 0 \; . \tag{6.34}$$

In the presence of collision, in which electrons are kicked in/out of the vicinity of the trajectory, a collision integral needs to be added to the right side. For a system in steady state and satisfying the isothermal condition (i.e., diffusion term absent), the Boltzmann equation in the relaxation-time approximation is given by

$$\dot{\boldsymbol{k}} \cdot \frac{\partial f}{\partial \boldsymbol{k}} = -\frac{f - f_0}{\tau} \; , \tag{6.35}$$

where τ is the characteristic relaxation time.

At the low field limit $\omega_c \tau \ll 1$ the collision processes are important and deserve a careful treatment. We show that even in the simple relaxation-time approximation, some correction is necessary. Because of its nature, the semiclassical formalism cannot give information on the change of τ in a magnetic field. We consider elastic impurity scattering, which is the dominant source of collision at low temperatures. The collision term is given by [4]

$$\frac{\partial f}{\partial t}\Big|_{\text{coll}} = -\int [\mathrm{d}\boldsymbol{k}'] D(\boldsymbol{k}') W_{\boldsymbol{k}\boldsymbol{k}'} [f(\boldsymbol{k}) - f(\boldsymbol{k}')] \; , \tag{6.36}$$

where $W_{\boldsymbol{k}\boldsymbol{k}'}$ is the transition probability from $\boldsymbol{k}'$ to $\boldsymbol{k}$ state. Note that the density of states explicitly enters into the expression. In the relaxation-time approximation we make the assumption that a characteristic relaxation time exists so that

$$\frac{f - f_0}{\tau} = D(\boldsymbol{k}) \int [\mathrm{d}\boldsymbol{k}'] \frac{D(\boldsymbol{k}')}{D(\boldsymbol{k})} W_{\boldsymbol{k}\boldsymbol{k}'} [f(\boldsymbol{k}) - f(\boldsymbol{k}')] \; . \tag{6.37}$$

Our hope is that the integral in the above equation becomes insensitive to the field. Then we can write

$$\tau = \frac{\tau_0}{D(\boldsymbol{k})} \approx \tau_0 \Big(1 - \frac{e}{\hbar} \boldsymbol{B} \cdot \boldsymbol{\Omega} \Big) \; . \tag{6.38}$$

More generally, we can always expand the relaxation time to first order of $(e/\hbar)\boldsymbol{B}\cdot\boldsymbol{\Omega}$,

$$\tau = \tau_0 + \tau_1 \frac{e}{\hbar} \boldsymbol{B} \cdot \boldsymbol{\Omega} \; , \tag{6.39}$$

where τ_1 should be regarded as a fitting parameter within this theory.

Finding the solution of the Boltzmann equation at the low field limit $\omega_c\tau \ll 1$ is relatively simple. Jones and Zener [66] proposed the following method to expand the solution in power series of $\omega_c\tau$. If we write $f = f_0 + g$, the Boltzmann equation becomes

$$(1 - \mathbf{U})g = -\hbar\tau\dot{\boldsymbol{k}} \cdot \boldsymbol{v}\frac{\partial f_0}{\partial \varepsilon} \ , \tag{6.40}$$

with the differential operator $\mathbf{U}$ defined by

$$\mathbf{U} \equiv -\tau\dot{\boldsymbol{k}} \cdot \frac{\partial}{\partial \boldsymbol{k}} \ . \tag{6.41}$$

If $\mathbf{U}$ is small compared to unity ($\omega_c\tau \ll 1$) and the inverse of $(1 - \mathbf{U})$ exists, we can write solution of g formally in power series of $\mathbf{U}$ as

$$\begin{aligned} g &= (1 - \mathbf{U})^{-1}\Big(-\hbar\tau\dot{\boldsymbol{k}} \cdot \boldsymbol{v}\frac{\partial f_0}{\partial \varepsilon}\Big) \\ &= (1 + \mathbf{U} + \mathbf{U}^2 + \cdots)\Big(-\hbar\tau\dot{\boldsymbol{k}} \cdot \boldsymbol{v}\frac{\partial f_0}{\partial \varepsilon}\Big) \ . \end{aligned} \tag{6.42}$$

Conventional approach – It is intuitive to see how this expansion is done using the conventional equations of motion [67]. Assuming the magnetic field is along the z-axis, we find that

$$\begin{aligned} g &= \Big(1 - \frac{e\tau}{\hbar}(\boldsymbol{v} \times \boldsymbol{B}) \cdot \frac{\partial}{\partial \boldsymbol{k}}\Big)^{-1}\Big(e\tau\boldsymbol{E} \cdot \boldsymbol{v}\frac{\partial f_0}{\partial \varepsilon}\Big) \\ &= e\tau\frac{\partial f_0}{\partial \varepsilon}\sum_{n=0}^{\infty}\Big[\frac{e\tau B}{\hbar}\Big(v_y\frac{\partial}{\partial k_x} - v_x\frac{\partial}{\partial k_y}\Big)\Big]^n(E_\beta v_\beta) \ . \end{aligned} \tag{6.43}$$

Consequently, the components of the conductivity tensor can be written in power series of B,

$$\begin{aligned} \sigma_{\alpha\beta}(B) &= \sum_{n=0}^{\infty}\sigma_{\alpha\beta}^{(n)}(B) \ , \\ \sigma_{\alpha\beta}^{(n)}(B) &= -e^2\tau\int[\mathrm{d}\boldsymbol{k}]\frac{\partial f_0}{\partial \varepsilon}v_\alpha\Big[\frac{e\tau B}{\hbar}\Big(v_y\frac{\partial}{\partial k_x} - v_x\frac{\partial}{\partial k_y}\Big)\Big]^n v_\beta \ . \end{aligned} \tag{6.44}$$

We explicitly write down the conductivity tensor to first order in B:

$$\sigma^{(0)}_{\alpha\beta} = -e^2\tau \int [\mathrm{d}\boldsymbol{k}] \frac{\partial f_0}{\partial \varepsilon} v_\alpha v_\beta \ , \tag{6.45}$$

$$\sigma^{(1)}_{\alpha\beta} = -e^2\tau \frac{e\tau B}{\hbar} \int [\mathrm{d}\boldsymbol{k}] \frac{\partial f_0}{\partial \varepsilon} v_\alpha \Big(v_y \frac{\partial}{\partial k_x} - v_x \frac{\partial}{\partial k_y} \Big) v_\beta \ . \tag{6.46}$$

If the crystal has rotational symmetry around the z-axis, then both $\sigma^{(0)}_{xy}$ and $\sigma^{(1)}_{xx}$ vanish. The conductivity tensor thus takes the form of

$$\overleftrightarrow{\sigma} = \begin{pmatrix} \sigma^{(0)}_{xx} + \sigma^{(2)}_{xx} & \sigma^{(1)}_{xy} \\ -\sigma^{(1)}_{xy} & \sigma^{(0)}_{xx} + \sigma^{(2)}_{xx} \end{pmatrix} \ . \tag{6.47}$$

To lowest power of B the magnetoresistance is given by

$$\frac{\Delta\rho}{\rho_0} = -\frac{\sigma^{(0)}_{xx}\sigma^{(2)}_{xx} + (\sigma^{(1)}_{xy})^2}{(\sigma^{(0)}_{xx})^2} \ , \tag{6.48}$$

which predicts a magnetoresistance quadratic in B.

However, in the presence of the Berry curvature, both $\sigma^{(1)}_{xx}$ and $\sigma^{(0)}_{xy}$ can be nonzero. The former comes from the expansion of $(e/\hbar)\boldsymbol{B}\cdot\boldsymbol{\Omega}$ and the latter is the anomalous Hall conductivity. The conductivity tensor can be written

$$\overleftrightarrow{\sigma} = \begin{pmatrix} \sigma^{(0)}_{xx} + \sigma^{(1)}_{xx} & \sigma^{(0)}_{xy} + \sigma^{(1)}_{xy} \\ -\sigma^{(0)}_{xy} - \sigma^{(1)}_{xy} & \sigma^{(0)}_{xx} + \sigma^{(1)}_{xx} \end{pmatrix} \ . \tag{6.49}$$

To first order in B the magnetoresistance is given by

$$\frac{\Delta\rho}{\rho_0} = -\frac{[(\sigma^{(0)}_{xx})^2 - (\sigma^{(0)}_{xy})^2]\sigma^{(1)}_{xx} + 2\sigma^{(0)}_{xx}\sigma^{(0)}_{xy}\sigma^{(1)}_{xy}}{\sigma^{(0)}_{xx}[(\sigma^{(0)}_{xx})^2 + (\sigma^{(0)}_{xy})^2]} \ . \tag{6.50}$$

In most cases we have $\sigma^{(0)}_{xx} \gg \sigma^{(0)}_{xy}$. Using this condition we can simplify the above equation:

$$\frac{\Delta\rho}{\rho_0} = -\Big[\frac{\sigma^{(1)}_{xx}}{\sigma^{(0)}_{xx}} + \frac{2\sigma^{(0)}_{xy}\sigma^{(1)}_{xy}}{(\sigma^{(0)}_{xx})^2}\Big] \ . \tag{6.51}$$

The first term is due to the implicit inclusion of the Berry curvature. In the second

term, $\sigma_{xy}^{(0)}$ is the anomalous Hall conductivity σ_{AH} and $\sigma_{xy}^{(1)}$ is the Hall conductivity σ_H. Weitering's data shows that

$$\frac{\sigma_{AH}}{\sigma_{xx}} \sim \frac{\sigma_H}{\sigma_{xx}} \sim 5\% \; .$$

Obviously the second term cannot explain the 5% magnetoresistance observed in the experiment. Thus the main contribution must come from the first term,

$$\frac{\Delta\rho}{\rho_0} = -\frac{\sigma_{xx}^{(1)}}{\sigma_{xx}^{(0)}} \; , \tag{6.52}$$

for which only the diagonal elements of the conductivity tensor need to be calculated. (But if it turns out that this part is also too small then our theory ... It is too desperate to even think about this possibility!)

Now we use equations (6.10) to solve the Boltzmann equation. We consider the geometry of crossed electric and magnetic fields, $\boldsymbol{E} \perp \boldsymbol{B}$. The Jones and Zener expansion (6.42) to first order in B reads

$$\begin{aligned} g &= \Big(1 + \frac{e\tau}{\hbar}\frac{\boldsymbol{v}\times\boldsymbol{B}}{D(\boldsymbol{k})}\cdot\frac{\partial}{\partial\boldsymbol{k}}\Big)\Big(e\tau\frac{\boldsymbol{E}\cdot\boldsymbol{v}}{D(\boldsymbol{k})}\frac{\partial f_0}{\partial\varepsilon}\Big) \\ &= \frac{\partial f_0}{\partial\varepsilon}\Big[e\tau\frac{\boldsymbol{E}\cdot\boldsymbol{v}}{D(\boldsymbol{k})} + \frac{e\tau_0}{\hbar}(\boldsymbol{v}\times\boldsymbol{B})\cdot\frac{\partial}{\partial\boldsymbol{k}}\Big(e\tau_0\boldsymbol{E}\cdot\boldsymbol{v}\Big)\Big] \; . \end{aligned} \tag{6.53}$$

In the second term we have neglected all the $D(\boldsymbol{k})$ dependence because it is already linear in B. If the crystal has rotational symmetry around the z-axis, the second term only contributes to the off-diagonal elements of the conductivity tensor, as shown in equation (6.46) in the conventional approach part. The only interesting part to us is

$$g = e\tau\frac{\partial f_0}{\partial\varepsilon}\frac{\boldsymbol{E}\cdot\boldsymbol{v}}{D(\boldsymbol{k})} \; . \tag{6.54}$$

It follows that the diagonal element of the conductivity tensor is

$$\sigma_{xx} = -e^2\int[\mathrm{d}\boldsymbol{k}]\tau\frac{\partial f_0}{\partial\varepsilon}\frac{v_x^2}{D(\boldsymbol{k})} \; . \tag{6.55}$$

This is just the zeroth order expansion based on $\omega_c\tau$. The linear magnetoresistance comes from the $(e/\hbar)B\Omega$ correction to this expression. Recalling that both the

relaxation time τ and the "normal" velocity $\boldsymbol{v}$ have a field dependent part:

$$\tau = \frac{\tau_0}{D(\boldsymbol{k})} ,$$
$$v_x = \frac{1}{\hbar}\frac{\partial(\varepsilon_0 - m_z B)}{\partial k_x} = v_x^{(0)} - \frac{1}{\hbar}\frac{\partial m_z}{\partial k_x} B ,$$

we expand expression (6.55) to first order of B,

$$\sigma_{xx} = -e^2\tau_0 \int [\mathrm{d}\boldsymbol{k}] \frac{\partial f_0}{\partial \varepsilon} \Big[(v_x^{(0)})^2 - B\Big(\frac{2e\Omega_z}{\hbar}(v_x^{(0)})^2 + \frac{2}{\hbar}\frac{\partial m_z}{\partial k_x} v_x^{(0)} \Big) \Big] . \tag{6.56}$$

In the following we shall just write v_x for $v_x^{(0)}$. So far we have not considered the change of Fermi volume yet. The first term in the above equation can be written as

$$-e^2\tau_0 \int [\mathrm{d}\boldsymbol{k}] \frac{\partial f_0}{\partial \varepsilon} v_x^2 = e^2\tau_0 \int [\mathrm{d}\boldsymbol{k}] f_0 (\mathbf{M})^{-1}_{xx} , \tag{6.57}$$

where $\mathbf{M}$ is the effect mass tensor defined by

$$(\mathbf{M})^{-1}_{\alpha\beta} \equiv \frac{1}{\hbar^2}\frac{\partial^2 \varepsilon}{\partial k_\alpha \partial k_\beta} . \tag{6.58}$$

The change of the Fermi volume leads to a change of the conductivity

$$e^2\tau_0 \int [\mathrm{d}\boldsymbol{k}] \frac{\partial f_0}{\partial \varepsilon} (\delta\varepsilon - \delta\mu)(\mathbf{M})^{-1}_{xx} . \tag{6.59}$$

If $(\mathbf{M})^{-1}$ has spherical symmetry on the surface, we can use equation (6.9) to convert this surface integral to a volume integral of the Berry curvature over the Fermi sea. Finally, we sum over all the linear-in-B terms and find that the change in the conductivity is

$$\sigma_{xx}^{(1)} = e^2\tau_0 \int [\mathrm{d}\boldsymbol{k}] \frac{\partial f_0}{\partial \varepsilon} \Big[\Big(\frac{2e\Omega_z}{\hbar} v_x^2 + \frac{2}{\hbar}\frac{\partial m_z}{\partial k_x} v_x \Big) B + (\delta\varepsilon - \delta\mu)(\mathbf{M})^{-1}_{xx} \Big] \tag{6.60}$$
$$= e^2\tau_0 B \Big[\int [\mathrm{d}\boldsymbol{k}] \frac{\partial f_0}{\partial \varepsilon} \Big(\frac{2e\Omega_z}{\hbar} v_x^2 + \frac{2}{\hbar}\frac{\partial m_z}{\partial k_x} v_x \Big) - \frac{e}{\hbar} \langle (\mathbf{M})^{-1}_{xx} \rangle_{k_F} \int [\mathrm{d}\boldsymbol{k}] f \Omega_z \Big] . \tag{6.61}$$

The zero-field conductivity takes the usual form

$$\sigma_{xx}^{(0)} = -e^2\tau_0 \int [\mathrm{d}\boldsymbol{k}] \frac{\partial f_0}{\partial \varepsilon} v_x^2 . \tag{6.62}$$

According to (6.52), the ratio $-\sigma_{xx}^{(1)}/\sigma_{xx}^{(0)}$ will then give us the Berry-phase induced magnetoresistance.

Chapter 7

Valley Hall Effect and Electrically Induced Magnetization in Graphene

7.1 Introduction

The extraordinary physical properties of graphene have offered great application potential of carbon based electronic devices [68]. The band structure of graphene has two degenerate valleys at the corners of the Brillouin zone, where the conduction and valence bands conically touch each other. Since the intervalley scattering is negligible in pure graphene samples, the valley degree of freedom can be exploited in electronic devices in the same way spin is used in spintronics [69]. The central question to valleytronics thus is how to generate and detect the valley polarization. Here we predict that in graphene with broken inversion symmetry, a valley Hall current can be induced by applying an electric field. As a result, a finite valley polarization will accumulate on the boundary. Moreover, we show that this valley polarization is always accompanied by a sizable magnetization. Our method provides an effective way to electrically induce magnetization in graphene.

The recently observed quantum Hall effect in graphene [70, 71] and bilayer graphene [72] has unambiguously demonstrated the existence of the Berry phase of the electron wavefunction and its importance in the quantization of energy levels. It has been shown [6, 7] that the Berry phase can also affect the electron dynamics

through a vector field called the Berry curvature. The Berry phase accumulated by an electron along a loop in the momentum space is equal to the flux of the Berry curvature through the surface enclosed by this loop. In the presence of an electric field, an electron will acquire a transverse velocity proportional to the Berry curvature. In ferromagnetic materials, summing this velocity over occupied electronic states leads to a large intrinsic contribution to the Hall current in the absence of a magnetic field, known as the anomalous Hall effect [40, 10, 11]. However, such an effect is absent in graphene due to time-reversal symmetry. In addition, graphene also has inversion symmetry. The presence of both symmetries requires that the Berry curvature vanishes everywhere except at those degenerate points called Dirac points, where it becomes singular. To engineer a Berry phase effect, we explicitly break the inversion symmetry of the lattice, which gives the Berry curvature a very rich structure. Our proposed valley Hall effect is a direct manifestation of the Berry curvature.

Figure 7.1 schematically shows the valley Hall effect in graphene. A direct band gap opens at those Dirac points due to inversion symmetry breaking. Because the two valleys, labeled by $\boldsymbol{K}_1$ and $\boldsymbol{K}_2$, are related by time-reversal symmetry, their Berry curvatures have opposite signs. As a result, each valley will possess an anomalous Hall effect but with their Hall currents in opposite directions. The charge Hall currents from different valleys cancel each other exactly, resulting in a pure valley Hall current in the bulk. It will lead to a finite valley polarization with opposite signs on opposite boundaries. Furthermore, the appearance of a finite valley polarization effectively breaks the local time-reversal symmetry. The resulting magnetization, which is also related to the Berry curvature, is sufficiently large to be detected by magnetic resonance force microscopy or SQUID.

7.2 Valley Hall Effect in Monolayer Graphene

We now demonstrate the valley Hall effect. For simplicity, we first consider single-layer graphene and later extend our result to bilayer graphene. Graphene is a single layer of carbon atoms packed into a honeycomb lattice composed of two hexagonal sublattices. Its electronic properties can be well described by a standard nearest-neighbor tight-binding model [73]. To realize the valley Hall effect, it is necessary to break the inversion symmetry of the lattice. This can be done by

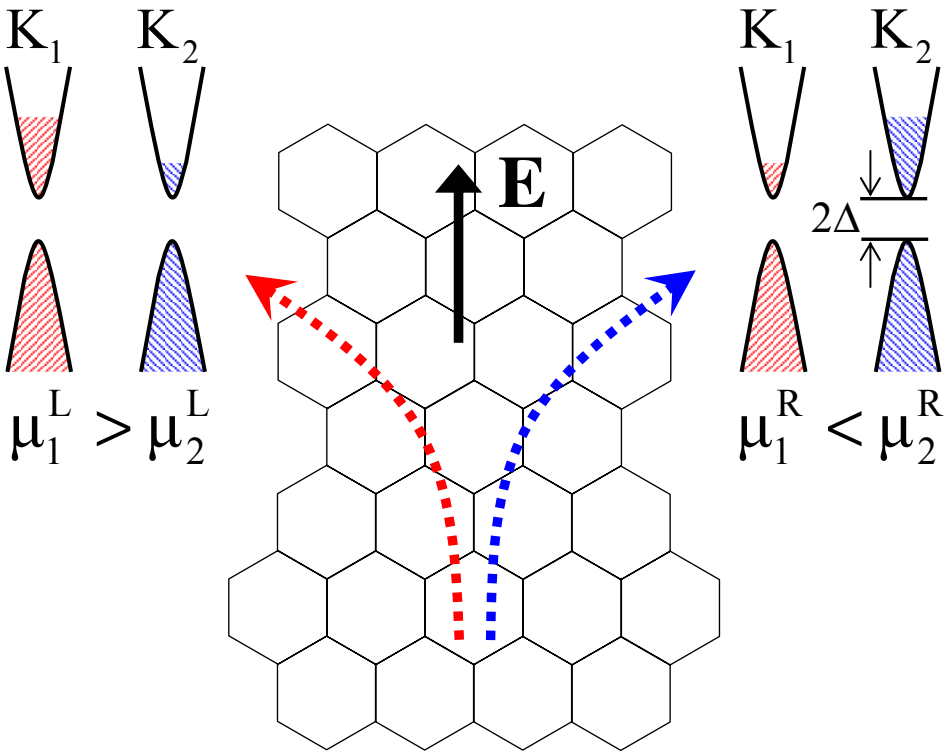

Figure 7.1: Schematic diagram of the valley Hall effect in graphene with inversion symmetry breaking. An energy gap (2Δ) opens at the Dirac points. In the presence of an electric field, electrons in different valleys will move towards opposite directions, giving rise to a pure valley Hall current. As a result, a finite valley polarization appears on the boundary. The valley polarization can be detected by measuring the magnetization along the boundary.

including a staggered sublattice potential $\pm\Delta$. The Hamiltonian takes the following form [74, 65, 75, 64]

$$H = -t \sum_{\langle i,j \rangle} c_i^\dagger c_j + \Delta \sum_i \xi_i c_i^\dagger c_i \ , \tag{7.1}$$

where $\langle i, j \rangle$ denotes nearest-neighbor pairs, t is the hopping energy, and $\xi_i = \pm 1$ for different sublattices. The electron spin degree of freedom is suppressed because of the extremely small spin-orbit coupling in graphene [76, 77]. In practice, the staggered sublattice potential can be induced by posing a strain on a graphene sheet so that one sublattice will move away from the substrate and the other will move towards the substrate. This possibility has been proposed to explain the spontaneous chiral symmetry breaking under a strong magnetic field [78].

Figure 7.2 shows the Berry curvature $\Omega(\boldsymbol{k})$ of the conduction band, defined as $\boldsymbol{\Omega}(\boldsymbol{k}) = \boldsymbol{\nabla}_{\boldsymbol{k}} \times \langle u(\boldsymbol{k}) | i \boldsymbol{\nabla}_{\boldsymbol{k}} | u(\boldsymbol{k}) \rangle$, where $|u(\boldsymbol{k})\rangle$ is the periodic part of the Bloch function [6, 7]. For two-dimensional systems $\boldsymbol{\Omega}(\boldsymbol{k}) = \Omega(\boldsymbol{k}) \hat{\boldsymbol{z}}$ is always along the $\hat{\boldsymbol{z}}$-axis. The valence-band Berry curvature has opposite sign. The distribution of $\Omega(\boldsymbol{k})$ has very sharp peaks around the corners of the Brillouin zone. Among these six corners, only two of them are inequivalent; we choose $\boldsymbol{K}_{1,2} = (\mp 4\pi/3a)\hat{\boldsymbol{x}}$, where $a = 2.46$ Å is the lattice constant. Note that Berry curvatures at valley $\boldsymbol{K}_1$ and $\boldsymbol{K}_2$ have opposite sign due to time-reversal symmetry, i.e., $\Omega(\boldsymbol{k}) = -\Omega(-\boldsymbol{k})$. At $\boldsymbol{K}_{1,2}$ the magnitude of $\Omega(\boldsymbol{k})$ reaches its maximum, $\Omega(\boldsymbol{K}_{1,2}) = \mp a^2/2\Delta_0^2$, where $\Delta_0 = 2\Delta/\sqrt{3}t$ is a dimensionless parameter. As Δ_0 approaches zero, $\Omega(\boldsymbol{k})$ becomes more and more concentrated in the valleys. When $\Delta_0 = 0$, the conduction and valence bands touch each other and $\Omega(\boldsymbol{k})$ vanishes everywhere except at $\boldsymbol{K}_{1,2}$ where it diverges. Despite of this fact, the Berry phase accumulated by an electron during one circle around the valley becomes exactly $\pm\pi$ when the gap closes. This Berry phase of π has been observed in the quantum Hall effect in graphene [71, 70].

In the following we consider n-doped graphene. Generalization to p-doped graphene is trivial due to electron-hole symmetry. To obtain analytical expressions, we resort to the low-energy description of the electron dynamics near $\boldsymbol{K}_{1,2}$. The

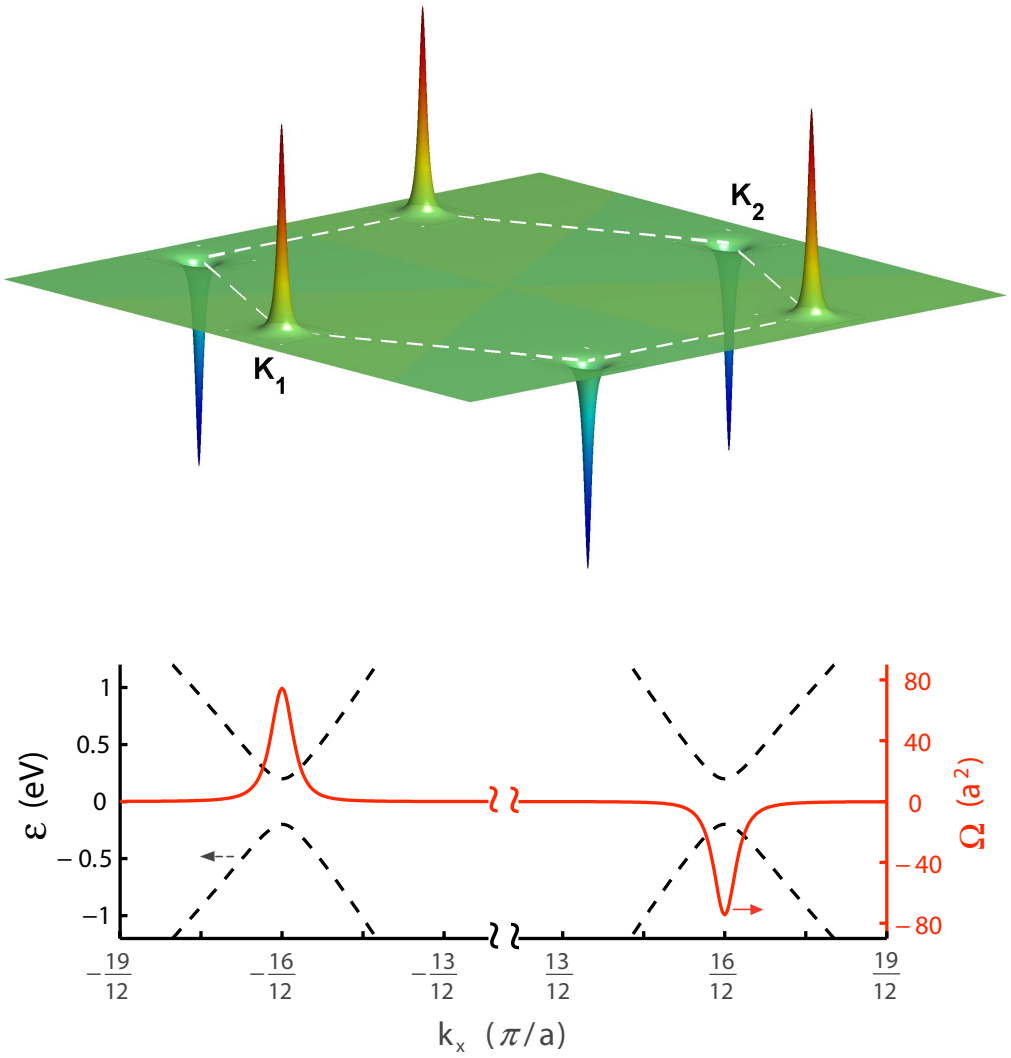

Figure 7.2: **Berry curvature of the conduction band.** The parameters used are $t = 2.82$ eV and $\Delta = 0.2$ eV. Top panel: The overall view of the Berry curvature in the Brillouin zone, indicated by dashed line. Bottom panel: Intersections of energy bands (dashed line) and the Berry curvature (solid line) around the valleys $\boldsymbol{K}_1$ and $\boldsymbol{K}_2$, along the line $k_y = 0$. The Berry curvature is sharped centered at the bottom of each valley.

Hamiltonian is given by (hereafter we set the lattice constant $a = 1$)

$$H = \begin{pmatrix} H_1(\boldsymbol{q}_1) & 0 \\ 0 & H_2(\boldsymbol{q}_2) \end{pmatrix} ,$$
$$H_{1,2}(\boldsymbol{q}) = q_y\sigma_y \mp q_x\sigma_x + \Delta_0\sigma_z ,$$

where $\boldsymbol{\sigma}$ is the Pauli matrix accounting for the sublattice index. The two diagonal blocks $H_{1,2}(\boldsymbol{q}_{1,2})$ describe electron dynamics around $\boldsymbol{K}_1$ and $\boldsymbol{K}_2$ with $\boldsymbol{q}_{1,2}$ measured from $\boldsymbol{K}_{1,2}$, respectively. They are time-reversal copies of each other. The vanishing off-diagonal block is a result of the negligible intervalley scattering. It allows us to treat electrons at different valleys independently.

Let us first consider valley $\boldsymbol{K}_1$, whose Berry curvature has the following form

$$\Omega_1(\boldsymbol{q}) = \frac{\Delta_0}{2(\Delta_0^2 + q^2)^{3/2}} . \tag{7.2}$$

The intrinsic contribution [40, 10, 11] to the Hall conductivity is given by $\sigma_H^{\rm int} = 2(e^2/\hbar)\sum_{\boldsymbol{q}} f(\boldsymbol{q})\Omega(\boldsymbol{q})$, where $f(\boldsymbol{q})$ is the Fermi-Dirac distribution function. In addition, there is a side jump contribution [79] from the Fermi surface that is also independent of scattering, $\sigma_H^{\rm sj} = 2(e^2/\hbar)\sum_{\boldsymbol{q}}(\partial f/\partial\mu)\Omega(\boldsymbol{q})(\partial\varepsilon_{\boldsymbol{q}}/\partial\boldsymbol{q})\cdot\boldsymbol{q}$. We have included a factor of 2 from the spin degeneracy in the above expressions. The scattering-independent Hall conductivity at valley $\boldsymbol{K}_1$ thus is

$$\begin{aligned} \sigma_{H1} &= \sigma_H^{\rm int} + \sigma_H^{\rm sj} \\ &= \frac{e^2}{h}\Big[1 - \frac{\Delta_0}{\sqrt{\Delta_0^2 + q_F^2}} - \frac{\Delta_0 q_F^2}{(\Delta_0^2 + q_F^2)^{3/2}}\Big] . \end{aligned} \tag{7.3}$$

As we discussed before, because of time-reversal symmetry, electrons at $\boldsymbol{K}_2$ will also contribute the same amount of Hall current but in the opposite direction. The net result is a pure valley Hall current in the bulk. Accordingly, at the boundary of the sample a finite valley "polarization" is expected,

$$\int \delta n_v \, dx = j\tau_v = 2\frac{\sigma_{H1}\tau_v}{e}E , \tag{7.4}$$

where δn_v is the population difference between the two valleys, $\hat{\boldsymbol{x}}$ is the normal

direction of the boundary, and τ_v is the characteristic intervalley scattering time.

In the above we only considered the scattering-independent contribution to σ_H, which is the dominate contribution when scattering is relatively strong. In principle, the Hall conductivity σ_H also has other contributions such as skew scattering, which becomes important in clean samples at low temperature [80]. It is noteworthy that in order for the intrinsic contribution to survive, the energy gap 2Δ has to be sufficiently large so that impurity scattering cannot mix the conduction and valence bands. Nonetheless, the existence of the valley Hall effect is general consequence of inversion symmetry breaking and does not depend on the underlying mechanism.

Next we show that a finite valley polarization is always accompanied by a magnetization. In addition to the Berry curvature $\boldsymbol{\Omega}(\boldsymbol{k})$, there is another characteristic quantity of electrons at different valleys, namely, the orbital magnetic moment $\boldsymbol{m}(\boldsymbol{k})$ defined as $\boldsymbol{m}(\boldsymbol{k}) = -i(e/2\hbar)\langle\nabla_{\boldsymbol{k}}u| \times [H(\boldsymbol{k}) - \varepsilon_{\boldsymbol{k}}]|\boldsymbol{\nabla}_{\boldsymbol{k}}u\rangle_z$ [6, 7]. This magnetic moment originates from the self-rotation of the electron wave packet, and has the property $\boldsymbol{m}(\boldsymbol{k}) = -\boldsymbol{m}(-\boldsymbol{k})$ in the presence of time-reversal symmetry. Intuitively, a finite valley polarization means that one valley has more magnetic moments than the other, which will give a net magnetization. This is indeed the case. Since the electron spin degree of freedom is frozen, the magnetization comes purely from the orbital part. At zero temperature the orbital magnetization is given by [35, 28] $M = 2\sum_{\boldsymbol{k}}[m(\boldsymbol{k}) + (e/\hbar)(\mu - \varepsilon_{\boldsymbol{k}})\Omega(\boldsymbol{k})]$, where μ is the chemical potential. Note that there is an additional term from the Berry correction. For the conduction band $m(\boldsymbol{k}) = (e/\hbar)\varepsilon_{\boldsymbol{k}}\Omega(\boldsymbol{k})$, we thus have $M = (e/\hbar)\mu\sum_{\boldsymbol{k}}\Omega(\boldsymbol{k})$. If $\mu_1 \neq \mu_2$, the net magnetization is given by

$$\delta M = 2\frac{e}{\hbar}[\mu_1\Omega_1(\mu_1) + \mu_2\Omega_2(\mu_2)] \approx 2\frac{e}{\hbar}\Omega_1(\mu)\delta\mu \;, \tag{7.5}$$

where $\Omega_i(\mu)$ is the sum of the Berry curvature over states below μ in valley $\boldsymbol{K}_i$. We have used the property that $\Omega(\boldsymbol{k})$ is highly concentrated around the valley bottom, therefore $\Omega_1(\mu_1) \approx -\Omega_2(\mu_2) \approx \Omega_1(\mu)$ with μ the unperturbed chemical potential. Hence the boundary magnetization is given by

$$M_{\text{edge}} = \int M\, dx = \frac{4}{\hbar}\frac{\partial\mu}{\partial n}\Omega_1(\mu)\sigma_{H1}\tau_v E \;. \tag{7.6}$$

7.3 Valley Hall Effect in Bilayer Graphene

So far we have demonstrated the valley Hall effect using a relatively simple model. While the strain induced inversion symmetry breaking in graphene remains to be seen, we propose that a more realistic system to observe the valley Hall effect is bilayer graphene. A recent study [81] using angle-resolved photoemission spectroscopy shows that in bilayer graphene with staggered stacking, a gap can be opened in the energy spectrum. This can be explained using the biased graphene bilayer model [82, 83] where an out-of-plane electric field breaks the inversion symmetry of the lattice. In this case, the energy gap is due to the difference in electrostatic potentials in the two layers. The Berry curvature of bilayer graphene is similar to that of the single-layer graphene, i.e., highly concentrated in each valley with different sign. Therefore our previous arguments about the single-layer graphene also applies here.

Figure 7.3 shows the predicted valley Hall effect in bilayer graphene. Our calculation is done by numerically diagonalizing the biased graphene bilayer Hamiltonian [82, 83] with three parameters, namely, the intralayer hopping t, the interlayer hopping $t_\perp$, and the energy gap Δ. The parameter values are chosen so that the band structure matches the experiment result [81]. Bilayer graphene has two positive energy bands (conduction) and two negative energy bands (valence). As we can see, the Berry curvature $\Omega(\boldsymbol{k})$ and the magnetic moment $m(\boldsymbol{k})$ of the lower conduction band are more prominent than those of the upper conduction band. The temperature dependence of σ_H, M and M_{edge} is not significant except in the range where μ is near the band bottom. As the Fermi energy sweeps through this range, a dip appears in σ_H and M_{edge} because of the fine structures of the Berry curvature. At low temperature, the sign change of the boundary magnetization (Fig. 7.3f) at around $\mu = 0.15$ eV provides a check of our theory. At high temperatures, these features are smeared out.

Since the actual value of the intervalley scattering time τ_v is unknown, we provide some crude estimations. The intravalley scattering time is about $\tau_0 = 0.1$ ps. We choose τ_v to be 10^2 ps. Then at the doping level that can be experimentally accessed [81], indicated by an arrow in Fig. 7.3f, the boundary magnetization is 2×10^3 μ_B/μm. The valley polarization will accumulate near the boundary within the range of the valley diffusion length, which is $v_F\sqrt{\tau_0\tau_v/2} \sim 10$ μm. This gives us

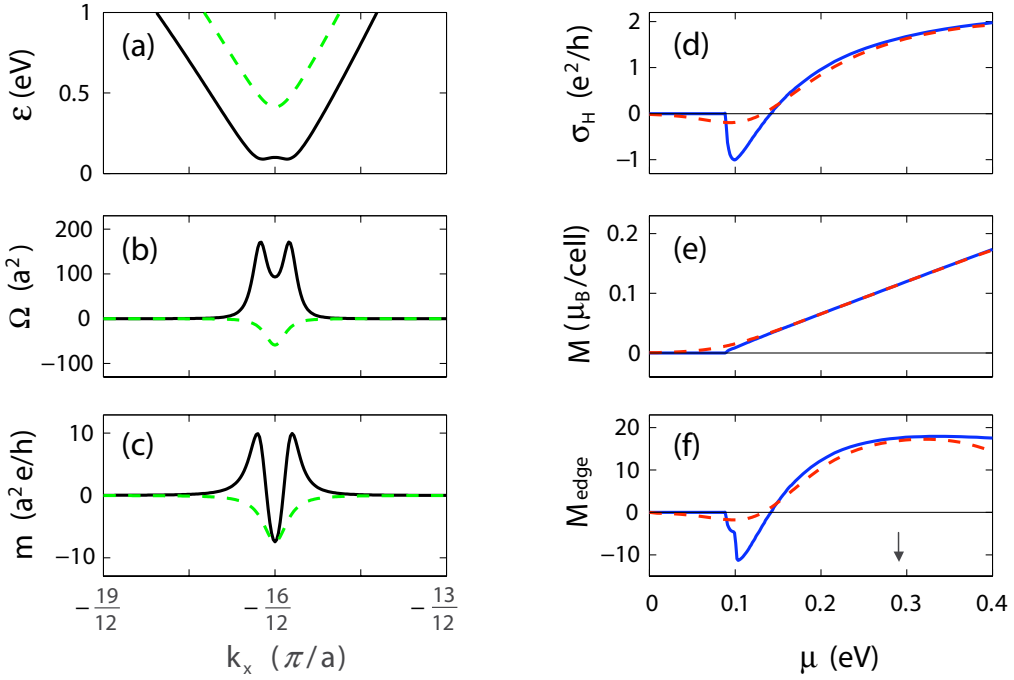

Figure 7.3: Valley Hall effect in bilayer graphene with inversion symmetry breaking. The parameters used are $t = 2.82$ eV, $\Delta = 0.2$ eV, and $t_\perp = 0.4$ eV. Left column: (a) Band structure, (b) Berry curvature, and (c) magnetic moment of the lower (black solid line) and upper (green dashed line) conduction bands around valley $\boldsymbol{K}_1$. Right column: (d) Hall conductivity and (e) magnetization of one valley, (f) accumulated boundary magnetization at $T = 4.5$ K (blue solid line) and $T = 300$ K (red dashed line). In (f) the units for $M_{\rm edge}$ is $\tau_V E\ \mu_B/\mu$m, where τ_V is in the units of ps and E mV/μm.

about 10^2 $\mu_B/\mu\mathrm{m}^2$ on the boundary. This is a magnetic signal that can be detected by magnetic resonance force microscopy or SQUID.

We emphasize that this method is not limited to the detection of the valley Hall effect. For example, in the recently proposed valley filter experiment [78], a finite valley polarization can be created by passing a current through a point contact with zigzag edge. This valley polarization can be also detected by our method.

Appendix A

Derivation of the Berry-Phase Modified Density of states

A.1 Time Evolution of a Volume Element in Phase Space

In this section we derive the equation of motion for a phase space volume element. Consider a dynamical system with coordinates $\boldsymbol{\xi} = (\boldsymbol{r}, \boldsymbol{k})$, whose dynamics is governed by

$$\dot{\xi}^a = f^a(\boldsymbol{\xi}, t) \; . \tag{A.1}$$

A volume element ΔV in phase space changes in time according to the equation

$$\Delta V(t) = J(t, t_0) \Delta V(t_0) \; , \tag{A.2}$$

where $J(t, t_0)$, the Jacobian of the transformation, is defined by

$$J(t, t_0) = \det |\mathbf{M}| \; , \qquad M_{ab} = \frac{\partial \xi^a(t)}{\partial \xi^b(t_0)} \; . \tag{A.3}$$

Let us now assume that the system evolves for a short time interval $\Delta t = t - t_0$. Then the coordinates of a point can be written as

$$\xi^a(t) = \xi^a(t_0) + \dot{\xi}^a(t_0) \Delta t \; . \tag{A.4}$$

To first order of Δt we find that

$$J(t,t_0) = \det\Big|\mathbf{I} + \frac{\partial\dot{\xi}^a(t_0)}{\partial\xi^b(t_0)}\Delta t\Big| = 1 + \frac{\partial\dot{\xi}^a(t_0)}{\partial\xi^a(t_0)}\Delta t \tag{A.5}$$

Inserting above equation into Eq. (A.2) yields

$$\Delta V(t_0+\Delta t) = \Big(1 + \frac{\partial\dot{\xi}^a(t_0)}{\partial\xi^a(t_0)}\Delta t\Big)\Delta V(t_0)\ , \tag{A.6}$$

or

$$1 + \frac{1}{\Delta V(t_0)}\frac{d\Delta V(t_0)}{dt_0}\Delta t = 1 + \frac{\partial\dot{\xi}^a(t_0)}{\partial\xi^a(t_0)}\Delta t\ . \tag{A.7}$$

Hence the time evolution of a volume element satisfies

$$\frac{1}{\Delta V}\frac{d\Delta V}{dt} = \boldsymbol{\nabla}_{\boldsymbol{r}}\cdot\dot{\boldsymbol{r}} + \boldsymbol{\nabla}_{\boldsymbol{k}}\cdot\dot{\boldsymbol{k}}\ . \tag{A.8}$$

For a system whose dynamics is determined by Hamiltonian's equations, i.e., $\dot{\boldsymbol{r}} = \partial H/\partial\boldsymbol{k}$ and $\dot{\boldsymbol{k}} = -\partial H/\partial\boldsymbol{r}$, it is obvious that the right hand side of the equation vanishes and the volume is a constant. But for the Berry phase modified dynamics this is generally not true, as shown below.

A.2 Liouville's Theorem for the Berry Phase Modified Dynamics

In this section we apply the general equation (A.8) to the Berry phase modified electron dynamics to find out how a volume element evolves in phase space. For simplicity of the notation, we set $e/\hbar = 1$; in other words, the electric and magnetic field absorb a factor of $e/\hbar$. The electron charge is taken to be $-e$. To begin with, we write down the semiclassical equations of motion

$$\dot{\boldsymbol{r}} = \boldsymbol{v}(\boldsymbol{k}) - \dot{\boldsymbol{k}}\times\boldsymbol{\Omega}(\boldsymbol{k})\ , \tag{A.9}$$

$$\dot{\boldsymbol{k}} = -\boldsymbol{E}(\boldsymbol{r}) - \dot{\boldsymbol{r}}\times\boldsymbol{B}(\boldsymbol{r})\ , \tag{A.10}$$

with $\boldsymbol{v}(\boldsymbol{k}) \equiv \partial\varepsilon(\boldsymbol{k})/\partial\boldsymbol{k}$. Here the energy $\varepsilon(\boldsymbol{k}) = \varepsilon_0(\boldsymbol{k}) - \boldsymbol{m}\cdot\boldsymbol{B}$ includes a correction due to the magnetic moment of the electron, or the Wilkinson term. Inserting Eq. (A.10) into Eq. (A.9) and using the vector identity $(\boldsymbol{A}\times\boldsymbol{B})\times\boldsymbol{C} = (\boldsymbol{A}\cdot\boldsymbol{C})\boldsymbol{B} -$

$(\boldsymbol{B}\cdot\boldsymbol{C})\boldsymbol{A}$ yields

$$\dot{\boldsymbol{r}} = \boldsymbol{v} + \boldsymbol{E}\times\boldsymbol{\Omega} + (\dot{\boldsymbol{r}}\cdot\boldsymbol{\Omega})\boldsymbol{B} - (\boldsymbol{B}\cdot\boldsymbol{\Omega})\dot{\boldsymbol{r}} \,. \tag{A.11}$$

It is easy to verify that $\dot{\boldsymbol{r}}\cdot\boldsymbol{\Omega} = \boldsymbol{v}\cdot\boldsymbol{\Omega}$ by multiplying $\boldsymbol{\Omega}\cdot$ on both sides of Eq. (A.9). Then the above equation becomes

$$D(\boldsymbol{r},\boldsymbol{k})\dot{\boldsymbol{r}} = \boldsymbol{v} + \boldsymbol{E}\times\boldsymbol{\Omega} + (\boldsymbol{v}\cdot\boldsymbol{\Omega})\boldsymbol{B} \,, \tag{A.12}$$

where $D(\boldsymbol{r},\boldsymbol{k})$ is defined by

$$D(\boldsymbol{r},\boldsymbol{k}) \equiv 1 + \boldsymbol{B}\cdot\boldsymbol{\Omega} \,. \tag{A.13}$$

Similarly we have

$$D(\boldsymbol{r},\boldsymbol{k})\dot{\boldsymbol{k}} = -\boldsymbol{E} - \boldsymbol{v}\times\boldsymbol{B} - (\boldsymbol{E}\cdot\boldsymbol{B})\boldsymbol{\Omega} \,. \tag{A.14}$$

Now we apply $\boldsymbol{\nabla}_{\boldsymbol{r}}\cdot$ on Eq. (A.12). Keeping it in mind that $\varepsilon_0(\boldsymbol{k})$ and $\boldsymbol{\Omega}(\boldsymbol{k})$ are functions of only $\boldsymbol{k}$, we have

$$\boldsymbol{\nabla}_{\boldsymbol{r}}D\cdot\dot{\boldsymbol{r}} + D\boldsymbol{\nabla}_{\boldsymbol{r}}\cdot\dot{\boldsymbol{r}} = \boldsymbol{\nabla}_{\boldsymbol{r}}\cdot(\boldsymbol{E}\times\boldsymbol{\Omega}) + (\boldsymbol{v}\cdot\boldsymbol{\Omega})(\boldsymbol{\nabla}_{\boldsymbol{r}}\cdot\boldsymbol{B}) \,. \tag{A.15}$$

We have neglected a higher order term $\mathrm{Tr}(\boldsymbol{\nabla}_{\boldsymbol{r}}\boldsymbol{B}\cdot\boldsymbol{\nabla}_{\boldsymbol{k}}\boldsymbol{m})$. Introducing the scalar and vector potential ϕ and $\boldsymbol{A}$, we can write the electric and magnetic fields as

$$\boldsymbol{E} = -\boldsymbol{\nabla}_{\boldsymbol{r}}\phi - \frac{\partial\boldsymbol{A}}{\partial t} \,, \quad \boldsymbol{B} = -\boldsymbol{\nabla}_{\boldsymbol{r}}\times\boldsymbol{A} \,. \tag{A.16}$$

Inserting these expression into Eq. (A.15) and exchanging the order of $\partial/\partial t$ and $\boldsymbol{\nabla}_{\boldsymbol{r}}$ leads to

$$D\boldsymbol{\nabla}_{\boldsymbol{r}}\cdot\dot{\boldsymbol{r}} = -\frac{\partial(\boldsymbol{B}\cdot\boldsymbol{\Omega})}{\partial t} - \boldsymbol{\nabla}_{\boldsymbol{r}}D\cdot\dot{\boldsymbol{r}} = -\frac{\partial D}{\partial t} - \boldsymbol{\nabla}_{\boldsymbol{r}}D\cdot\dot{\boldsymbol{r}} \,. \tag{A.17}$$

For Eq. (A.14), because the Berry curvature $\boldsymbol{\Omega}(\boldsymbol{k})$ can be derived from the vector potential $\boldsymbol{\mathcal{A}}(\boldsymbol{k}) = \langle u(\boldsymbol{k})|\mathrm{i}\boldsymbol{\nabla}_{\boldsymbol{k}}|u(\boldsymbol{k})\rangle$, $\boldsymbol{\Omega} = \boldsymbol{\nabla}_{\boldsymbol{k}}\times\boldsymbol{\mathcal{A}}$, we can use the same method to obtain

$$D\boldsymbol{\nabla}_{\boldsymbol{k}}\cdot\dot{\boldsymbol{k}} = -\boldsymbol{\nabla}_{\boldsymbol{k}}D\cdot\dot{\boldsymbol{k}} \,. \tag{A.18}$$

Finally, adding Eq. (A.17) and Eq. (A.18) together gives

$$D(\boldsymbol{\nabla}_{\boldsymbol{r}}\cdot\dot{\boldsymbol{r}} + \boldsymbol{\nabla}_{\boldsymbol{k}}\cdot\dot{\boldsymbol{k}}) = -\frac{\partial D}{\partial t} - \boldsymbol{\nabla}_{\boldsymbol{r}}D\cdot\dot{\boldsymbol{r}} - \boldsymbol{\nabla}_{\boldsymbol{k}}D\cdot\dot{\boldsymbol{k}} = -\frac{dD}{dt} \,, \tag{A.19}$$

or

$$\boldsymbol{\nabla}_{\boldsymbol{r}} \cdot \dot{\boldsymbol{r}} + \boldsymbol{\nabla}_{\boldsymbol{k}} \cdot \dot{\boldsymbol{k}} = -\frac{1}{D}\frac{dD}{dt} = -\frac{d\ln D}{dt} = -\frac{d\ln(1+\boldsymbol{B}\cdot\boldsymbol{\Omega})}{dt}\ . \tag{A.20}$$

The more general result, e.g., Eq. (2.13) in Chap. 2, can be derived in the same way if one notice that the Berry curvature is a differential two-form, derived from the $U(1)$-gauge field defined over the Bloch basis.

Appendix B

Gradient Expansion of Wave Packet

We derive part of the total current that is due to the self-rotation of the wave packet, i.e, the second term in Eq. (4.2). Details can be found in Ref. [6]. The wave packet is constructed from Bloch wave functions of a single band,

$$|W\rangle = \int d\boldsymbol{k}\, a(\boldsymbol{k})|\psi_n(\boldsymbol{k})\rangle \ . \tag{B.1}$$

The operator product needs to be anti-symmetrized to make it Hermitian. By defining $v_a = \dot{r}_a$ and $\tilde{a}(\boldsymbol{k}) = e^{i\boldsymbol{k}\cdot\boldsymbol{r}_c}a(\boldsymbol{k})$, we have

$$\begin{aligned} m_{ab} &= \mathrm{Re}\langle W|(r_b - r_b^c)v_a|W\rangle \\ &= \mathrm{Re}\int d\boldsymbol{k}' \int d\boldsymbol{k}\, a^*(\boldsymbol{k}')a(\boldsymbol{k})\langle\psi_n(\boldsymbol{k}')|(r_b - r_b^c)v_a|\psi_n(\boldsymbol{k})\rangle \\ &= \mathrm{Re}\int d\boldsymbol{k}' \int d\boldsymbol{k}\, \tilde{a}^*(\boldsymbol{k}')\tilde{a}(\boldsymbol{k})\langle u_n(\boldsymbol{k}')|e^{i(\boldsymbol{k}-\boldsymbol{k}')\cdot(\boldsymbol{r}-\boldsymbol{r}_c)}(r_b - r_b^c)\tilde{v}_a|u_n(\boldsymbol{k})\rangle \ , \end{aligned} \tag{B.2}$$

where $\tilde{v}_a$ is the velocity operator on the $|u_n\rangle$ basis,

$$\tilde{v}_a = e^{-i\boldsymbol{k}\cdot\boldsymbol{r}}v_a e^{i\boldsymbol{k}\cdot\boldsymbol{r}} = \frac{\partial\tilde{\mathcal{H}}_0}{\partial k_a} \ , \tag{B.3}$$

with $\tilde{\mathcal{H}}_0$ defined in a similar way. Since

$$\tilde{v}_a|u_n(\boldsymbol{k})\rangle = \sum_{n'}|u_{n'}(\boldsymbol{k})\rangle\langle u_{n'}(\boldsymbol{k})|\tilde{v}_a|u_n(\boldsymbol{k})\rangle \ , \tag{B.4}$$

$$\langle u_n(\boldsymbol{k}')|e^{i(\boldsymbol{k}-\boldsymbol{k}')\cdot(\boldsymbol{r}-\boldsymbol{r}_c)}(r_b - r_b^c)|u_{n'}(\boldsymbol{k})\rangle = i\delta_{nn'}\frac{\partial}{\partial k'_b}\delta(\boldsymbol{k}-\boldsymbol{k}') - i\delta(\boldsymbol{k}-\boldsymbol{k}')\Big\langle\frac{\partial u_n}{\partial k'_b}\Big|u_{n'}\Big\rangle \ , \tag{B.5}$$

we have (by inserting the complete set $\sum_{n'}|u_{n'}(\boldsymbol{k})\rangle\langle u_{n'}(\boldsymbol{k})| = 1$)

$$m_{ab} = \mathrm{Re}\Big\{-i\int d\boldsymbol{k}\,\frac{\partial\tilde{a}^*(\boldsymbol{k})}{\partial k_b}\tilde{a}(\boldsymbol{k})\langle u_n|\tilde{v}_a|u_n\rangle - i\int d\boldsymbol{k}\,|\tilde{a}(\boldsymbol{k})|^2\Big\langle\frac{\partial u_n}{\partial k_b}\Big|\tilde{v}_a\Big|u_n\Big\rangle\Big\} \ . \tag{B.6}$$

The integrand of the second term can be written as

$$\begin{aligned}
\mathrm{Im}\Big\langle\frac{\partial u_n}{\partial k_b}\Big|\frac{\partial\tilde{\mathcal{H}}_0}{\partial k_a}\Big|u_n\Big\rangle &= \mathrm{Im}\Big\{\frac{\partial}{\partial k_a}\Big\langle\frac{\partial u_n}{\partial k_b}\Big|\tilde{\mathcal{H}}_0\Big|u_n\Big\rangle - \Big\langle\frac{\partial u_n}{\partial k_b}\Big|\tilde{\mathcal{H}}_0\Big|\frac{\partial u_n}{\partial k_a}\Big\rangle\Big\} \\
&= \mathrm{Im}\Big\{\Big\langle\frac{\partial u_n}{\partial k_b}\Big|\frac{\partial u_n}{\partial k_a}\Big\rangle\varepsilon_n + \Big\langle\frac{\partial u_n}{\partial k_b}\Big|u_n\Big\rangle\frac{\partial\varepsilon_n}{\partial k_a} - \Big\langle\frac{\partial u_n}{\partial k_b}\Big|\tilde{\mathcal{H}}_0\Big|\frac{\partial u_n}{\partial k_a}\Big\rangle\Big\} \\
&= \mathrm{Im}\Big\{\Big\langle\frac{\partial u_n}{\partial k_b}\Big|(\varepsilon_n - \tilde{\mathcal{H}}_0)\Big|\frac{\partial u_n}{\partial k_a}\Big\rangle + \Big\langle\frac{\partial u_n}{\partial k_b}\Big|u_n\Big\rangle\frac{\partial\varepsilon_n}{\partial k_a}\Big\} \ .
\end{aligned} \tag{B.7}$$

Therefore the magnetic moment is

$$m_{ab} = \mathrm{Im}\Big\{\int d\boldsymbol{k}\,\frac{\partial\tilde{a}^*(\boldsymbol{k})}{\partial k_b}\tilde{a}(\boldsymbol{k})\frac{\partial\varepsilon_n}{\partial k_a} + |\tilde{a}(\boldsymbol{k})|^2\Big\langle\frac{\partial u_n}{\partial k_b}\Big|u_n\Big\rangle\frac{\partial\varepsilon_n}{\partial k_a} + |\tilde{a}(\boldsymbol{k})|^2\Big\langle\frac{\partial u_n}{\partial k_b}\Big|(\varepsilon_n - \tilde{\mathcal{H}}_0)\Big|\frac{\partial u_n}{\partial k_a}\Big\rangle\Big\} \ . \tag{B.8}$$

The first two terms cancel. Thus

$$m_{ab} = \mathrm{Im}\Big\langle\frac{\partial u_n}{\partial k_b}\Big|(\varepsilon_n - \tilde{\mathcal{H}}_0)\Big|\frac{\partial u_n}{\partial k_a}\Big\rangle \ . \tag{B.9}$$

If we define

$$m_c = \frac{1}{2}\epsilon_{abc}m_{ab} = \frac{i}{2}\Big\langle\frac{\partial u_n}{\partial\boldsymbol{k}}\Big| \times (\tilde{\mathcal{H}}_0 - \varepsilon_n)\Big|\frac{\partial u_n}{\partial\boldsymbol{k}}\Big\rangle_c \ , \quad \Leftrightarrow \quad m_{ab} = \epsilon_{abc}m_c \ , \tag{B.10}$$

$$\tilde{M}_{ab} = \epsilon_{abc}\tilde{M}_c = \epsilon_{abc}\int\frac{d\boldsymbol{k}}{(2\pi)^3}f(\boldsymbol{r},\boldsymbol{k})m_c \ , \tag{B.11}$$

then

$$J_a = \nabla_b \tilde{M}_{ab} = \epsilon_{abc} \nabla_b \tilde{M}_c = \boldsymbol{\nabla} \times \tilde{\boldsymbol{M}} \ . \tag{B.12}$$

Finally, several remarks of the calculation are in order. In deriving Eq. (B.6) we need calculate the derivative of a δ-function, this is done by integrating by parts, i.e.,

$$\begin{aligned} & i \int d\boldsymbol{k}' \int d\boldsymbol{k}\, \tilde{a}^*(\boldsymbol{k}') \tilde{a}(\boldsymbol{k}) \frac{\partial}{\partial k'_b} \delta(\boldsymbol{k} - \boldsymbol{k}') \\ & \qquad = i \int d\boldsymbol{k}' \int d\boldsymbol{k} \left\{ \frac{\partial}{\partial k'_b} \Big[\tilde{a}^*(\boldsymbol{k}') \tilde{a}(\boldsymbol{k}) \delta(\boldsymbol{k} - \boldsymbol{k}') \Big] - \frac{\partial \tilde{a}^*(\boldsymbol{k}')}{\partial k'_b} \tilde{a}(\boldsymbol{k}) \delta(\boldsymbol{k} - \boldsymbol{k}') \right\} . \end{aligned} \tag{B.13}$$

The first integral reduces to a surface term, hence vanishes. In Eq. (B.7) we did not count the term below, since its imaginary part is zero:

$$\left\langle \frac{\partial^2 u_n}{\partial k_a \partial k_b} \middle| u_n \right\rangle = \left\langle u_n \middle| \frac{\partial^2 u_n}{\partial k_a \partial k_b} \right\rangle . \tag{B.14}$$

Bibliography

[1] Y. Aharonov and D. Bohm, Phys. Rev. **115**, 485 (1959).

[2] S. Pancharatnam, Proc. Indian Acad. Sci. A **44**, 247 (1956).

[3] M. V. Berry, Proc. R. Soc. Lond. **A392**, 45 (1984).

[4] N. W. Ashcroft and N. D. Mermin, *Solid State Physics* (Saunders College, Philadelphia, 1976).

[5] F. Bloch, Zeitschrift für physik **52**, 555 (1928).

[6] M.-C. Chang and Q. Niu, Phys. Rev. B **53**, 7010 (1996).

[7] G. Sundaram and Q. Niu, Phys. Rev. B **59**, 14915 (1999).

[8] J. Smit, Physica **21**, 877 (1955).

[9] L. Berger, Phys. Rev. B **2**, 4559 (1970).

[10] T. Jungwirth, Q. Niu, and A. H. MacDonald, Phys. Rev. Lett. **88**, 207208 (2002).

[11] Z. Fang, N. Nagaosa, K. S. Takahashi, A. Asamitsu, R. Mathieu, T. Ogasawara, H. Yamada, M. Kawasaki, Y. Tokura, and K. Terakura, Science **302**, 92 (2003).

[12] Y. Yao, L. Kleinman, A. H. MacDonald, J. Sinova, T. Jungwirth, D.-s. Wang, E. Wang, and Q. Niu, Phys. Rev. Lett. **92**, 037204 (2004).

[13] A. Bohm, A. Mostafazadeh, H. Koizumi, Q. Niu, and J. Zwanziger, *The Geometric Phase in Quantum Systems: Foundations, Mathematical Concepts, and Applications in Molecular and Condensed Matter Physics* (Springer-Verlag, Berlin, 2003).

[14] D. J. Thouless, M. Kohmoto, M. P. Nightingale, and M. den Nijs, Phys. Rev. Lett. **49**, 405 (1982).

[15] D. J. Thouless, Phys. Rev. B **27**, 6083 (1983).

[16] R. D. King-Smith and D. Vanderbilt, Phys. Rev. B **47**, 1651 (1993).

[17] R. Resta, Rev. Mod. Phys. **66**, 899 (1994).

[18] F. D. M. Haldane, Phys. Rev. Lett. **93**, 206602 (2004).

[19] S. Murakami, N. Nagaosa, and S.-C. Zhang, Science **301**, 1348 (2003).

[20] J. Sinova, D. Culcer, Q. Niu, N. A. Sinitsyn, T. Jungwirth, and A. H. MacDonald, Phys. Rev. Lett. **92**, 126603 (2004).

[21] H. Kuratsuji and S. Iida, Phys. Rev. D **37**, 441 (1988).

[22] R. G. Littlejohn and W. G. Flynn, Phys. Rev. A **44**, 5239 (1991).

[23] G. Panati, H. Spohn, and S. Teufel, Commun. Math. Phys. **242**, 547 (2003).

[24] P. Středa, J. Phys. C: Solid State Phys. **15**, L717 (1982).

[25] L. E. Reichl, *A Modern Course in Statistical Physics* (University of Texas Press, Austin, TX, 1980).

[26] D. Culcer, J. Sinova, N. A. Sinitsyn, T. Jungwirth, A. H. MacDonald, and Q. Niu, Phys. Rev. Lett. **93**, 046602 (2004).

[27] O. Gat and J. E. Avron, Phys. Rev. Lett. **91**, 186801 (2003).

[28] T. Thonhauser, D. Ceresoli, D. Vanderbilt, and R. Resta, Phys. Rev. Lett. **95**, 137205 (2005).

[29] J. Shi, G. Vignale, D. Xiao, and Q. Niu, to be published.

[30] P. Zhang and Q. Niu, `cond-mat/0406436`.

[31] P. Senjanovic, Ann. Phys. **100**, 227 (1976).

[32] D. M. Gitman and I. V. Tyutin, *Quantization of Fields with Constraints* (Springer-Verlag, New York, 1990).

[33] H. P. Robertson, Phys. Rev. **46**, 794 (1934).

[34] P. A. Horváthy, L. Martina, and P. C. Stichel, Phys. Lett. B **615**, 87 (2005).

[35] D. Xiao, J. Shi, and Q. Niu, Phys. Rev. Lett. **95**, 137204 (2005).

[36] B. I. Halperin, Phys. Rev. B **25**, 2185 (1982).

[37] P. Středa and L. Smrčka, J. Phys. C: Solid State Phys. **16**, L895 (1983).

[38] W.-L. Lee, S. Watauchi, V. L. Miller, R. J. Cava, and N. P. Ong, Phys. Rev. Lett. **93**, 226601 (2004).

[39] P. Středa, Phys. Rev. B **74**, 113306 (2006).

[40] R. Karplus and J. M. Luttinger, Phys. Rev. **95**, 1154 (1954).

[41] W.-L. Lee, S. Watauchi, V. L. Miller, R. J. Cava, and N. P. Ong, Science **303**, 1647 (2004).

[42] C. Zeng, Y. Yao, Q. Niu, and H. H. Weitering, Phys. Rev. Lett. **96**, 037204 (2006).

[43] N. R. Cooper, B. I. Halperin, and I. M. Ruzin, Phys. Rev. B **55**, 2344 (1997).

[44] J. D. Jackson, *Classical Electrodynamics* (John Wiley & Sons, New York, 1999), 3rd ed.

[45] J. Smit, Physica **24**, 39 (1958).

[46] J. M. Luttinger, Phys. Rev. **135**, A1505 (1964).

[47] M. P. Marder, *Condensed Matter Physics* (John Wiley & Sons, new York, 2000).

[48] Y. Wang, Z. A. Xu, T. Kakeshita, S. Uchida, S. Ono, Y. Ando, and N. P. Ong, Phys. Rev. B **64**, 224519 (2001).

[49] Y. Yao, Y. Liang, D. Xiao, Q. Niu, S.-Q. Shen, X. Dai, and Z. Fang, Phys. Rev. B **75**, 020401(R) (2006).

[50] Y. K. Kato, R. C. Myers, A. C. Gossard, and D. D. Awschalom, Science **306**, 1910 (2004).

[51] J. Wunderlich, B. Kaestner, J. Sinova, and T. Jungwirth, Phys. Rev. Lett. **94**, 047204 (2005).

[52] S. Murakami, N. Nagaosa, and S.-C. Zhang, Phys. Rev. Lett. **93**, 156804 (2004).

[53] G. Y. Guo, Y. Yao, and Q. Niu, Phys. Rev. Lett. **94**, 226601 (2005).

[54] Y. Yao and Z. Fang, Phys. Rev. Lett. **95**, 156601 (2005).

[55] J. Shi, P. Zhang, D. Xiao, and Q. Niu, Phys. Rev. Lett. **96**, 076604 (2006).

[56] S. O. Valenzuela and M. Tinkham, Nature **442**, 176 (2006).

[57] H. Zhao, E. J. Loren, H. M. Van Driel, and A. L. Smirl, Phys. Rev. Lett. **96**, 246601 (2006).

[58] B. Liu, J. Shi, W. Wang, H. Zhao, D. Li, S. Zhang, Q. Xue, and D. Chen, `cond-mat/0610150`.

[59] D. Xiao, Y. Yao, Z. Fang, and Q. Niu, Phys. Rev. Lett. **97**, 026603 (2006).

[60] S. Murakami, Phys. Rev. Lett. **97**, 236805 (2006).

[61] P. Zhang, Z. Wang, J. Shi, D. Xiao, and Q. Niu, `cond-mat/0701293`.

[62] J. E. Avron, R. Seiler, and B. Simon, Phys. Rev. Lett. **51**, 51 (1983).

[63] C. L. Kane and E. J. Mele, Phys. Rev. Lett. **95**, 146802 (2005).

[64] C. L. Kane and E. J. Mele, Phys. Rev. Lett. **95**, 226801 (2005).

[65] F. D. M. Haldane, Phys. Rev. Lett. **61**, 2015 (1988).

[66] J. M. Ziman, *Electrons and Phonons: The Theory of Transport Phenomena in Solids* (Oxford University Press, Oxford, UK, 1960).

[67] W. Kesternich, Phys. Rev. B **13**, 4227 (1976).

[68] A. K. Geim and K. S. Novoselov, Nature Mater. **6**, 183 (2007).

[69] S. A. Wolf, D. D. Awschalom, R. A. Buhrman, J. M. Daughton, S. von Molnár, M. L. Roukes, A. Y. Chtchelkanova, and D. M. Treger, Science **294**, 1488 (2001).

[70] Y. Zhang, Y.-W. Tan, H. L. Stormer, and P. Kim, Nature **438**, 201 (2005).

[71] K. S. Novoselov, A. K. Geim, S. V. Morozov, D. Jiang, M. I. Katsnelson, I. V. Grigorieva, S. V. Dubonos, and A. A. Firsov, Nature **438**, 197 (2005).

[72] K. S. Novoselov, E. McCann, S. V. Morozov, V. I. Fal'ko, M. I. Katsnelson, U. Zeitler, D. Jiang, F. Schedin, and A. K. Geim, Nature Phys. **2**, 177 (2006).

[73] P. R. Wallace, Phys. Rev. **71**, 622 (1947).

[74] G. W. Semenoff, Phys. Rev. Lett. **53**, 2449 (1984).

[75] G. Sundaram, Ph.D. thesis, The University of Texas at Austin (2000).

[76] H. Min, J. E. Hill, N. A. Sinitsyn, B. R. Sahu, L. Kleinman, and A. H. MacDonald, Phys. Rev. B **74**, 165310 (2006).

[77] Y. Yao, F. Ye, X.-L. Qi, S.-C. Zhang, and Z. Fang, Phys. Rev. B **75**, 041401 (2007).

[78] J.-N. Fuchs and P. Lederer, Phys. Rev. Lett. **98**, 016803 (2007).

[79] N. A. Sinitsyn, Q. Niu, and A. H. MacDonald, Phys. Rev. B **73**, 075318 (2006).

[80] N. A. Sinitsyn, J. E. Hill, H. Min, J. Sinova, and A. H. MacDonald, Phys. Rev. Lett. **97**, 106804 (2006).

[81] T. Ohta, A. Bostwick, T. Seyller, K. Horn, and E. Rotenberg, Science **313**, 951 (2006).

[82] E. McCann and V. I. Fal'ko, Phys. Rev. Lett. **96**, 086805 (2006).

[83] F. Guinea, A. H. C. Neto, and N. M. R. Peres, Phys. Rev. B **73**, 245426 (2006).

Vita

Di Xiao was born in the town of Songzi near the Yangtze River of China on August 16th, 1979, the second child and the son of Xupei Zhang and Zhaoqin Xiao. After three years in the National Science Class at the Affiliated High School of Peking University, he enrolled at Peking University and received his Bachelor of Science degree in Physics in July 2001. A month later, he entered the University of Texas at Austin and started graduate studies in their physics program. He married his wife Yuan Li in Austin in the winter of 2001.

Permanent Address: 176 Minzhu St.
Songzi, Hubei 434200, China

This dissertation was typeset with LaTeX 2_ε[1] by the author.

[1] LaTeX 2_ε is an extension of LaTeX. LaTeX is a collection of macros for TeX. TeX is a trademark of the American Mathematical Society. The macros used in formatting this dissertation were written by Dinesh Das, Department of Computer Sciences, The University of Texas at Austin, and extended by Bert Kay, James A. Bednar, and Ayman El-Khashab.